Published for SISSA by Springer

Received: *August 21, 2021*
Revised: *August 7, 2022*
Accepted: *September 30, 2022*
Published: *October 31, 2022*

Stringy ER = EPR

Daniel Louis Jafferis and Elliot Schneider

Center for the Fundamental Laws of Nature, Harvard University, Cambridge, MA, U.S.A.

E-mail: jafferis@physics.harvard.edu, elliot.andrew.schneider@gmail.com

Abstract: The ER = EPR correspondence relates a superposition of entangled, disconnected spacetimes to a connected spacetime with an Einstein-Rosen bridge. We construct examples in which both sides may be described by weakly-coupled string theory. The relation between them is given by a Lorentzian continuation of the FZZ duality of the two-dimensional Euclidean black hole CFT in one example, and in another example by continuation of a similar duality that we propose for the asymptotic Euclidean AdS_3 black hole. This gives a microscopic understanding of ER = EPR: one has a worldsheet duality between string theory in a connected, eternal black hole, and in a superposition of disconnected geometries in an entangled state. The disconnected description includes a condensate of entangled folded strings emanating from a strong-coupling region in place of a bifurcation point. Our construction relies on a Lorentzian interpretation of Euclidean time winding operators via angular quantization, as well as some lesser known worldsheet string theories, such as perturbation theory around a thermofield-double state, which we define using Schwinger-Keldysh contours in target space.

Keywords: Black Holes in String Theory, Long Strings, String Duality

ArXiv ePrint: 2104.07233

https://doi.org/10.1007/JHEP10(2022)195

JHEP10(2022)195

Contents

JHEP10(2022)195

1 Introduction and overview

The beautiful relation between quantum entanglement and geometric spatial connection, known colloquially as ER = EPR, has given a new perspective on the gauge/gravity correspondence [1–6]. The prototypical example is that a pair of entangled black holes are joined by an Einstein-Rosen bridge in their interiors.

In asymptotic AdS_{d+1}, for example, the two-sided (large) black hole in its Hartle-Hawking (HH) state at inverse Hawking temperature β is dual, above the Hawking-Page temperature, to the thermofield-double (TFD) state in two copies of the boundary CFT Hilbert space on S^{d-1} (figure 1) [7–10]. The TFD is a maximally entangled state, prepared by the Euclidean functional integral on $[0,\beta/2]\times S^{d-1}$, and given by a sum over product

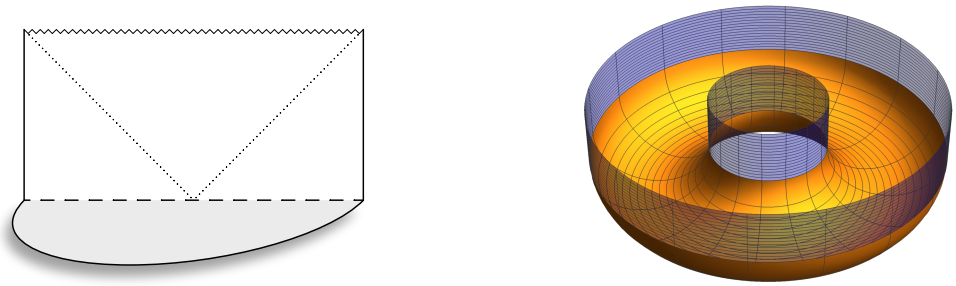

(a) (b)

Figure 1. *The* AdS_3 *HH State and the Dual TFD.* The conformal diagram of the asymptotic AdS_3 two-sided black hole (or, rather, its top half) is shown on the left. Over each point is an additional circle, which is suppressed in the figure. The left and right asymptotic AdS_3 regions are causally separated by the horizons, represented by the diagonal dotted lines. The future singularity is the zigzag line at the top of the diagram. The Hartle-Hawking state is prepared by halving the Euclidean continuation of the black hole, shown by the half-disk, and gluing it to the zero-time slice of the black hole on the horizontal dashed line. The Euclidean time periodicity is β, the inverse Hawking temperature of the black hole. The zero-time slice has the topology of an annulus and the halved Euclidean black hole resembles a half-bagel, obtained by revolving the dashed line and half-disk around the suppressed circle. Above the Hawking-Page temperature, this bulk state is dual to the thermofield-double state in two copies of the boundary CFT on a circle (times time), shown on the right. The yellow half-torus prepares the state on its two circle boundaries, which then evolve forward in Lorentzian time along the two blue cylinders. The Hartle-Hawking cap that prepared the bulk state corresponds to the solid half-torus obtained by filling in the interior of the yellow surface.

states of the two uncoupled CFTs, $|\text{TFD}\rangle \propto \sum e^{-\beta E_n/2} |n^*\rangle_{\text{L}} \otimes |n\rangle_{\text{R}}$.[1] It is a purification of the thermal state at inverse temperature β, the reduced density matrix in a single copy of the CFT being $\text{tr}_{\mathcal{H}_{\text{L}}} |\text{TFD}\rangle \langle\text{TFD}| \propto e^{-\beta H}$.

It is natural that each side of the black hole is dual to a thermal state of the CFT, the reduced density-matrix of the HH state in the bulk likewise being a thermal state of inverse Hawking temperature β [11, 12]. Moreover, that the two-sided black hole is dual to a state in two independent copies of the CFT is a boundary manifestation of the fact that the left and right asymptotic AdS regions in the bulk are causally separated by the horizons.

On the other hand, it is surprising that a superposition of product states in two uncoupled CFTs admits a bulk description as a connected spacetime [1, 2]. Each term $|n^*\rangle_{\text{L}} \otimes |n\rangle_{\text{R}}$ in the TFD sum corresponds to a pair of disconnected spacetimes. Thus, the linearity of quantum mechanics would seem to imply that their superposition would in turn be dual to a superposition of disconnected geometries. And yet, the superposition admits a connected description as a two-sided black hole due to the entanglement[2] between the two sides (figure 2), so the existence of an Einstein-Rosen bridge is a non-linear property of the state.

[1] The star denotes the action of CPT.

[2] Below the Hawking-Page temperature, the boundary TFD state is instead dual to the bulk TFD in two disconnected copies of AdS (figure 13a). Then the boundary TFD, and likewise the bulk disconnected superposition, is not sufficiently entangled to admit a dual semi-classical connected description.

JHEP10(2022)195

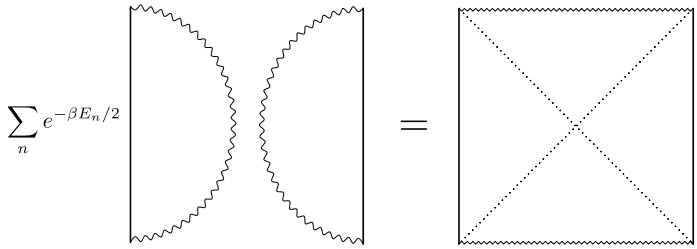

Figure 2. *Schematic of* ER = EPR. The connected, two-sided, asymptotically AdS black hole admits a dual description as an entangled superposition of disconnected spacetimes, represented schematically by the wedges on the left, each of which is dual to an energy eigenstate $|n\rangle_{\mathrm{L}}, |n\rangle_{\mathrm{R}}$ of the two copies of the boundary CFT. The ER = EPR correspondence asserts that this equivalence of entangled quantum states to connected spacetimes holds more generally. We find examples of string dualities of this type, relating a string in a connected target space to a string in an entangled superposition of disconnected targets.

There is no sharp contradiction because the Einstein-Rosen bridge is cloaked behind a horizon, and its existence cannot be measured at the boundary. Moreover, scenarios in which it is operationally observable, such as the traversable wormhole protocol [13], require that the two sides are coupled together and only apply to a small subspace of states, giving results consistent with linearity.

All this suggests that there should exist examples of quantum gravity dualities, relating a connected spacetime to an entangled superposition of disconnected spacetimes. In this work, we exhibit exact string theory dualities of this type. The form of the relations is between string theory in a two-sided black hole[3] made of fundamental strings in the HH state (figure 1a), and string theory in a pair of disconnected spacetimes in the TFD state (in the bulk sense), with an entangled condensate of folded strings (figure 6a). Expanding the condensate, one indeed finds a dual EPR-like description of the black hole given by a superposition of disconnected geometries, each with a number of entangled strings. On the disconnected side, the black hole bifurcation point is replaced by a strong-coupling region from which the folded strings emanate.[4] In the semi-classical limit, the black hole description is weakly coupled in the α' sense, and the EPR description is strongly coupled. Both sides may be taken at weak string coupling, however.[5]

These string dualities are defined by the Lorentzian continuation in the sense of the target time coordinate of CFT dualities for Euclidean black hole target spaces in two and three dimensions. In two dimensions, the Euclidean duality with which we begin is the well-known Fateev-Zamolodchikov-Zamolodchikov (FZZ) duality of the asymptotic

[3]Or more simply in a two-sided Rindler decomposition of AdS_3, with asymptotic AdS_3 regions separated by coordinate horizons.

[4]The disconnected geometries may or may not be horizonless, however, once the backreaction of the folded strings is taken into account. It is reasonable to suspect that a typical microstate with many folded strings falling into the strong-coupling region will result in the formation of a black hole with a horizon, though we have not attempted to verify this.

[5]In the sense that the boundary correlators or scattering amplitudes can be computed in string perturbation theory since they are governed by regions of the target space with tunably-weak string coupling. The target space in the EPR side of the dualities includes a strong-coupling region, however.

JHEP10(2022)195

linear-dilaton Euclidean black hole CFT [15, 16]. In three dimensions, one of the goals of this paper is to propose that there exists an analogous duality of the asymptotic Euclidean AdS_3 black hole CFT. We provide evidence for this duality by demonstrating that all symmetries match between the two sides, and by showing that upon gauging translations symmetry along the "third direction", it reduces to the original FZZ duality.

Each of these CFT dualities relates worldsheet string theory with a Euclidean black hole target space characterized by a contractible Euclidean time circle, to a dual geometry with a non-contractible time circle, together with a potential built of winding operators. Continuing the target time in the first case yields the ER description of a string in a two-sided, Lorentzian black hole. The other yields the EPR description of a string in a disconnected target. The challenge in the latter case is to understand what it means to define a Lorentzian string theory by continuation from a Euclidean background containing insertions of Euclidean time winding operators.

Developing a formalism for the Lorentzian treatment of backgrounds built with Euclidean time winding operators is the other main goal of our work. We will argue that these string theories are defined by choosing an appropriate contour of integration on the string moduli space. In the neighborhood of Euclidean time winding insertions, the contour involves a deformation in the sense of angular quantization (as opposed to the more familiar contour of radial quantization [38]), that renders the moduli integral well-defined when Lorentzian scattering operators collide with Euclidean winding insertions. This results in a Hilbert space picture in which the euclidean time winding operators define particular states in the BRST quantization of extended strings with asymptotics determined by the angularly quantized operator.

We apply this formalism to the winding operators in sine-Liouville theory and its AdS_3 cousin described above, and show that they correspond to pairs of entangled folded strings emanating from the strongly coupled interiors of the disconnected targets. The full theories have a condensate of such strings. In the "infinitesimal" versions of these dualities, which relate different descriptions of the same operator in the black hole target CFT, the winding side corresponds to a specific state in the extended string Hilbert space with both endpoints at the bifurcation point.

In the remainder of this introduction, we give an overview of these results. As just mentioned, the ER = EPR dualities that we propose are defined by the Lorentzian continuation of CFT dualities for Euclidean black hole target spaces. The essential feature of a Euclidean duality required to realize ER = EPR upon continuation is that the Euclidean time circle should be contractible on one side of the duality and non-contractible on the other. The contractible ER description produces a state in a connected Lorentzian geometry with a horizon upon continuation, while the non-contractible EPR description gives a state in a disconnected geometry. By consistency, the non-contractible description must feature a mechanism that violates the winding number conservation law around the Euclidean time circle, since the string can unwind in the contractible dual. One could imagine that this winding violation is accomplished by the inclusion of D-branes or by a potential that explicitly breaks the symmetry.[6]

[6] Or by strong-coupling effects.

JHEP10(2022)195

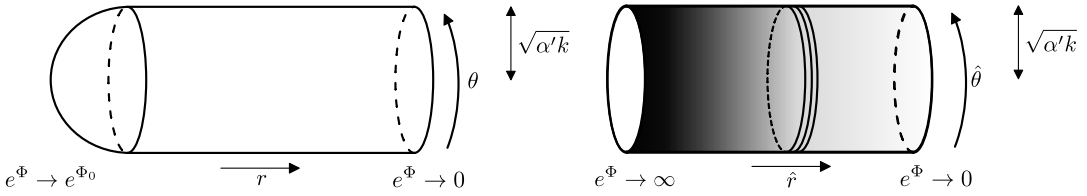

(a) *The Cigar Background.* The cigar sigma-model is a weakly-coupled Lagrangian description of the $\mathrm{SL}(2,\mathbb{R})_k/\mathrm{U}(1)$ CFT when k is large. For large r, the geometry is a cylinder of radius $\sqrt{\alpha' k}$, and as $r \to 0$ the cylinder smoothly caps off. The dilaton is a monotonically decreasing function of r. Its maximal value Φ_0 is attained at the tip, and at large r it falls off linearly as $-r$ and the string coupling goes to zero. Although a string in the weak-coupling region appears to be able to wind around the cylinder, there is no conserved topological charge because the string can unwind at the tip.

(b) *The sine-Liouville Background.* According to the FZZ duality, the sine-Liouville sigma-model is a dual description of the $\mathrm{SL}(2,\mathbb{R})_k/\mathrm{U}(1)$ CFT, better suited when k is small (compared to 2). The geometry is an infinite cylinder of radius $\sqrt{\alpha' k}$. The dilaton is $\Phi = -Q\hat{r}$, so that the string coupling e^{Φ} diverges as $\hat{r} \to -\infty$ and vanishes as $\hat{r} \to \infty$. The sine-Liouville potential $e^{-\sqrt{(k-2)/\alpha'}\hat{r}} \mathrm{Re}\, e^{i\sqrt{k/\alpha'}(\hat{\theta}_\mathrm{L} - \hat{\theta}_\mathrm{R})}$ includes a pure-winding mode of $\hat{\theta}$ (represented by the circles wrapping the middle of the cylinder), times a linear-dilaton primary (represented by the gradient).

Figure 3. The Cigar and sine-Louiville Backgrounds.

The presence of D-branes would allow closed strings wrapping the Euclidean time direction to break into pairs of open strings ending on the brane. Equivalently, the boundary state of the D-brane in the worldsheet CFT is a linear combination of states with different Euclidean time winding numbers. Such a duality would necessarily involve the cancellation of string loop diagrams on the EPR side with tree-level effects on the ER side, however, which may be complicated.

The EPR side of the duality can be interpreted as describing the constituent objects that make up the black hole. In backgrounds with Ramond-Ramond fluxes, one would therefore expect to find D-branes. In our examples, however, the dualities only involve closed strings, corresponding to black holes that are made of fundamental strings. It will instead be a winding potential that is responsible for breaking the symmetry in these EPR theories, corresponding to a condensate of strings that wrap the non-contractible Euclidean time circle.

Our first example is found in two-dimensional dilaton-gravity, where the $\mathrm{SL}(2,\mathbb{R})_k/\mathrm{U}(1)$ CFT describes for large k a string in a cigar-shaped Euclidean black hole with an asymptotically linear dilaton (figure 3a) [14]. The dual description of this CFT due to FZZ is given by a sigma-model into a cylinder, now with an infinite linear-dilaton direction, plus a condensate of winding strings (figure 3b). It is known as the sine-Liouville background, and the condensate is called the sine-Liouville potential.

The cigar description is weakly coupled for large k, while the sine-Liouville description is strongly coupled. Both backgrounds asymptote to identical cylinders in the region where the linear dilaton goes to minus infinity and the string coupling subsequently vanishes. Whereas the cigar geometry terminates at finite string coupling at its tip, in sine-Liouville

JHEP10(2022)195

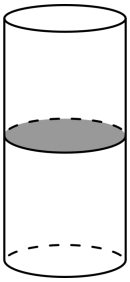

(a) *The Euclidean* AdS_3 *Black Hole.* $EAdS_3$ may be described as a solid cylinder. Compactifying the length of the cylinder to form a solid torus yields the Euclidean continuation of the asymptotic AdS_3 black hole, where the continuation is performed with respect to the contractible cycle. The coset manifold $SL(2,\mathbb{C})/SU(2)$ is equivalent to $EAdS_3$, and a string in $EAdS_3$ may therefore be described by the $SL(2,\mathbb{C})_k/SU(2)$ coset WZW model, where $\alpha' k = l^2_{AdS}$ sets the AdS length. The quotient $\mathbb{Z}\backslash SL(2,\mathbb{C})_k/SU(2)$ thus describes a string in the asymptotic $EAdS_3$ black hole, known as Euclidean BTZ (EBTZ).

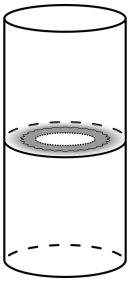

(b) *The 3D sine-Liouville Background.* In the dual description we propose for the $SL(2,\mathbb{C})_k/SU(2)$ CFT and its black hole quotient $\mathbb{Z}\backslash SL(2,\mathbb{C})_k/SU(2)$, the radial direction of the cylinder or solid torus is replaced by an infinite linear-dilaton direction, and a condensate of strings winding the resulting non-contractible cycle is added. Gauging the translation symmetry along the length of the cylinder produces the two-dimensional sine-Liouville background (figure 3b), whereas gauging the same symmetry in the first description yields the two-dimensional cigar (figure 3a). Thus, this duality is an uplift of the FZZ duality to a three-dimensional target space.

Figure 4. The Euclidean AdS_3 Black Hole and 3D sine-Liouville Background.

the cylinder extends forever and the string coupling diverges. In this description it is instead the sine-Liouville potential that is responsible for suppressing string configurations that extend into the strong-coupling region. In both backgrounds the apparent winding number conservation law of the common asymptotic cylinder region is violated — in the cigar because a wound string may unwind at the tip, and in sine-Liouville because the winding potential explicitly breaks the symmetry.

In three-dimensional spacetime, we propose a similar duality of the $\mathbb{Z}\backslash SL(2,\mathbb{C})_k/SU(2)$ CFT that describes a string in the asymptotic Euclidean AdS_3 black hole, known as Euclidean BTZ (EBTZ), which has the topology of a solid torus (figure 4a). The duality in fact applies as well to $SL(2,\mathbb{C})_k/SU(2)$ itself, prior to the $\mathbb{Z}$ quotient. The latter describes a string in Euclidean AdS_3 ($EAdS_3$), which is equivalent to the $SL(2,\mathbb{C})/SU(2)$ coset manifold. $EAdS_3$ may be described as a solid cylinder, and compactifying its length yields the EBTZ solid torus $\mathbb{Z}\backslash SL(2,\mathbb{C})/SU(2)$, where the circumference $4\pi^2/\beta$ of the compactification is fixed by the inverse Hawking temperature β of the black hole. In the dual description, the radial direction of the torus or cylinder is replaced by an infinite linear-dilaton direction as in the sine-Liouville background, and a condensate of winding strings wrapping the resulting non-contractible cycle is again added (figure 4b).[7] The original description is weakly coupled for large k while the dual description is strongly coupled, and once again g_s diverges at

[7] As we explain in section 2.2, the duality requires that we express the boundary cylinder or torus variables of $SL(2,\mathbb{C})_k/SU(2)$ or $\mathbb{Z}\backslash SL(2,\mathbb{C})_k/SU(2)$ in the first-order formalism.

JHEP10(2022)195

the strong-coupling boundary of the dual geometry.[8] Gauging the translation symmetry around the original non-contractible cycle of the torus or the length of the cylinder in the two descriptions reproduces the cigar and sine-Liouville backgrounds. Thus, this duality may be thought of as a three-dimensional uplift of the FZZ duality.[9,10,11]

These dualities share the essential feature that the two related target space geometries are of different topologies. In the cigar description of $\mathrm{SL}(2,\mathbb{R})_k/\mathrm{U}(1)$, the geometry has the topology of a disk, with the asymptotic cylinder capping off at the origin. By contrast, in the sine-Liouville description the cylinder is infinite, and the topology is an annulus. Thus, the circle direction of the two geometries, which is defined as the Euclidean time, is contractible on one side of the duality and non-contractible on the other. Similarly, in the $\mathbb{Z}\backslash\mathrm{SL}(2,\mathbb{C})_k/\mathrm{SU}(2)$ duality the contractible cycle of the torus in the original description is replaced by a non-contractible cycle in the dual, exchanging the disk $\times$ S^1 topology with an annulus $\times$ S^1. It is again this cycle that one defines as the Euclidean time in order to obtain the Lorentzian black hole upon continuation.[12]

Indeed, continuing with respect to a contractible Euclidean time circle yields a Lorentzian geometry with a horizon; the vanishing coefficient of the Euclidean time in the metric at the point where the circle shrinks implies that the continuation is a Lorentzian wedge bounded by a horizon at the same point. The simplest example is the continuation of $\mathbb{R}^2$ with respect to angular Euclidean time $\theta = it$: $\mathrm{d}s^2 = \mathrm{d}r^2 + r^2\mathrm{d}\theta^2 \to \mathrm{d}r^2 - r^2\mathrm{d}t^2$. The result is the right wedge of the Rindler decomposition of Minkowski spacetime, bounded by the Rindler horizon at $r = 0$ where the coefficient of $\mathrm{d}t^2$ vanishes (figure 8b). The Lorentzian continuation of the cigar, whose metric is $\mathrm{d}s^2 \propto \mathrm{d}r^2 + \tanh^2(r)\mathrm{d}\theta^2$, is an eternal, two-sided black hole of two-dimensional dilaton-gravity (figure 5a) [14]. In fact, in the neighborhood of the tip of the cigar where $\tanh^2(r)$ approaches r^2, the geometry is simply $\mathbb{R}^2$, and thus the near-horizon geometry of the black hole is again Rindler.[13] Likewise, the continuation of the EBTZ solid torus with respect to its contractible cycle is the asymptotic AdS_3 black hole, known as BTZ [23, 24], whose near-horizon geometry is Rindler $\times$ S^1.

Continuing with respect to a non-contractible Euclidean time circle, on the other hand, naturally produces a disconnected Lorentzian geometry, as we recall momentarily. In both cases, the compactness of the Euclidean time direction leads to a thermal state.

Although a black hole such as figure 5a is time dependent with respect to the global

[8] For small k (relative to its minimal value $k = 2$), on the other hand, the original description of $\mathrm{SL}(2,\mathbb{C})_k/\mathrm{SU}(2)$ is strongly coupled. Then we expect that the dual sigma-model is the better description of the AdS_3 vacuum for small k. It would be interesting to understand the connection between the sine-Liouville description and recent work on string theory in AdS_3 at small k [17–20].

[9] $\mathrm{SL}(2,\mathbb{C})/\mathrm{SU}(2)$ is a Euclidean continuation of $\mathrm{SL}(2,\mathbb{R}) = \mathrm{AdS}_3$, and the two-dimensional black hole may equivalently be thought of as a coset of the former.

[10] Potentially related work on a three-dimensional uplift of the FZZ duality was discussed in [21].

[11] We expect there is also a supersymmetric version of this duality, as in the supersymmetric FZZ duality of [22]. We focus on the bosonic string in this paper for simplicity, though we expect similar examples of ER = EPR would hold for the superstring in the cigar and the supersymmetric $\mathrm{AdS}_3 \times \mathrm{S}^3$ background.

[12] In the three-dimensional case one may alternatively continue with respect to the other cycle, which prepares a thermal state in AdS_3, or simply the vacuum state prior to the $\mathbb{Z}$ quotient. See Ft. 8.

[13] Of course, in Rindler the horizon is an artifact of the coordinates, whereas it is a genuine horizon in the case of the black hole.

JHEP10(2022)195

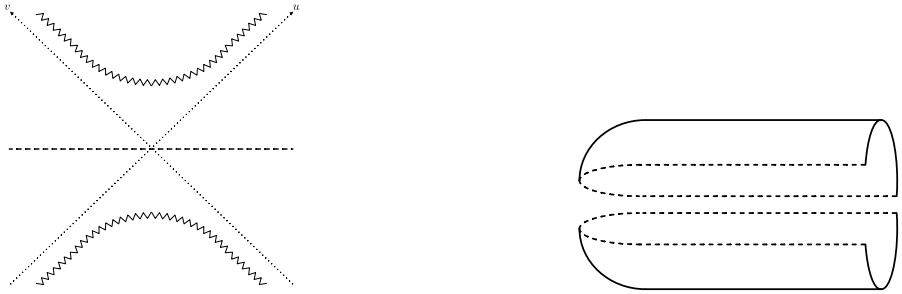

(a) (b)

Figure 5. *The Two-Dimensional Black Hole.* The Lorentzian continuation of the Euclidean cigar is a two-sided, eternal black hole. The horizons are the diagonal dotted lines, and the past and future singularities are the zigzag hyperbolas at the bottom and top. The geometry is invariant under time reflection about the dashed line, which enables the construction of the Hartle-Hawking state. The cigar, which has the topology of a disk, is cut in half and glued to the black hole along the fixed line of the reflection symmetry, similar to figure 1a but resembling the Schwarzschild causal diagram rather than BTZ. This Euclidean cap prepares the state on the dashed line, which is then evolved forward in Lorentzian time.

Kruskal time that flows vertically, it is symmetric under time reversal, which is a reflection about the horizontal dashed line in the figure. The existence of this Z_2 symmetry ensures that the Euclidean continuation of the geometry is real, and that the fixed-point locus is common to both the Lorentzian and Euclidean sections. Thus, the two may be cut in half and glued together along this line as shown in figure 1a in the AdS case. The functional integral over the Euclidean section prepares the HH state on the asymptotic linear-dilaton black hole background [7, 8, 10]. This state is a generalized notion of a vacuum, and its existence is due to the Z_2 symmetry of the black hole.

The infinite cylinder of the sine-Liouville background may similarly be cut and continued to prepare a state in a Lorentzian geometry (figure 6). Now the half-annulus topology prepares a state in the disconnected union of two copies of $\mathbb{R}^{1,1}$. This is the TFD state in the bulk disconnected spacetime. On each copy of $\mathbb{R}^{1,1}$, one has a linear dilaton along the spatial direction, with one asymptotic boundary at weak string coupling and the other at strong coupling, represented by the solid and dotted lines.

On top of this free-field background, one has the condensate of strings that wind the non-contractible Euclidean time circle, which by the FZZ duality is equivalent to the connected linear-dilaton black hole. A winding string worldsheet is also shown in the figure. An important aspect of our construction is to explain the interpretation of these winding strings in the Lorentzian continuation, which we will argue produce pairs of entangled folded strings emanating from the strong-coupling boundaries.

Note that although one could T-dualize the sine-Liouville background, and thereby replace the winding potential with a momentum potential whose Lorentzian interpretation is more straightforward, its continuation would not be dual to the Lorentzian black hole. To obtain a Lorentzian duality, one must continue with respect to the same Z_2 symmetry

JHEP10(2022)195

(a) (b)

Figure 6. *The Bulk TFD State.* The infinite cylinder geometry of the sine-Liouville background has the topology of an annulus (right). The linear dilaton implies that the string coupling vanishes at one asymptotic boundary and diverges at the other, represented by the solid and dotted circles. When the annulus is halved and glued to the Lorentzian continuation, it prepares the TFD state in two disconnected copies of flat linear-dilaton spacetime (left). The state prepared by halving the dual EBTZ background is similar but with an additional circle suppressed. Also pictured is the embedding of a string worldsheet with a pair of Euclidean time winding operator insertions from the sine-Liouville potential. The image of the worldsheet wraps the Euclidean time circle, extending out from the dotted strong-coupling boundary toward finite coupling, before folding back on itself and falling back to strong coupling. When the worldsheet is sliced in angular quantization, each spatial slice is then mapped to a folded string, shown in red, that comes in and out of the strong-coupling region. The full sine-Liouville potential adds a condensate of such folded strings on top of the disconnected union of linear-dilaton × time backgrounds. Expanding the condensate, one obtains an EPR description of a string in a superposition of entangled disconnected spacetimes, dual to string theory in the connected black hole.

on both sides of the Euclidean duality. The continuation of the T-dualized sine-Liouville background would instead be dual to the continuation of the so-called trumpet geometry [25], which has a naked singularity where the θ circle of the cigar shrinks.

One may likewise prepare the HH state for the AdS_3 black hole by slicing the EBTZ solid torus in half across its contractible Euclidean time cycle, producing a manifold in the shape of a halved bagel, and gluing its annulus boundary to the identical zero-time slice of the two-sided black hole (figure 1a). The two circle boundaries of the annulus correspond to slices of the left and right asymptotic AdS_3 cylinder boundaries. Cutting the now non-contractible cycle of the dual geometry, on the other hand, prepares a TFD state in two disconnected copies of linear-dilaton × time × S^1, together with the condensate.[14]

Complexified spacetimes such as figure 1a and 6a are familiar in quantum field theory. The Euclidean cap specifies the domain on which the fields in the functional integral are defined, and by gluing two Euclidean caps together with a Lorentzian excursion in between, one obtains a Schwinger-Keldysh contour on which the functional integral computes expectation values in the states specified by the caps [26, 27]. Such expectation values may be obtained by computing the Euclidean correlation function and then continuing the operator insertions to the Lorentzian section.

[14]The linear-dilaton × time × S^1 coincides with the asymptotics of AdS_3 written in first-order variables, as explained in section 2.2.

JHEP10(2022)195

From the point of view of string theory, the Schwinger-Keldysh contour is now interpreted as the integration cycle in a complexification of the target space over which the worldsheet functional integral is evaluated. Note that it is imprecise to merely ask for a string amplitude in e.g. the black hole background — one must also specify a state in order to define a string perturbation theory. For example, one could ask for a string amplitude in AdS_3 in the vacuum state or in a thermal state; the Lorentzian section is the same in both cases, but the string perturbation theories are different. The state is fixed by the incoming and outgoing Euclidean segments of the target space Schwinger-Keldysh contour. Thus, the target space contour obtained by gluing together two copies of figure 1a produces string amplitudes for the black hole background in the HH state. Similarly, the contour obtained by gluing together two copies of figure 6a—prior to adding the condensate — computes amplitudes for string theory in $\mathbb{R}^{1,1} \cup \mathbb{R}^{1,1}$ in the TFD state, or $\mathbb{R}^{1,1} \times S^1 \cup \mathbb{R}^{1,1} \times S^1$ in the three-dimensional case.

The two-dimensional linear-dilaton black hole is asymptotically flat, and the simplest string amplitudes for the black hole in the HH state compute conventional scattering amplitudes for strings $\mathcal{O}_{jE}$ scattering off the horizon [25]. They are labeled by their energy E and linear-dilaton momentum $j \in \frac{1}{2} + i\mathbb{R}$, subject to the on-shell condition.[15] The energy spectrum is continuous at leading order in string perturbation theory, as is consistent with effective field theory in the black hole background. Such amplitudes may be obtained by continuation from cigar amplitudes of operators $\mathcal{O}_{jn}$ with momentum $n \to iE$ around the compact Euclidean time circle.[16] In doing so, one must continue from the discrete set of Matsubara frequencies n of the Euclidean theory to the continuous set of Lorentzian energies E, as is often necessary in thermal systems.

In three dimensions the continuation is in fact simpler. Because AdS is effectively a box, string amplitudes do not compute an S-matrix, but rather correlation functions of the dual CFT on the spacetime conformal boundary [28–31]. One may choose a basis of worldsheet vertex operators labeled by the point on the conformal boundary where a dual operator is inserted [32]. Then Lorentzian string amplitudes are obtained by continuation from Euclidean amplitudes in the usual sense of continuation of the dual CFT. For example, a vertex operator $\Phi_j(z, \bar{z}; \xi, \theta)$ of $SL(2, \mathbb{C})_k/SU(2)$ describing string theory in $EAdS_3$ in the spacetime vacuum state[17] is labeled by a point $(\xi, \theta) \in \mathbb{R} \times S^1$ on the Euclidean conformal boundary cylinder, where z is a worldsheet coordinate. A string amplitude of such operators computes a dual CFT correlation function with insertions at those points, and by continuing $\xi \to it$ to the Lorentzian section of the Schwinger-Keldysh contour, one obtains an expectation value of the dual CFT in the vacuum state.

Similarly, vertex operators of $\mathbb{Z}\backslash SL(2, \mathbb{C})_k/SU(2)$ may be labeled by a point on the spacetime conformal boundary T^2 of the EBTZ solid torus. A Euclidean string amplitude

[15] As well as a contribution h from the internal CFT, in general, and a left/right label depending from which asymptotically flat region the particle originates.

[16] More generally, the $SL(2, \mathbb{R})_k/U(1)$ CFT includes primaries $\mathcal{O}_{jnw}$ labeled by a third number w, related to the (non-conserved) winding number of S^1 at infinity. To compute a scattering amplitude of a string in the Lorentzian black hole one continues $\mathcal{O}_{j,n=iE,w=0}$.

[17] Once combined with an appropriate internal CFT to cancel the conformal anomaly.

JHEP10(2022)195

computes a correlation function of local operators inserted at those boundary points, and by continuing the insertions one obtains a string amplitude in the BTZ black hole in the HH state [33–35]. Above the Hawking-Page temperature, these amplitudes compute the dominant contribution to dual CFT expectation values in the TFD state.

Alternatively, one may Fourier transform the vertex operators from the boundary position basis to obtain eigenstates of the spacetime energy and momentum, analogous to the aforementioned operators in two dimensions. These correspond to the conventional modes of the spacetime effective field theory. Their energy spectrum is again continuous in BTZ in the HH state — and discrete in AdS_3 in the vacuum state. To directly compute the Lorentzian string amplitudes of such vertex operators requires performing the continuation from the Euclidean Matsubara frequencies, which may be more technically challenging because one is continuing from a discrete set of data. The amplitudes compute dual CFT expectation values of the modes of its local operators. Of course, one may alternatively compute a string amplitude in the boundary position basis where the continuation to Lorentzian signature is easy, and then Fourier transform the result to obtain an expectation value in the momentum basis.

In this way, cutting and continuing the dual descriptions of the $\mathrm{SL}(2,\mathbb{R})_k/\mathrm{U}(1)$ and $\mathbb{Z}\backslash\mathrm{SL}(2,\mathbb{C})_k/\mathrm{SU}(2)$ CFTs yield Schwinger-Keldysh contours for the ER = EPR dual string theories that we propose in this paper. On the ER side, one has string theory in the two or three-dimensional eternal black hole in the HH state. On the EPR side, one has string theory in the disconnected union of two copies of $\mathbb{R}^{1,1}$ or $\mathbb{R}^{1,1}\times\mathrm{S}^1$ in the TFD state, deformed by the sine-Liouville condensate. The condensate is the most subtle aspect of the continuation; it is built of strings that wind the Euclidean time circle, and therefore its interpretation in the Lorentzian continuation is not obvious.

In two dimensions, the condensate takes the form $V_{\mathrm{sL}} \propto W_+ + W_-$, where $W_\pm = e^{-2b_{\mathrm{sL}}\hat{r}}e^{\pm ik(\theta_{\mathrm{L}}-\theta_{\mathrm{R}})}$ are linear-dilaton $\times\,\mathrm{S}^1$ vertex operators for a string with unit winding around the Euclidean time circle θ, times a Liouville-like factor in the linear-dilaton direction $\hat{r}$ (figure 3b). The latter serves to reflect strings away from the strong-coupling region $\hat{r}\to-\infty$, where b_{sL} is a positive real number chosen such that these vertex operators are marginal. Let us treat the condensate as a large deformation of the free linear-dilaton $\times\,\mathrm{S}^1$ background; one obtains a series of W_+W_- insertions of the form $e^{-\int V_{\mathrm{sL}}} \sim \sum \frac{1}{(N!)^2}\left(\int W_+W_-\right)^N$.[18] Note that only paired operators W_+W_- contribute to the expansion due to the winding number conservation law of the undeformed cylinder. We emphasize that it is only after resumming the series that one recovers the black hole CFT.

Let us therefore consider the effect of a pair of W_+, W_- insertions in the Lorentzian continuation of the linear-dilaton $\times\,\mathrm{S}^1$ string theory. Let W_+ be inserted at the origin and W_- at the point-at-infinity on a Euclidean worldsheet CP^1. One typically fixes the worldsheet diffeomorphism and Weyl gauge redundancies in string theory by choosing a locally flat metric $\mathrm{d}s^2 = \mathrm{d}z\,\mathrm{d}\bar{z}$. Afterward, there remains a residual gauge redundancy given by conformal transformations. In free theories, or more generally in backgrounds with a

[18] This expansion is formal and requires regularization in the strong-coupling region. Our aim, however, is to give an abstract picture of the EPR string background, not a practical scheme for computing amplitudes.

JHEP10(2022)195

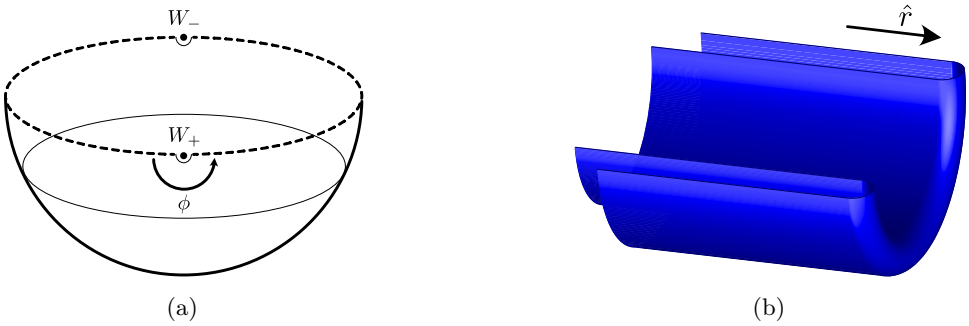

(a) (b)

Figure 7. *The TFD State of a Pair of Folded Strings.* With insertions of Euclidean time winding operators W_+, W_-, the worldsheet should be treated in angular quantization to discuss the continuation to Lorentzian target time. One foliates the worldsheet in radial lines, such as the two dashed semi-circles shown on the left, with the angular direction interpreted as Euclidean time. The resulting Hilbert space $\mathcal{H}_{+-}(\mathbb{R})$ lives on a line, labeled by asymptotic conditions associated to the operator insertions at either end. The functional integral over the halved worldsheet shown prepares the TFD state in two copies of $\mathcal{H}_{+-}(\mathbb{R})$. The asymptotic conditions for $W_\pm$ send $\hat{r} \to -\infty$ with winding ± 1. A schematic of the spacetime image of the halved worldsheet is shown on the right. In particular, the two dashed spatial slices map to the folded strings bounding the blue figure, emanating from the strong-coupling region.

time-translation isometry, one sometimes adopts the static gauge condition $\theta = \rho$ on-shell to fix the residual redundancy and obtain a target space picture, wherein the target time θ is set equal to the worldsheet radial coordinate ρ, where $z = e^{\rho + i\phi}$. Indeed, in the usual radial quantization, one interprets ρ as the worldsheet Euclidean time coordinate, and the spatial slices are circles centered at the origin. The functional integral over a disk with an operator inserted at the origin prepares the corresponding state in the CFT Hilbert space $\mathcal{H}(\mathrm{S}^1)$ on the boundary circle.

However, the gauge choice $\theta = \rho$ is incompatible with the operator insertion $W_+(0)$, which requires that $\theta \to \phi$ has winding one as $\rho \to -\infty$. Instead, one may adopt the angular gauge $\theta = \phi$, identifying the compact target time with the angular coordinate on the worldsheet. This suggests that in the neighborhood of a winding operator one should treat the worldsheet in angular quantization rather than the usual radial quantization. In this formulation, the worldsheet is foliated in radial lines rather than circles, and the angular direction ϕ running transverse to these spatial slices is defined as the Euclidean time. The Hilbert space $\mathcal{H}_{+-}(\mathbb{R})$ in this quantization scheme lives on a line, labeled by asymptotic conditions at either end associated to the insertions of W_+ and W_- there. When the worldsheet is cut in half across this Euclidean time circle as in figure 7a, the functional integral on the half-space prepares yet another TFD state, now valued in $\mathcal{H}_{+-}(\mathbb{R}) \otimes \mathcal{H}_{+-}(\mathbb{R})$.

Though less conventional than radial quantization, angular quantization is likely familiar in the context of the Unruh effect in Rindler spacetime. There, one considers a field theory on $\mathbb{R}^2$, again with the angular direction interpreted as Euclidean time (figure 8a). After the continuation one obtains the Rindler decomposition of Minkowski spacetime, with its coordinate horizon separating the left and right Rindler wedges (figure 8b). This coordinate horizon results in a quantization in a mixed state on a space with an asymptotic endpoint.

JHEP10(2022)195

(a) (b)

Figure 8. *Angular Quantization.* When $\mathbb{R}^2$ in polar coordinates (left) is continued with respect to the angular direction, the result is a wedge of the Rindler decomposition of Minkowski spacetime (right). With no operator insertions, the Euclidean functional integral over the half-plane prepares the Minkowski vacuum on the dashed line. In angular quantization, the Minkowski vacuum is identified with the TFD state in the two copies of the Hilbert space on the left and right Rindler wedges. The reduced density matrix in a single wedge is a thermal state at the Unruh temperature. To understand a Lorentzian string background with Euclidean time winding operator insertions, the neighborhood of the winding operator should be treated in angular quantization. The Hilbert space of angular quantization is a generalization of the Rindler Hilbert space, now labeled by the asymptotic condition imposed by the boundary operator.

With no insertions, the functional integral over the Euclidean half-space prepares the Minkowski vacuum, which may equivalently be understood as the TFD state in the product Hilbert space of the left and right Rindler wedges in angular quantization. The reduced density matrix in a single wedge is a thermal state, resulting in the Unruh effect, and the TFD state in the product Hilbert space is its purification.

The angular quantization that we propose is a generalization of the Rindler example, with operator insertions at one or both ends of the spatial slice fixing asymptotic conditions for the fields on the line. The asymptotic conditions for the marginal winding operators $W_\pm$ of the linear-dilaton $\times$ S^1 background that make up the sine-Liouville potential are[19]

$$\hat{r} \overset{\rho\to-\infty}{\longrightarrow} 2\alpha' b_{\mathrm{sL}} \rho \tag{1.1a}$$

$$\theta \overset{\rho\to-\infty}{\longrightarrow} \pm\phi. \tag{1.1b}$$

Since b_{sL} is positive, these asymptotic conditions map the worldsheet neighborhood of each $W_\pm$ insertion to the strong-coupling region of the target cylinder, with winding ± 1, as shown in figure 7b. In particular, the spatial slices at $\phi = 0$ and π that bound the diagram in figure 7a map to folded strings in spacetime at $\theta = 0$ and π that emanate from the strong-coupling region.[20] The Lorentzian interpretation of the pair of Euclidean time winding insertions is thus that, atop the disconnected union of linear-dilaton $\times$ time

[19] When inserted in the far past on the cylinder, the linear-dilaton asymptotic condition is modified to $\hat{r} \to 2\alpha'(b_{\mathrm{sL}} - Q/2)\rho$ due to the contribution from the background charge, where $Q = 1/\sqrt{\alpha'(k-2)}$ is the linear-dilaton slope. In the $k \to \infty$ limit, however, this contribution is sub-leading.

[20] This picture is somewhat formal in that there is no saddle for the linear-dilaton $\times$ S^1 theory plus the expanded condensate unless additional operators are inserted, due to the anomalous momentum conservation law. Moreover, to properly define string theory in this background, one should introduce a regulator to suppress the strong-coupling region, which will completely break the translation symmetry.

JHEP10(2022)195

backgrounds in the bulk TFD state, a pair of folded strings is added, themselves entangled in the worldsheet TFD state of angular quantization (figure 9a). After continuing[21] $\theta = it$ and $\phi = i\mathfrak{t}$, the folded string evolves forward in Lorentzian time $t = \mathfrak{t}$, as sketched in figure 6.[22]

Ideas relating Euclidean time winding operators and folded string solutions were previously explored in [36]. In that context, the folded strings emanated from the weak-coupling region. Here we extend the connection between Euclidean time winding operators and folded strings from the $c = 1$ analysis of [36, 37] to the true black hole regime of $k > 3$.

There remains to address an important issue of mutual locality that arises in computing Lorentzian string amplitudes in the EPR microstates that describe strings scattering off the background of entangled folded strings. In the ER description, scattering amplitudes in the HH state are obtained from cigar amplitudes with insertions $\mathcal{O}_{jn}$ by continuing from the discrete Matsubara frequencies n to the continuous Lorentzian energies $n \to iE$. One may perform the continuation at the level of the CFT correlation function, and then integrate over the moduli space to produce a Lorentzian string amplitude.

In the asymptotic cylinder region of the cigar, $\mathcal{O}_{jn}$ approaches a superposition of linear-dilaton $\times$ S^1 primaries. To compute a Euclidean amplitude in the sine-Liouville description, one would insert these limiting free-field operators in the sine-Liouville functional integral and integrate over the moduli space.

Upon attempting the same continuation $n \to iE$ in a linear-dilaton $\times\, \mathrm{S}^1$ correlator after expanding the sine-Liouville condensate, however, one will in general obtain a multi-valued function, the reason being that the Euclidean time winding insertions and the Lorentzian momentum operators are not mutually local. Namely, the OPE of winding $e^{\pm ik\tilde{\theta}(z,\bar{z})}$ and momentum $e^{in\theta(z,\bar{z})}$ operators of the compact boson is single-valued only for $n \in \mathbb{Z}$, which is the expected momentum quantization law. When these insertions approach one another, the correlation function behaves as $(z/\bar{z})^{\pm n/2} = e^{\pm in\phi}$, yielding $e^{\mp E\phi}$ after continuation and violating the periodicity of ϕ. Thus, the result is single-valued only on an infinite-sheeted cover of the worldsheet, over which the moduli integral would diverge in one direction or the other.

On the other hand, the Lorentzian string amplitude for each term in the expansion with a given number of winding insertions may be obtained by integrating the Euclidean correlation function over the moduli space, and only then continuing the Matsubara frequencies n to the Lorentzian energies E in the final answer. The question is how to evaluate the integral of a Lorentzian correlation function over the moduli, such that one obtains the same result. To do so, one must define the moduli integral along a deformed contour in a complexification of the moduli space on which the integral converges and the integrand is single-valued.

Even in the ER description — indeed, even in ordinary flat space string theory — the naive integral over moduli diverges in general, and should instead be defined by integrating over a deformed complex contour [38]. The prescription for ordinary operator insertions described in [38] is to cut out the neighborhood of each point in the original moduli space where two insertions collide and glue in the Lorentzian cylinder of radial quantization.

[21] Or $\theta = \pi + it_{\mathrm{L}}$ and $\phi = \pi + i\mathfrak{t}_{\mathrm{L}}$ on the opposite side of the TFD.

[22] For an ordinary insertion $e^{in\theta}$, on the other hand, the asymptotic condition $\theta \to -i\frac{\alpha'}{R^2}n\rho$ becomes $t \to E\mathfrak{t}$ after continuing $\theta = it$, $\rho = i\mathfrak{t}$, and $n = i\frac{R^2}{\alpha'}E$ in the usual sense of radial quantization.

JHEP10(2022)195

(a) (b)

Figure 9. *The Contour of Angular Quantization.* Near any pair of W_+, W_- insertions on the worldsheet of a linear-dilaton $\times$ S^1 string diagram, one may slice their neighborhood as shown on the left. The upper cap prepares a pair of folded strings in the TFD state of angular quantization, which is glued to the rest of the worldsheet below. In computing a string amplitude of linear-dilaton $\times$ time including Euclidean time winding insertions, one must choose a deformed contour of integration in evaluating the sum over moduli. On the right is sketched the contour used to evaluate the integral of a Lorentzian scattering operator. When the integrated insertion approaches another ordinary operator, the contour is deformed along the Lorentzian cylinder of radial quantization according to the prescription of [38]. When it approaches a winding operator, the Euclidean cap that prepared the TFD state of folded strings is replaced by the pair of Rindler diamonds shown and glued along the red zero-time slice. The radial deformation prevents two scattering insertions from colliding, while the angular deformation prohibits a scattering operator from looping around a winding operator.

To evaluate a Lorentzian string amplitude in the background of Euclidean time winding operators, we similarly propose that their neighborhood should be replaced by a Rindler wedge of angular quantization (figure 9b). In particular, continuing $\phi \to i\mathfrak{t}$ in the neighborhood where Euclidean winding and Lorentzian energy operators collide, the problematic limiting behavior $e^{\mp E\phi}$ is replaced by the single-valued and oscillatory measure $e^{\mp iE\mathfrak{t}}$.

In three dimensions, the situation is again even simpler when working in the basis of operators labeled by spacetime conformal boundary points. Then there is no violation of mutual locality between the sine-Liouville potential and vertex operators labeled by the target Lorentzian section. Of course, if one Fourier transforms to the momentum basis one must again employ the deformed contour of angular quantization in evaluating the sum over moduli, and the construction is similar to the preceding discussion in two dimensions. Likewise, the three-dimensional analog of the sine-Liouville potential again produces a condensate of folded strings entangled between the two disconnected copies of the asymptotic AdS_3 spacetimes.

Having established the necessary ingredients, the Lorentzian string dualities we propose now follow by continuation from the $SL(2,\mathbb{R})_k/U(1)$ and $\mathbb{Z}\backslash SL(2,\mathbb{C})_k/SU(2)$ CFT dualities. The weakly-coupled side (in the α' sense) is string theory in the connected two-dimensional linear-dilaton (or three-dimensional AdS) black hole in the HH state. The strongly-coupled side is string theory in the disconnected union of two copies of linear-dilaton $\times$ time (or linear-dilaton $\times$ time $\times$ S^1) in the bulk TFD state, with a condensate of pairs of

JHEP10(2022)195

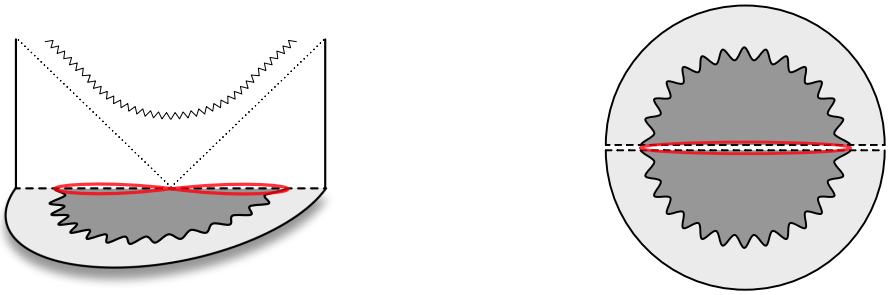

(a) (b)

Figure 10. *The Infinitesimal Duality.* When the $\mathrm{SL}(2,\mathbb{R})_k/\mathrm{U}(1)$ or $\mathbb{Z}\backslash\mathrm{SL}(2,\mathbb{C})_k/\mathrm{SU}(2)$ Euclidean black hole CFT is deformed by a marginal operator known as the sine-Liouville operator — so-called because its free-field limit is the sine-Liouville potential — a condensate of strings that wrap the Euclidean horizon is introduced (right). The red loop is a spatial slice of string, corresponding to the image of the dashed line in figure 7a bounding the worldsheet TFD state with a pair of winding insertions. It may be thought of as a pair of folded strings emanating from the horizon, contrasted with the disconnected folded strings emanating from the strong-coupling region in the EPR description (figure 6b and 7b). When continued to the Lorentzian ER string theory, one finds a pair of folded strings joined at the horizon bifurcation point in an entangled state. The deformation introduces a condensate of such strings, and the infinitesimal duality asserts that the same effect is described by shifting the constant mode of the dilaton. In both descriptions the mass of the black hole is in turn shifted.

entangled folded strings emanating from the strong-coupling boundaries, themselves in the worldsheet TFD state of angular quantization.[23] By expanding the condensate, one obtains a superposition of entangled disconnected microstates. The dualities are therefore explicit examples of ER = EPR, each relating a connected, two-sided spacetime to an entangled superposition of disconnected geometries.

We point out that we will not construct string theories for the individual disconnected microstates, but only for the thermal gas of such states that constitutes the EPR description of the black hole. It would however be very interesting to better understand these individual microstates in future work. Note that in contrast to microstates of extremal black holes such as those constructed in [39], the typical solutions in our context will be time dependent. Moreover, one might expect the backreaction of the many folded strings in a generic microstate to lead to the formation of a black hole, and it would therefore be interesting if one could demonstrate that a horizon forms around the folded strings in typical disconnected geometries. One open question is the extent to which perturbative string techniques can be used to characterize these solutions, given the presence of a strongly coupled region in the deep interior.

Finally, we will also describe an "infinitesimal" version of each of these dualities that relates two equivalent descriptions in the ER string theory of a marginal deformation that

[23] By continuing the duality of $\mathrm{SL}(2,\mathbb{C})_k/\mathrm{SU}(2)$ with respect to the same cycle, but prior to the $\mathbb{Z}$ quotient that makes the Euclidean black hole, one likewise obtains an even simpler duality between string theory in a connected Rindler decomposition of AdS_3 and the analogous EPR theory in linear-dilaton $\times$ time $\times\,\mathbb{R}$. The quotient replaces the ER side with the black hole and compactifies $\mathbb{R}$ to S^1 on the EPR side.

JHEP10(2022)195

shifts the mass of the black hole. The marginal operator is known as the sine-Liouville operator, whose limiting form in the weak-coupling region is the sine-Liouville potential. In one description of this operator, the deformation shifts the constant mode of the dilaton. In the dual description, the asymptotic condition for the sine-Liouville operator sends the string to the horizon with unit winding [40], and so the deformation introduces a condensate of horizon-wrapping strings.[24] The identification of the two descriptions is based on an isomorphism of the corresponding CFT states discussed in [41]. Whereas the condensate of Euclidean time winding strings as a deformation of the free linear-dilaton $\times$ $S^1(\times S^1)$ produced in the Lorentzian continuation pairs of disconnected folded strings emanating from the strong-coupling boundaries (figure 6), in the ER description of the infinitesimal duality the perturbation introduces folded strings joined at the horizon bifurcation point (figure 10). They may be thought of as the fundamental strings that make up the black hole, whose mass is in turn shifted under the deformation.

These horizon-bound strings, and their strong-coupling-bound EPR counterparts, resemble the open strings conjectured in [42, 43] to account for the black hole entropy. It would be very interesting to understand how to compute the entropy in these string backgrounds. Our work may also be relevant to understanding entanglement entropy in string theory, related to ideas discussed in [44, 45].

Recent potentially related work involving a condensate of folded strings behind the black hole horizon and the Lorentzian continuation of the FZZ duality has appeared in [46–53]. It would also be very interesting to establish the precise connection between these results.

The remainder of the paper is organized as follows. In section 2 we review the Euclidean FZZ duality of $SL(2,\mathbb{R})_k/U(1)$, and we propose the new duality of $SL(2,\mathbb{C})_k/SU(2)$ and $\mathbb{Z}\backslash SL(2,\mathbb{C})_k/SU(2)$. We also describe here the infinitesimal interpretation of these Euclidean dualities. In section 3 we discuss the formulation of string perturbation theory in various states using Schwinger-Keldysh contours in a complexified spacetime, which enables us to define the string theories in the TFD and HH states that appear in the Lorentzian dualities that we propose in section 4. There, we formulate the Lorentzian string dualities, and explain via angular quantization the Lorentzian interpretation of the Euclidean time winding operators, and the corresponding deformation of the moduli space integration contour.

The fairly substantial length of the paper is in part due to an effort to make it self-contained. Expert readers may wish to skip our review of the FZZ duality (section 2.1) and the formulation of string perturbation theory in AdS_3 in its vacuum state (sections 2.2.1 and 3.2.1). The discussion of Schwinger-Keldysh contours for string theory in thermofield-double or Hartle-Hawking states may also be more-or-less known to experts (section 3.2.2–3.2.3). The principal new ingredients that we discuss in order to establish our examples of ER = EPR include the uplifted duality of the $SL(2,\mathbb{C})_k/SU(2)$ and $\mathbb{Z}\backslash SL(2,\mathbb{C})_k/SU(2)$ CFTs, the Lorentzian interpretation of Euclidean time winding operators in terms of folded strings in the thermofield-double state of angular quantization, the deformed contour of integration for the sum over moduli in the background of Euclidean time winding operators, and the infinitesimal interpretation of the various dualities in terms of conformal

[24] Note that a single abstract operator may admit multiple semi-classical descriptions via asymptotic conditions.

JHEP10(2022)195

perturbation theory.

2 The Euclidean dualities

In this section, we review the FZZ duality of the two-dimensional Euclidean black hole CFT $\mathrm{SL}(2,\mathbb{R})_k/\mathrm{U}(1)$, and we propose an uplifted three-dimensional duality of the asymptotically Euclidean AdS_3 black hole $\mathbb{Z}\backslash\mathrm{SL}(2,\mathbb{C})_k/\mathrm{SU}(2)$ and its Euclidean AdS_3 parent $\mathrm{SL}(2,\mathbb{C})_k/\mathrm{SU}(2)$. We also discuss an infinitesimal interpretation of each duality that relates two semi-classical descriptions of a conformal perturbation that shifts the mass of the black hole.

2.1 The FZZ duality

We begin[25] by reviewing the two-dimensional FZZ duality [15, 16], which relates two Lagrangian descriptions of the $\mathrm{SL}(2,\mathbb{R})_k/\mathrm{U}(1)$ CFT. This CFT is a coset of the $\mathrm{SL}(2,\mathbb{R})_k$ WZW model. The group $\mathrm{SL}(2,\mathbb{R})$ is equivalent to Lorentzian AdS_3, and the WZW model describes a string propagating on that manifold, with the WZW level k corresponding to the AdS length, $l^2_{\mathrm{AdS}} = k l_{\mathrm{s}}^2$ [28–32, 54–57]. AdS_3 may be described as a solid cylinder with time running along its length (figure 4a), and the coset is defined by gauging this timelike isometry. The result is the unitary $\mathrm{SL}(2,\mathbb{R})_k/\mathrm{U}(1)$ CFT, of central charge

$$c = \frac{3k}{k-2} - 1, \tag{2.1}$$

the first term being the central charge of the $\mathrm{SL}(2,\mathbb{R})_k$ WZW model, less one for the quotient. k is a real number greater than two, which need not be an integer.

2.1.1 The cigar background and the 2D black hole

The $\mathrm{SL}(2,\mathbb{R})_k/\mathrm{U}(1)$ coset is remarkable because it describes, for large k, a string in a Euclidean black hole of two-dimensional dilaton-gravity [14]. In that limit, it admits a weakly-coupled Lagrangian description in terms of the following sigma-model metric and dilaton:

$$\mathrm{d}s^2 = \alpha' k \left(\mathrm{d}r^2 + \tanh^2(r)\mathrm{d}\theta^2\right) \tag{2.2a}$$

$$\Phi = -\log\cosh(r) + \Phi_0. \tag{2.2b}$$

We will recall how this background follows by gauging the $\mathrm{SL}(2,\mathbb{R})_k$ WZW model in section 2.2.1. The action on a closed worldsheet Σ of metric h is

$$S_{\mathrm{cigar}} = \frac{k}{4\pi}\int_\Sigma \mathrm{d}^2\sigma\,\sqrt{h}\left\{(\nabla r)^2 + \tanh^2(r)(\nabla\theta)^2 + \frac{1}{k}\mathcal{R}[h]\left(-\log\cosh r + \Phi_0\right)\right\}. \tag{2.3}$$

$r \in [0,\infty)$ and $\theta \sim \theta + 2\pi$ are coordinates on a target space with the topology of a disk. In the neighborhood of the origin, the geometry is simply $\mathbb{R}^2$ in polar coordinates,

$$\mathrm{d}s^2 \to \alpha' k\left(\mathrm{d}r^2 + r^2\mathrm{d}\theta^2\right) + \mathcal{O}\left(r^3\right) \tag{2.4a}$$

$$\Phi \to \Phi_0 + \mathcal{O}\left(r^2\right), \tag{2.4b}$$

[25] Readers familiar with the FZZ duality may wish to skip to section 2.2.

JHEP10(2022)195

while for large r the geometry approaches a cylinder of radius $\sqrt{\alpha' k}$:

$$\mathrm{d}s^2 \to \alpha' k(\mathrm{d}r^2 + \mathrm{d}\theta^2) + \mathcal{O}\left(e^{-2r}\right) \tag{2.5a}$$

$$\Phi \to -r + \mathcal{O}(1). \tag{2.5b}$$

The target space therefore resembles a cigar (figure 3a), with an asymptotic cylinder at large r that caps off at the tip $r = 0$, hence the background is also known as the cigar sigma-model. The leading $\mathcal{O}(e^{-2r})$ correction to the metric is $-4\alpha' k e^{-2r}\mathrm{d}\theta^2$, and the corresponding operator $e^{-2r}\partial\theta\bar{\partial}\theta$ is the leading correction to the cylinder background as one heads back toward finite r. It is important to note that although the asymptotic cylinder suggests the sigma-model has a topological winding number, there is no conserved charge because a string that appears to wind the cylinder can unwind at the tip.

The cigar is large and weakly curved for large k,

$$\mathcal{R}[g] = \frac{4}{\cosh^2(r)}\frac{1}{\alpha' k}, \tag{2.6}$$

and the sigma-model is weakly coupled in the α' sense. The string coupling $g_{\mathrm{s}} = e^{\Phi}$, meanwhile, is determined by the dilaton eq. (2.2b). The unusual profile $\Phi(r)$ ensures conformal invariance of the curved background at leading order,

$$\beta_{IJ} = \alpha'\left(R_{IJ} + 2\nabla_I\nabla_J\Phi\right) + \mathcal{O}\left(\alpha'^2\right) = \mathcal{O}\left(\alpha'^2\right). \tag{2.7}$$

$\Phi(r)$ is a monotonically decreasing function, with the constant Φ_0 setting its maximal value at the tip of the cigar, $\Phi(0) = \Phi_0$. At large r it falls off linearly. The string coupling therefore attains its maximum e^{Φ_0} at the tip and decays to zero at large r, which we refer to as the weak-coupling region. The parameter Φ_0 is a modulus of the theory. It reflects the usual freedom to shift the dilaton by a constant, the only effect being to shift the action by $\Phi_0\chi$, with χ the Euler characteristic of Σ.

From the spacetime perspective, the cigar background (g, Φ) is a solution of two-dimensional dilaton-gravity,

$$S_{\text{spacetime}} = -\frac{1}{2\kappa^2}\int \mathrm{d}r\mathrm{d}\theta\sqrt{g}\, e^{-2\Phi}\left(\mathcal{R}[g] + 4\left(\nabla\Phi\right)^2 + \frac{4}{\alpha' k}\right), \tag{2.8}$$

whose equations of motion may be written

$$R_{IJ} + 2\nabla_I\nabla_J\Phi = 0 \tag{2.9a}$$

$$\left(\nabla\Phi\right)^2 - \frac{1}{2}\nabla^2\Phi - \frac{1}{\alpha' k} = 0. \tag{2.9b}$$

The first is again the leading order beta function equation from the perspective of the worldsheet. The second computes the central charge $c = 2 + 6\alpha'\left(\left(\nabla\Phi\right)^2 - \frac{1}{2}\nabla^2\Phi\right)$ at large k, $\frac{3k}{k-2} - 1 = 2 + \frac{6}{k} + \mathcal{O}(k^{-2})$. At finite k, both the metric and dilaton receive corrections [25].

With θ interpreted as the Euclidean time coordinate, this solution describes a Euclidean black hole [14]. The horizon bifurcation point is found at the tip where the θ circle shrinks. The geometry in that neighborhood is $\mathbb{R}^2$ (eq. (2.4a)), whose continuation with respect to

JHEP10(2022)195

angular Euclidean time yields Rindler spacetime — the near-horizon geometry of the black hole. Continuing $\theta = it$ gives the Lorentzian metric in the right wedge:

$$\mathrm{d}s^2 = \alpha' k \left(\mathrm{d}r^2 - \tanh^2(r) \mathrm{d}t^2 \right). \tag{2.10}$$

The geometry approaches flat space at large r, $\mathrm{d}s^2 \to \alpha' k(\mathrm{d}r^2 - \mathrm{d}t^2)$, together with the asymptotically linear dilaton. This coordinate patch ends at the horizon $r = 0$, where the coefficient of $\mathrm{d}t^2$ vanishes. The complete, two-sided black hole may be described in Kruskal coordinates

$$u = e^{-t} \sinh(r), \qquad v = -e^{t} \sinh(r), \tag{2.11}$$

in terms of which the metric reads

$$\mathrm{d}s^2 = \alpha' k \frac{\mathrm{d}u\, \mathrm{d}v}{uv - 1}, \tag{2.12}$$

and the dilaton is $\Phi = -\frac{1}{2}\log(1 - uv) + \Phi_0$. The extended black hole geometry is pictured in figure 5a. There is of course a second asymptotic boundary in the left wedge. The singularities are found at $uv = 1$. Note that the dilaton and string coupling also diverge there. The mass of the black hole is [14]

$$M = \frac{1}{\sqrt{\alpha' k}} e^{-2\Phi_0}. \tag{2.13}$$

Returning to the Euclidean theory, in the next sub-section we enumerate the spectrum of the $\mathrm{SL}(2,\mathbb{R})_k/\mathrm{U}(1)$ CFT, after which we discuss the FZZ dual description.

2.1.2 $\mathbf{SL(2,\mathbb{R})_k/U(1)}$ spectrum

Above we have focused on the large k limit where the cigar sigma-model is weakly coupled, but thanks to its relation to the $\mathrm{SL}(2,\mathbb{R})_k$ WZW model via the coset construction, which we review in section 2.2.1, the exact spectrum of the $\mathrm{SL}(2,\mathbb{R})_k/\mathrm{U}(1)$ CFT is known [25, 54, 58]. Its Virasoro primaries $\mathcal{O}_{jnw}(z,\bar{z})$ are labeled by integers n and w and a complex number j, taking the following values:

$$(i) \qquad j = \frac{1}{2}(1 + is), \quad s \in \mathbb{R}_+ \tag{2.14a}$$

$$(ii) \qquad j_N = \frac{k|w| - |n|}{2} - N \in \left(\frac{1}{2}, \frac{k-1}{2} \right), \quad N \in \mathbb{N}, \tag{2.14b}$$

and carrying conformal weights

$$h_{jnw} = -\frac{j(j-1)}{k-2} + \frac{(n - kw)^2}{4k}, \qquad \bar{h}_{jnw} = -\frac{j(j-1)}{k-2} + \frac{(n + kw)^2}{4k}. \tag{2.15}$$

These two sets are referred to as the complex and real branches of primaries based on the value of j. The complex branch primaries correspond to delta-function normalizable scattering states on the cigar with momentum s, while the real branch primaries with $j = j_N$ correspond to bound states living at the tip. The upper bound $j_N < \frac{k-1}{2}$ ensures

JHEP10(2022)195

positivity of the weights $h_{j_N nw}$, while the lower bound $j_N > \frac{1}{2}$ ensures normalizability of the wavefunctions. In all cases the spin $h_{jnw} - \bar{h}_{jnw} = -nw$ is appropriately quantized. One may also consider the continuation of j to general complex values, including real branch operators for which j is not valued in the discrete set j_N. The latter map to non-normalizable states.

Since the cigar sigma-model approaches a free linear-dilaton $\times$ S^1 background at large r (eq. (2.5)), the abstract primaries $\mathcal{O}_{jnw}$ may be expanded in free-field primaries in that limit. To do so it is convenient to define canonically normalized coordinates,

$$\hat{r} = \frac{1}{Q} r, \qquad \hat{\theta} = \sqrt{\alpha' k}\,\theta, \tag{2.16}$$

where Q is evidently given by $1/\sqrt{\alpha' k}$ in the large k limit. However, at finite k it is corrected to [25]

$$Q = \frac{1}{\sqrt{\alpha'(k-2)}}, \tag{2.17}$$

and we use the exact value here so that we need not assume k is large.[26] Note also that $\hat{\theta}$ is periodic in $2\pi\sqrt{\alpha' k}$. In the rescaled coordinates the asymptotic background is

$$\mathrm{d}s^2 \overset{\hat{r}\to\infty}{\longrightarrow} \mathrm{d}\hat{r}^2 + \mathrm{d}\hat{\theta}^2 \tag{2.18a}$$

$$\Phi \overset{\hat{r}\to\infty}{\longrightarrow} -Q\hat{r}. \tag{2.18b}$$

The Virasoro primaries of this free linear-dilaton $\times$ S^1 theory, considered in its own right with $\hat{r}$ permitted to range over the entire real line, may be written

$$\mathcal{V}_{\alpha p_{\mathrm{L}} p_{\mathrm{R}}}(z,\bar{z}) = e^{-2\alpha\hat{r}(z,\bar{z})} e^{i p_{\mathrm{L}} \hat{\theta}_{\mathrm{L}}(z) + i p_{\mathrm{R}} \hat{\theta}_{\mathrm{R}}(\bar{z})}. \tag{2.19}$$

p_{L} and p_{R} are valued in the lattice

$$p_{\mathrm{L}} = \frac{n}{\sqrt{\alpha' k}} - \sqrt{\frac{k}{\alpha'}}\, w, \qquad p_{\mathrm{R}} = \frac{n}{\sqrt{\alpha' k}} + \sqrt{\frac{k}{\alpha'}}\, w, \qquad n, w \in \mathbb{Z}, \tag{2.20}$$

where n is the momentum number around the cylinder and w is minus the winding number.[27] The linear-dilaton momentum α may be continued to a general complex number, and in a correlation function of primaries it satisfies the anomalous conservation law

$$\sum_j \alpha_j = \frac{1}{2} Q \chi, \tag{2.21}$$

with χ the Euler characteristic of the worldsheet. These primaries carry conformal weights

$$h_{\alpha p_{\mathrm{L}} p_{\mathrm{R}}} = \alpha'\alpha(Q-\alpha) + \alpha' \frac{p_{\mathrm{L}}^2}{4}, \qquad \bar{h}_{\alpha p_{\mathrm{L}} p_{\mathrm{R}}} = \alpha'\alpha(Q-\alpha) + \alpha' \frac{p_{\mathrm{R}}^2}{4}, \tag{2.22}$$

[26] That is, the k-corrected background of [25] still approaches the linear-dilaton $\times$ S^1 background at large r, but with a modified scaling in the r direction: $\mathrm{d}s^2 \to \alpha'(k-2)\mathrm{d}r^2 + \alpha' k \mathrm{d}\theta^2$.

[27] We let w denote the negative of the winding number so that it coincides with the spectral-flow number in $\mathrm{SL}(2,\mathbb{R})_k$, as explained in section 2.2.1.

JHEP10(2022)195

with respect to the holomorphic stress-tensor

$$T(z) = -\frac{1}{\alpha'}(\partial\hat{r})^2 - Q\partial^2\hat{r} - \frac{1}{\alpha'}(\partial\hat{\theta})^2 \tag{2.23}$$

and its anti-holomorphic counterpart. The central charge of the Virasoro algebra is $c_{\mathrm{LD}\times\mathrm{S}^1} = 2 + 6\alpha' Q^2$, which reproduces the exact central charge of the coset eq. (2.1) using eq. (2.17).

In the asymptotic region the CFT primary $\mathcal{O}_{jnw}$ may then be expanded in the free-field primaries $\mathcal{V}_{\alpha p_{\mathrm{L}} p_{\mathrm{R}}}$ [25]:

$$\mathcal{O}_{jnw} \overset{\hat{r}\to\infty}{\longrightarrow} \left(e^{-2Q(1-j)\hat{r}} + R(j,n,w)e^{-2Qj\hat{r}}\right) e^{ip_{\mathrm{L}}\hat{\theta}_{\mathrm{L}} + ip_{\mathrm{R}}\hat{\theta}_{\mathrm{R}}}. \tag{2.24}$$

p_{L} and p_{R} are as in eq. (2.20); namely, the operator labels n and $-w$ correspond to the momentum and winding numbers around the asymptotic cylinder. j is meanwhile related to the asymptotic linear-dilaton momentum. $R(j,n,w)$ is the reflection coefficient [31, 32, 59]:

$$\begin{aligned} R(j,n,w) = (\nu(k))^{2j-1} &\frac{\Gamma\left(1-\frac{2j-1}{k-2}\right)}{\Gamma\left(1+\frac{2j-1}{k-2}\right)} \\ &\times 4^{2j-1}\frac{\Gamma(1-2j)}{\Gamma(2j-1)}\frac{\Gamma\left(j+\frac{|n|-kw}{2}\right)\Gamma\left(j+\frac{|n|+kw}{2}\right)}{\Gamma\left(1-j+\frac{|n|-kw}{2}\right)\Gamma\left(1-j+\frac{|n|+kw}{2}\right)}. \end{aligned} \tag{2.25}$$

Semi-classically, R is the amplitude for a string sent from the weak-coupling region to reflect and return to infinity. As an abstract CFT quantity, it characterizes a redundancy in the space of CFT operators $\mathcal{O}_{jnw}$ when analytically continued to the complex j-plane: operators labeled by j and $1-j$ are identical, up to rescaling by the reflection coefficient. To avoid double-counting operators, one restricts the domain to $\mathrm{Re}(j) > \frac{1}{2}$ or $j \in \frac{1}{2} + i\mathbb{R}_+$ as in eq. (2.14). R satisfies $R(1-j,n,w)R(j,n,w) = 1$. $\nu(k)$ is a convention-dependent function of k, but not of j.

The zero-mode wavefunction of the state prepared by $\mathcal{O}_{jnw}$ may likewise be expanded at large $\hat{r}$. The radial wavefunction differs from the operator by a factor of $e^{-\Phi} \to e^{Q\hat{r}}$ due to the dilaton's coupling to curvature:[28]

$$\Psi_{jnw}(\hat{r}) \underset{\propto}{\overset{\hat{r}\to\infty}{\longrightarrow}} e^{2Q\left(j-\frac{1}{2}\right)\hat{r}} + R(j,n,w)e^{-2Q\left(j-\frac{1}{2}\right)\hat{r}}. \tag{2.26}$$

With $j \in \frac{1}{2} + i\mathbb{R}_+$, both exponentials are oscillatory, and one obtains a delta-function normalizable state. These are the scattering states of eq. (2.14a), the two terms in the asymptotic wavefunction describing the incoming and reflected waves at infinity. The asymptotic operator is identified with the linear-dilaton primary $e^{-2\alpha\hat{r}}$ with $\alpha = Q(1-j)$

[28] With the cylinder metric on S^2, $\mathrm{d}s^2 = \frac{\mathrm{d}z\mathrm{d}\bar{z}}{z\bar{z}}$, the scalar curvature $\mathcal{R}[h] = \frac{4\pi}{\sqrt{h}}\left(\delta(z,\bar{z}) + \delta(z-z_\infty, \bar{z}-\bar{z}_\infty)\right)$ is singular at the two poles. Then the effect of the dilaton coupling to curvature $e^{-\frac{1}{4\pi}\int \mathrm{d}^2\sigma\sqrt{h}\mathcal{R}[h]\Phi}$ is to insert so called background-charge operators $e^{-\Phi}$ at the ends of the cylinder which contribute to the wavefunction. See e.g. [40] for a review.

JHEP10(2022)195

plus its reflection $e^{-2(Q-\alpha)\hat{r}}$, together with the compact boson primary of momentum n and winding $-w$. The corresponding free-field weights (eq. (2.22)), which are invariant under $\alpha \to Q-\alpha$, reproduce the exact weights (eq. (2.15)).

Away from the complex branch, the first exponential in eqs. (2.24) and (2.26) dominates the second for $\mathrm{Re}(j) > \frac{1}{2}$. Then, generically, the operator approaches $\mathcal{V}_{\alpha p_{\mathrm{L}} p_{\mathrm{R}}}$ with $\alpha = Q(1-j)$ at weak coupling, the wavefunction diverges exponentially, and the associated state is non-normalizable. However, at the discrete values $j = j_N$ of eq. (2.14b), $R(j_N, n, w)$ is singular due to one of the two Gamma functions $\Gamma\left(j + \frac{|n| \pm kw}{2}\right)$. Then it is the reflected term $e^{-2Qj_N\hat{r}}$ of eq. (2.24) that dominates in the asymptotic region, and the radial wavefunction decays:

$$\frac{1}{R}\Psi_{j_N n w}(\hat{r}) \overset{\hat{r}\to\infty}{\underset{\propto}{\longrightarrow}} e^{-2Q\left(j_N - \frac{1}{2}\right)\hat{r}}. \tag{2.27}$$

In this way, one finds a discrete spectrum of normalizable bound states on eq. (2.14b), the lower bound $j_N > \frac{1}{2}$ ensuring the wavefunction decays at infinity.

The simplest bound states have $n = 0$, $w = \mp 1$, and $j = \frac{k}{2} - 1$.[29] The asymptotic form of these operators, which we will denote by $\mathcal{W}_{\pm}$, is

$$\mathcal{W}_{\pm} \equiv \frac{1}{R}\mathcal{O}_{j=\frac{k}{2}-1, n=0, w=\mp 1} \overset{\hat{r}\to\infty}{\longrightarrow} e^{-\sqrt{\frac{k-2}{\alpha'}}\hat{r}} e^{\pm i\sqrt{\frac{k}{\alpha'}}(\hat{\theta}_{\mathrm{L}} - \hat{\theta}_{\mathrm{R}})}, \tag{2.28}$$

with radial wavefunction $\Psi_{\pm}(\hat{r}) \to e^{-Q(k-3)\hat{r}}$. Their sum,

$$\mathcal{O}_{\mathrm{sL}} \equiv \mathcal{W}_{+} + \mathcal{W}_{-}, \tag{2.29}$$

is called the sine-Liouville operator [41], and will be important in what follows. It is of conformal weight $(1,1)$, and one may therefore consider the effect of deforming the CFT by this operator, which we will take up in section 2.3. The wavefunction is normalizable for $k > 3$, consistent with the lower bound $j > \frac{1}{2}$.

Finally, we note for later use the asymptotic conditions associated to these operators [40, 60, 61]. Beginning with the free theory, when $\mathcal{V}_{\alpha p_{\mathrm{L}} p_{\mathrm{R}}}$ is inserted in the functional integral it adds a source term to free the equations of motion. The solutions in the neighborhood of the source inserted in the far past on the cylinder are the Green functions[30]

$$\hat{r}(\rho, \phi) \overset{\rho\to-\infty}{\longrightarrow} 2\alpha'\left(\alpha - \frac{Q}{2}\right)\rho + \mathcal{O}(1) \tag{2.30a}$$

$$\hat{\theta}(\rho, \phi) \overset{\rho\to-\infty}{\longrightarrow} -i\sqrt{\frac{\alpha'}{k}}n\rho - \sqrt{\alpha' k}w\phi + \mathcal{O}(1), \tag{2.30b}$$

where $z = e^{\rho + i\phi}$. These asymptotic conditions specify how the fields behave as one approaches the operator insertion point on the worldsheet. For $\mathrm{Re}(\alpha) < \frac{Q}{2}$ the asymptotic condition maps the insertion point to the weak-coupling region $\mathrm{Re}(\hat{r}) \to \infty$, while for $\mathrm{Re}(\alpha) > \frac{Q}{2}$ it is mapped to the strong-coupling region $\mathrm{Re}(\hat{r}) \to -\infty$ where $g_{\mathrm{s}} = e^{-Q\hat{r}}$

[29] Note that the set eq. (2.14b) is empty for $w = 0$, consistent with the fact that there are no normalizable solutions of the Laplace equation on the cigar.

[30] The shift $\alpha \to \alpha - \frac{Q}{2}$ in eq. (2.30a) is due to the background charge at the end of the cylinder. See Ft. 28.

JHEP10(2022)195

diverges. The zero-mode wavefunction $\Psi(\hat{r}) = e^{2(\frac{Q}{2}-\alpha)\hat{r}}$ correspondingly diverges at weak or strong coupling depending on the sign of $\mathrm{Re}(\alpha) - \frac{Q}{2}$.

In the cigar, meanwhile, for generic $\mathrm{Re}(j) > \frac{1}{2}$ the coset primary $\mathcal{O}_{jnw}$ approaches the free-field primary $\mathcal{V}_{\alpha p_{\mathrm{L}} p_{\mathrm{R}}}$ in the weak-coupling region, where $\alpha = Q(1-j)$ satisfies $\mathrm{Re}(\alpha) < \frac{Q}{2}$. Then the neighborhood of the insertion is mapped to the asymptotic cylinder region where the curvature corrections are sub-leading, and the free-field solution is self-consistent. The asymptotic condition describing such an operator is thus as in the free theory, eq. (2.30) with $\alpha = Q(1-j)$. Complex branch operators may similarly be understood by deforming $j \to j + \varepsilon$.

On the bound state spectrum $j = j_N$, however, we have seen that the asymptotic linear-dilaton momentum of $\mathcal{O}_{jnw}$ is instead $\alpha = Qj$. Now $\alpha > \frac{Q}{2}$, and the free-field asymptotic condition would send $\hat{r} \to -\infty$. In this case the string is mapped out of the free-field region, where the curvature corrections from the cigar are important, and eq. (2.30) is no longer a self-consistent solution of the cigar equations of motion.

Since the neighborhood of a bound state insertion is not mapped to the weak-coupling region, the limiting form eq. (2.24) of the operator is insufficient to determine the behavior of the string. The radial dependence of the operator on the full cigar was determined in [25]. For example, for the bound states $\mathcal{W}_{\pm}$,

$$\mathcal{W}_{\pm} \propto \left(\sinh^2(r) - \frac{1}{k-2}\right) \mathrm{sech}^k(r). \tag{2.31}$$

In [40] we found the associated asymptotic conditions:

$$r \overset{\rho\to-\infty}{\longrightarrow} e^{\rho} \tag{2.32a}$$

$$\theta \overset{\rho\to-\infty}{\longrightarrow} \pm\phi. \tag{2.32b}$$

Thus, in the neighborhood of the bound state insertions $\mathcal{W}_{\pm}$, the string asymptotically wraps the tip of the cigar with winding ± 1.

2.1.3 The dual sine-Liouville background

Having reviewed the spectrum of the $\mathrm{SL}(2,\mathbb{R})_k/\mathrm{U}(1)$ CFT and its description in terms of the cigar sigma-model at large k, we now come to the dual description of Fateev, Zamolodchikov, and Zamolodchikov [15, 16].

We have seen that the cigar asymptotes to the free linear-dilaton $\times\, \mathrm{S}^1$ background at large $\hat{r}$ (eq. (2.18)). The full linear-dilaton background, with $\hat{r}$ permitted to range over the whole real line, is not a unitary CFT or a well-defined string background. As a CFT, the operator product does not close on the space of delta-function normalizable states (for which $\alpha \in \frac{Q}{2} + i\mathbb{R}$), and as a string background the string coupling $g_{\mathrm{s}} = e^{-Q\hat{r}}$ diverges as $\hat{r} \to -\infty$.

In the cigar background, this strong-coupling region is eliminated by ending the geometry at $r = 0$. Another familiar way of regulating the free linear dilaton is to turn on a potential $V_{\mathrm{L}} \propto e^{-2b_{\mathrm{L}}\hat{r}}$ that serves as a barrier, suppressing string configurations which extend too

JHEP10(2022)195

deeply into the strong-coupling region. The linear-dilaton momentum $b_{\rm L}$ is chosen such that the potential is of weight $(1,1)$: $\alpha' b_{\rm L}(Q-b_{\rm L})=1$. The result is the Liouville CFT, together with the free compact boson.

The cigar and Liouville $\times$ S^1 backgrounds are identical at large $\hat{r}$ and reproduce the same central charge (eq. (2.1)). One might ask if they are dual descriptions of the same CFT. The answer is no, as is clear, for example, from the fact that the Liouville $\times$ S^1 theory conserves the string winding number around the cylinder, which is broken in the cigar.[31] There is, however, a close relative of the Liouville $\times$ S^1 background, called sine-Liouville, that is dual to the cigar, and this is the content of the FZZ duality.

In sine-Liouville, the linear-dilaton$\times\mathrm{S}^1$ is instead deformed by $V_{\rm sL}\propto e^{-2b_{\rm sL}\hat{r}}\mathrm{Re}\, e^{i\sqrt{\frac{k}{\alpha'}}(\hat{\theta}_{\rm L}-\hat{\theta}_{\rm R})}$. The potential consists of a Liouville-like radial factor $e^{-2b_{\rm sL}\hat{r}}$, together with the unit-winding operator around the S^1 direction. The presence of the winding operator explicitly breaks the winding number conservation law of the free theory, consistent with winding non-conservation in the cigar. The momentum of the linear-dilaton factor,

$$b_{\rm sL}=\frac{1}{2}\sqrt{\frac{k-2}{\alpha'}}, \tag{2.33}$$

is again chosen such that the potential is weight $(1,1)$,

$$\alpha' b_{\rm sL}(Q-b_{\rm sL})+\frac{k}{4}=1, \tag{2.34}$$

$k/4$ being the contribution of the unit-winding operator. At large $\hat{r}$, the potential decays and one recovers the same asymptotic linear-dilaton $\times$ S^1 theory as for the cigar. One thinks of the sine-Liouville background as being built up of a condensate of winding strings on top of the cylinder, as pictured in figure 3b. The dual description of the coset is best[32] near $k=2$, where $b_{\rm sL}$ is small. At large k it is a strongly-coupled description of the CFT.

The sine-Liouville action on a closed worldsheet Σ is thus

$$S_{\rm sL}=\frac{1}{4\pi\alpha'}\int_\Sigma \mathrm{d}^2\sigma\sqrt{h}\left\{(\nabla\hat{r})^2+(\nabla\hat{\theta})^2+4\pi\lambda(W_++W_-)-\alpha' Q\mathcal{R}[h]\hat{r}\right\}, \tag{2.35}$$

where

$$W_\pm=e^{-2b_{\rm sL}\hat{r}}e^{\pm i\sqrt{\frac{k}{\alpha'}}(\hat{\theta}_{\rm L}-\hat{\theta}_{\rm R})} \tag{2.36}$$

are the winding ±1 components of the sine-Liouville potential. λ is a positive constant.

The duality relates two target spaces of different topologies. In the cigar description the target space is a disk, whose contractible Euclidean time circle indicates the Lorentzian continuation is a connected geometry with a horizon (eq. (2.10)). In the sine-Liouville description the target space is an annulus, and continuation with respect to the non-contractible Euclidean time circle produces a disconnected Lorentzian geometry. Both descriptions share the same asymptotic linear-dilaton $\times$ S^1 region. The leading departure

[31] However, for $2<k<3$, the Liouville $\times$ S^1 and $\mathrm{SL}(2,\mathbb{R})_k/\mathrm{U}(1)$ CFTs are conjectured to be connected by a conformal manifold [16].

[32] Though not strictly-speaking weakly coupled, since the circle radius is not large.

JHEP10(2022)195

from the free theory at finite r in the cigar is the metric deformation $e^{-2r}\partial\theta\bar{\partial}\theta$, while sine-Liouville results from the potential deformation $e^{-2b_{\rm sL}\hat{r}}\cos\left(\sqrt{k/\alpha'}(\hat{\theta}_{\rm L}-\hat{\theta}_{\rm R})\right)$.

One is again free to add a constant mode Φ_0 to the dilaton, but it may be eliminated by the field redefinition $\hat{r}\to\hat{r}+\frac{\Phi_0}{Q}$, up to a rescaling of λ by $e^{-(k-2)\Phi_0}$. In particular, only the combination $e^{-2\Phi_0}\lambda^{\frac{2}{k-2}}$ is a meaningful parameter of the string theory, which sets the mass of the black hole; we can therefore choose $\Phi_0=0$ in the sine-Liouville description.

Relatedly, although the action eq. (2.35) takes the form of the free linear-dilaton $\times$ S^1 action deformed by the sine-Liouville potential with coefficient λ, the sine-Liouville background is not a small perturbation of the free theory. The freedom to rescale λ by a field redefinition of $\hat{r}$ implies that correlation functions are not analytic functions of λ, and one cannot in general write a sine-Liouville correlator as a Taylor expansion in λ with coefficients computed from the free theory. As in Liouville [62], the λ dependence of a correlator of primaries in the sine-Liouville frame may be evaluated by performing the zero-mode integral over the linear-dilaton coordinate [16]. The functional integral with asymptotic primary insertions $\prod_N e^{-2Q(1-j_N)\hat{r}}\mathcal{S}_N(\hat{\theta})$, where $\mathcal{S}_N$ are S^1 primaries, may be written

$$\begin{aligned}&\int \mathrm{D}\hat{r}\mathrm{D}\hat{\theta}\; e^{-S_{\rm sL}[\hat{r},\hat{\theta}]}\prod_N e^{-2Q(1-j_N)\hat{r}}\mathcal{S}_N \\ &=\int \mathrm{D}\hat{r}'\mathrm{D}\hat{\theta}\; e^{-S_{\rm LD}[\hat{r}']-S_{\rm S^1}[\hat{\theta}]}\prod_N e^{-2Q(1-j_N)\hat{r}'}\mathcal{S}_N \\ &\quad\times\int \mathrm{d}\hat{r}_0\; e^{Q\left(\chi-2\sum_N(1-j_N)\right)\hat{r}_0-\left(\frac{\lambda}{\alpha'}V_{\rm sL}[\hat{r}',\hat{\theta}]\right)e^{-2b_{\rm sL}\hat{r}_0}},\end{aligned} \tag{2.37}$$

where $\hat{r}(z,\bar{z})=\hat{r}_0+\hat{r}'(z,\bar{z})$ and $V_{\rm sL}[\hat{r}',\hat{\theta}]=2\int \mathrm{d}^2\sigma\sqrt{h}e^{-2b_{\rm sL}\hat{r}'}\cos\left(\sqrt{k/\alpha'}(\hat{\theta}_{\rm L}-\hat{\theta}_{\rm R})\right)$. Using the identity

$$\int_{-\infty}^{\infty}\mathrm{d}\xi\; e^{\kappa\xi-\beta e^{-\xi}}=\beta^{\kappa}\Gamma(-\kappa),\qquad \mathrm{Re}(\kappa)<0,\quad \mathrm{Re}(\beta)>0, \tag{2.38}$$

the zero-mode integral may be evaluated for $\sum_N(\mathrm{Re}(j_N)-1)<-\frac{1}{2}\chi$ as

$$\int_{-\infty}^{\infty}\mathrm{d}\hat{r}_0\; e^{2b_{\rm sL}\kappa\hat{r}_0-\left(\frac{\lambda}{\alpha'}V_{\rm sL}\left[\hat{r}',\hat{\theta}\right]\right)e^{-2b_{\rm sL}\hat{r}_0}}=\frac{1}{2b_{\rm sL}}\left(\frac{\lambda}{\alpha'}V_{\rm sL}\left[\hat{r}',\hat{\theta}\right]\right)^{\kappa}\Gamma\left(-\kappa\right), \tag{2.39}$$

where

$$\kappa=\frac{Q}{2b_{\rm sL}}\left(\chi-2\sum_N\left(1-j_N\right)\right). \tag{2.40}$$

When $\mathrm{Re}(\kappa)>0$, the zero-mode integral over the real line diverges, and must be deformed to a complex contour that preserves convergence and analyticity.[33]

[33] Of course, since one is in general interested in complex values of j, it is inevitable that the functional integral is complexified.

JHEP10(2022)195

Thus, the sine-Liouville correlation function is reduced to a linear-dilaton$\times$S^1 correlation function, with the linear-dilaton zero-mode measure omitted, plus κ powers of the integrated sine-Liouville potential:

$$\left\langle \prod_N e^{-2Q(1-j_N)\hat{r}} \mathcal{S}_N \right\rangle_{\text{sL}} \tag{2.41}$$
$$= \frac{1}{2b_{\text{sL}}} \left(\frac{\lambda}{\alpha'}\right)^{\kappa} \Gamma(-\kappa) \left\langle V_{\text{sL}}[\hat{r},\hat{\theta}]^{\kappa} \prod_N e^{-2Q(1-j_N)\hat{r}} \mathcal{S}_N \right\rangle_{\text{LD}\times\text{S}^1,\emptyset} .$$

Such an expression with the integrated potential inserted κ times, which is in general a complex number, does not admit an obvious interpretation as a correlation function of local operators, and is defined by the functional integral.

On a genus g Riemann surface, one obtains the scaling $\lambda^{\frac{2}{k-2}\left(1-g+\sum_N (j_N-1)\right)}$. The answer is analytic in λ only when κ is a natural number, in which the case the κ insertions of the potential ${V_{\text{sL}}}^{\kappa}$ is most straightforward. The subsequent divergence of the pre-factor $\Gamma(-\kappa)$ is attributable to the volume of the non-compact target space.

Observe that the sine-Liouville potential $W_+ + W_-$ coincides with the weak-coupling limit of the previously defined coset operator $\mathcal{O}_{\text{sL}} = \mathcal{W}_+ + \mathcal{W}_-$ (eqs. (2.28)–(2.29)), hence the common terminology. A conformal perturbation of $\text{SL}(2,\mathbb{R})_k/\text{U}(1)$ by the marginal operator $\mathcal{O}_{\text{sL}}$ is trivial at the level of the CFT — the deformation merely shifts the coefficient λ of the sine-Liouville potential, which may be undone by a field redefinition of $\hat{r}$ at the cost of introducing a dilaton zero-mode. The latter is a trivial improvement term from the perspective of the CFT. As a string background, on the other hand, the deformation by $\mathcal{O}_{\text{sL}}$ is important because it shifts the mass of the black hole. We explore this point further in section 2.3.

2.2 An AdS$_3$ duality

In this section we propose a new duality that may be considered the uplift of FZZ to the Euclidean AdS$_3$ CFT $\text{SL}(2,\mathbb{C})_k/\text{SU}(2)$, or its quotient $\mathbb{Z}\backslash\text{SL}(2,\mathbb{C})_k/\text{SU}(2)$ that describes a string in the asymptotic Euclidean AdS$_3$ black hole.[34] The familiar description of these CFTs is of a string propagating in a solid cylinder or solid torus geometry, with respect to which the disk topology of the cigar may be thought of as a cross-sectional slice (figure 4a). As in FZZ, one may attempt to define a dual description by extending the semi-infinite radial direction $r \in [0,\infty)$ to an infinite line $\hat{r} \in (-\infty,\infty)$, with the dual action given by the same limiting form at infinity plus the marginal, unit-winding operator around the resulting non-contractible cycle (figure 4b). To do so requires adopting a first-order description near the conformal boundary, such that the limiting theories are free. Gauging the translation symmetry along the length of the cylinder in the two descriptions yields the same cigar and sine-Liouville backgrounds of the two-dimensional duality, providing strong evidence that the uplifted duality holds in the parent CFTs.

[34] Or, equivalently, thermal AdS$_3$.

JHEP10(2022)195

2.2.1 $\mathbf{SL(2,\mathbb{R})_k}$ and $\mathbf{SL(2,\mathbb{C})_k/SU(2)}$

We begin by reviewing relevant details of AdS_3, the $SL(2,\mathbb{R})_k$ and $SL(2,\mathbb{C})_k/SU(2)$ WZW models, and the coset construction of $SL(2,\mathbb{R})_k/U(1)$.

AdS_3 may be described as a solid cylinder (figure 4a) with radial coordinate $r \in [0,\infty)$, angular coordinate $\theta \sim \theta + 2\pi$, and Lorentzian time coordinate $t \in (-\infty,\infty)$ running along its length. The metric in these cylinder coordinates is

$$\mathrm{d}s^2_{\mathrm{AdS}} = l^2_{\mathrm{AdS}}\left(-\cosh^2(r)\mathrm{d}t^2 + \mathrm{d}r^2 + \sinh^2(r)\mathrm{d}\theta^2\right). \tag{2.42}$$

As a (pseudo) Riemannian manifold, AdS_3 is equivalent to the Lie group $SL(2,\mathbb{R})$, as may be seen from the parameterization[35]

$$g = e^{i(t+\theta)\mathrm{T}_3}e^{2ir\mathrm{T}_2}e^{i(t-\theta)\mathrm{T}_3} \in \mathrm{SL}(2,\mathbb{R}), \tag{2.43}$$

where $\mathrm{T}_1 = -\frac{i}{2}\sigma_1$, $\mathrm{T}_2 = -\frac{i}{2}\sigma_3$, and $\mathrm{T}_3 = \frac{1}{2}\sigma_2$ are a basis of $\mathfrak{sl}(2,\mathbb{R})$, satisfying $[\mathrm{T}_i,\mathrm{T}_j] = i\epsilon_{ijk}\eta^{kl}\mathrm{T}_l$, with metric $\eta_{ij} = 2\mathrm{tr}(\mathrm{T}_i\mathrm{T}_j) = \mathrm{Diag}(-1,-1,1)_{ij}$. The AdS_3 metric eq. (2.42) is then reproduced by the usual group metric $\frac{1}{2}l^2_{\mathrm{AdS}}\mathrm{tr}\left(g^{-1}\mathrm{d}g g^{-1}\mathrm{d}g\right)$.

One may therefore describe a string propagating in AdS_3 by the $SL(2,\mathbb{R})_k$ WZW model [28–31, 54, 55]. The WZW level k, which is a real number greater than 2, sets the AdS length scale, $l_{\mathrm{AdS}} = \sqrt{\alpha' k}$. AdS_3 has constant negative curvature $\mathcal{R} = -6/l^2_{\mathrm{AdS}}$, and conformal symmetry on the worldsheet is supported by a B-field that is contributed by the Wess-Zumino term, $\mathrm{tr}\left(\left(g^{-1}\mathrm{d}g\right)^{\wedge 3}\right) \propto \mathrm{d}B$, with $B \propto \cosh(2r)\mathrm{d}t \wedge \mathrm{d}\theta$. The dilaton, meanwhile, is a constant, and the central charge is $c = 3k/(k-2)$.

However, one must be careful to define what one means by the $SL(2,\mathbb{R})_k$ WZW model. Since the metric eq. (2.42) is Lorentzian, the WZW action includes wrong-sign kinetic terms, and the functional integral is ill-defined. The ambiguity is meaningful and corresponds to the need to choose a state in spacetime around which one wishes to build a string perturbation theory. The Lorentzian string dualities that we describe in this paper will refer to string perturbation theories in various states. The appropriate worldsheet theories are defined by analytic continuation from unitary CFTs, which encode the choice of state. We elaborate on this point in section 3. For now, by the $SL(2,\mathbb{R})_k$ WZW model we mean string perturbation theory in AdS_3 in the spacetime vacuum state, which is defined by continuation from the theory with target Euclidean AdS_3 ($EAdS_3$).

$EAdS_3$ is obtained from eq. (2.42) by continuing $\xi = it$,

$$\mathrm{d}s^2_{\mathrm{EAdS}} = l^2_{\mathrm{AdS}}\left(\cosh^2(r)\mathrm{d}\xi^2 + \mathrm{d}r^2 + \sinh^2(r)\mathrm{d}\theta^2\right), \tag{2.44}$$

with $\xi \in (-\infty,\infty)$. The same continuation in eq. (2.43) yields not a group, but a parameterization of the vector space of 2×2 Hermitian matrices with unit determinant and positive eigenvalues. The group $SL(2,\mathbb{C})$ acts transitively on this space by conjugation, $g \to \Lambda g \Lambda^\dagger$, with stabilizer $SU(2)$. Thus, $EAdS_3$ is equivalent to the coset manifold $SL(2,\mathbb{C})/SU(2)$, and one may describe a string in $EAdS_3$ by the $SL(2,\mathbb{C})_k/SU(2)$ coset CFT [28–30, 32, 56, 57].

[35] $e^{\pm 2\pi i\mathrm{T}_3} = -1$, and therefore g is invariant under both $t \to t + 2\pi$ and $\theta \to \theta + 2\pi$. By $AdS_3 = SL(2,\mathbb{R})$, we mean the covering space where t is decompactified.

JHEP10(2022)195

The $\mathrm{SL}(2,\mathbb{C})_k/\mathrm{SU}(2)$ action is most conveniently written in Poincarè coordinates,

$$\mathrm{d}s^2_{\mathrm{EAdS}} = l^2_{\mathrm{AdS}}\left(\mathrm{d}\sigma^2 + e^{2\sigma}\mathrm{d}\gamma\mathrm{d}\bar{\gamma}\right), \tag{2.45}$$

where γ is a complex coordinate, $\bar{\gamma}$ is its complex conjugate, and $\sigma \in (-\infty, \infty)$. They are related to the cylinder coordinates by

$$\sigma = -\xi + \log\cosh r \tag{2.46a}$$
$$\gamma = \tanh(r)e^{\xi+i\theta} \tag{2.46b}$$
$$\bar{\gamma} = \tanh(r)e^{\xi-i\theta}. \tag{2.46c}$$

At the conformal boundary $r \to \infty$, note that $\gamma \to e^{\xi+i\theta}$ is the usual map between the boundary sphere with complex coordinate γ and the boundary cylinder with complex coordinate $W \equiv \xi + i\theta$.

The action, including the contribution from the B-field, is then [28]

$$S = \frac{k}{2\pi}\int \mathrm{d}^2z\left(\partial\sigma\bar{\partial}\sigma + e^{2\sigma}\partial\bar{\gamma}\bar{\partial}\gamma\right). \tag{2.47}$$

By the change of variables eq. (2.46) we obtain the action in cylinder coordinates[36]

$$S = \frac{k}{2\pi}\int \mathrm{d}^2z\left\{\partial r\bar{\partial}r + \partial\xi\bar{\partial}\xi + (\partial\xi - i\partial\theta)\left(\bar{\partial}\xi + i\bar{\partial}\theta\right)\sinh^2(r)\right\}. \tag{2.48}$$

The cigar is obtained by gauging the translation isometry along the length of the AdS_3 or EAdS_3 cylinder. Promoting $\partial\xi \to \partial\xi + A$, $\bar{\partial}\xi \to \bar{\partial}\xi + \bar{A}$, one obtains the gauged action

$$S \to S + \frac{k}{2\pi}\int \mathrm{d}^2z\left(J^3\bar{A} + \bar{J}^3A + \cosh^2(r)A\bar{A}\right), \tag{2.49}$$

where

$$J^3(z) = \partial\xi + \sinh^2(r)(\partial\xi - i\partial\theta) \tag{2.50}$$

is the holomorphic component of the current for translations in ξ, and $\bar{J}^3$ is the anti-holomorphic component. Solving the auxiliary equations of motion for $A, \bar{A}$ and evaluating the action on the solution one obtains

$$S_{\mathrm{cigar}} = \frac{k}{2\pi}\int \mathrm{d}^2z\left(\partial r\bar{\partial}r + \tanh^2(r)\partial\theta\bar{\partial}\theta\right). \tag{2.51}$$

Thus, classically gauging the length of the cylinder produces a disk topology with the cigar metric $\mathrm{d}s^2 = \alpha' k(\mathrm{d}r^2 + \tanh^2(r)\mathrm{d}\theta^2)$, as claimed in eq. (2.2). Quantum mechanically, integrating out the gauge fields produces the dilaton, as necessitated by conformal invariance (eq. (2.7)), as well as additional sub-leading corrections to the background eq. (2.2) [25].

One may then obtain the spectrum eq. (2.14) of the gauged WZW model by starting from the $\mathrm{SL}(2,\mathbb{R})_k$ spectrum and applying the coset construction. To do so we first review the Hilbert space of $\mathrm{SL}(2,\mathbb{R})_k$ as obtained in [54].

[36] We drop an additional total derivative term $i\tanh(r)(\partial r\bar{\partial}\theta - \bar{\partial}r\partial\theta)$ that corresponds to an exact B-field $\mathrm{d}(\log\cosh(r)\mathrm{d}\theta)$.

JHEP10(2022)195

Observe from eq. (2.43) that the obvious isometries of the AdS_3 metric in cylinder coordinates (eq. (2.42)), namely time translations $t \to t + \delta t$ and rotations $\theta \to \theta + \delta\theta$, are implemented in $SL(2,\mathbb{R})$ by $g \to e^{i\delta t \mathrm{T}_3} g e^{i\delta t \mathrm{T}_3}$ and $g \to e^{i\delta\theta \mathrm{T}_3} g e^{-i\delta\theta \mathrm{T}_3}$. The time translation and rotation generators are therefore the WZW charges $J_0^3 + \bar{J}_0^3$ and $J_0^3 - \bar{J}_0^3$, whose eigenvalues are the spacetime energy and angular momentum. The complete isometry algebra of $AdS_3 = SL(2,\mathbb{R})$ is $\mathfrak{sl}(2,\mathbb{R})_{\mathrm{L}} \oplus \mathfrak{sl}(2,\mathbb{R})_{\mathrm{R}} \simeq \mathfrak{so}(2,2)$, whose generators $\{J_0^3, J_0^\pm\} \cup \{\bar{J}_0^3, \bar{J}_0^\pm\}$ in the raising/lowering basis satisfy

$$\left[J_0^3, J_0^\pm\right] = \pm J_0^\pm, \quad \left[J_0^+, J_0^-\right] = -2J_0^3, \tag{2.52}$$

and similarly for $\bar{J}_0^a$, with $[J_0^a, \bar{J}_0^b] = 0$.

As is usual in WZW models, the target isometry algebra $\mathfrak{sl}(2,\mathbb{R})_{\mathrm{L}} \oplus \mathfrak{sl}(2,\mathbb{R})_{\mathrm{R}}$ is extended to a current algebra $\widehat{\mathfrak{sl}}_k(2,\mathbb{R})_{\mathrm{L}} \oplus \widehat{\mathfrak{sl}}_k(2,\mathbb{R})_{\mathrm{R}}$:

$$\left[J_A^3, J_B^3\right] = -\frac{k}{2} A \delta_{A+B} \tag{2.53a}$$

$$\left[J_A^3, J_B^\pm\right] = \pm J_{A+B}^\pm \tag{2.53b}$$

$$\left[J_A^+, J_B^-\right] = -2J_{A+B}^3 + kA\delta_{A+B}, \tag{2.53c}$$

J_A^a being the modes of the currents $\{J^a(z)\}_{a=3,\pm}$, $J^a(z) = \sum_{A\in\mathbb{Z}} J_A^a / z^{A+1}$. Likewise one has anti-holomorphic modes $\bar{J}_A^a$ of the currents $\bar{J}^a(\bar{z})$, which satisfy the same algebra and commute with the holomorphic modes. The isometry algebra corresponds to the global sub-algebra generated by the zero-modes $J_0^a, \bar{J}_0^a$.

The $SL(2,\mathbb{R})_k$ Hilbert space is organized in representations of this current algebra [54]:

$$\mathcal{H}_{SL(2,\mathbb{R})_k} = \bigoplus_{j,\alpha,w} \begin{cases} \widehat{D}_j^{+,w} \otimes \widehat{D}_j^{+,w} & j \in \left(\frac{1}{2}, \frac{k-1}{2}\right),\ w \in \mathbb{Z} \\ \widehat{C}_{j,\alpha}^w \otimes \widehat{C}_{j,\alpha}^w & j \in \frac{1}{2} + i\mathbb{R}_+,\ \alpha \in [0,1),\ w \in \mathbb{Z}. \end{cases} \tag{2.54}$$

The notation here is as follows. D_j^+ denotes the spin $j \in \mathbb{R}_+$ lowest-weight discrete-series representation of the global $\mathfrak{sl}(2,\mathbb{R})$ sub-algebra, which consists of states $\{|j,m\rangle : m \in j + \mathbb{N}\}$, with m being the eigenvalue of J_0^3 and $-j(j-1)/(k-2)$ being the conformal weight with respect to the $SL(2,\mathbb{R})_k$ stress tensor. The lowest-weight state $|j,j\rangle$ is annihilated by J_0^-, and the remainder of the representation is obtained by acting with J_0^+. Similarly, one may consider highest-weight discrete-series representations D_j^-, consisting of states $\{|j,m\rangle : m \in -j - \mathbb{N}\}$. $C_{j,\alpha}$ denotes the spin $j \in \frac{1}{2} + i\mathbb{R}$ continuous-series representation of $\mathfrak{sl}(2,\mathbb{R})$, consisting of states $\{|j,m\rangle : m \in \alpha + \mathbb{Z}\}$, with $\alpha \in [0,1)$ an additional parameter that fixes the J_0^3 eigenvalue modulo $\mathbb{Z}$. Note that continuous-series representations are infinite towers with no relation between j and m, while the discrete series are semi-infinite towers in which j and m are related by integer shifts.

On any such global $\mathfrak{sl}(2,\mathbb{R})$ representation, one may in the usual way build an $\widehat{\mathfrak{sl}}_k(2,\mathbb{R})$ current-algebra representation by demanding that the states $|j,m\rangle$ are primary with respect to the positive current modes, $J_{A>0}^a |j,m\rangle = 0$. Then the current-algebra representations, denoted $\widehat{D}_j^\pm$ and $\widehat{C}_{j,\alpha}$, are built by the action of the negative modes $J_{A<0}^a$ on the primaries.

JHEP10(2022)195

In addition to these standard varieties of current-algebra representations built atop primaries, the $\mathrm{SL}(2,\mathbb{R})_k$ spectrum includes less familiar representations $\widehat{D}_j^{\pm,w}$ and $\widehat{C}_{j,\alpha}^{w}$, labeled by an integer w, which arise from an automorphism $J_A^a \to J_A^a[w]$ of the current algebra known as the spectral-flow automorphism:

$$J_A^3 = J_A^3[w] + \frac{k}{2} w \delta_A \tag{2.55a}$$

$$J_A^\pm = J_{A\mp w}^\pm[w]. \tag{2.55b}$$

w may roughly be thought of as a winding number around the θ circle of AdS_3 [54]. Of course, since this cycle is contractible, w is not conserved.

States in spectral-flowed representations transform as ordinary representations under $J_A^a[w]$, with the action of J_A^a then determined by eq. (2.55). The Virasoro modes, being obtained from the currents by the Sugawara construction, in turn transform under spectral flow:

$$L_A = L_A[w] - w J_A^3[w] - \frac{k}{4} w^2 \delta_A. \tag{2.56}$$

For example, the J^3 and conformal weights of a spectral-flowed primary state $|j,m;w\rangle$ are

$$J_0^3 \,|j,m;w\rangle = \left(m + \frac{k}{2} w\right) |j,m;w\rangle \tag{2.57a}$$

$$L_0 \,|j,m;w\rangle = \left(-\frac{j(j-1)}{k-2} - wm - \frac{1}{4} k w^2\right) |j,m;w\rangle \,. \tag{2.57b}$$

In general, we denote by $M = m + \frac{k}{2} w$ the eigenvalue of J_0^3 to distinguish it from the eigenvalue m of $J_0^3[w]$ prior to spectral flow. Of course, in unflowed representations the two coincide.

A current-algebra primary $|j,m\rangle$ is also Virasoro primary, and from eqs. (2.55)–(2.56) it follows that the spectral-flowed state $|j,m;w\rangle$ remains Virasoro primary. We also point out for later use that, for $w > 0$, $|j,m;w\rangle$ transforms as a lowest-weight state $|J, M = J\rangle$ with respect to the global sub-algebra, $J_0^- \,|j,m;w\rangle = J_w^-[w] \,|j,m;w\rangle = 0$. Thus, $|j,m;w\rangle$ sits at the bottom of a lowest-weight representation D_J^+ of spin $J = m + \frac{k}{2} w$. Likewise, for $w < 0$, $|j,m;w\rangle \in D_{J'}^-$ is a highest-weight state $|J', M' = -J'\rangle$ of spin $J' = -\left(m + \frac{k}{2} w\right)$. For further details of these representations, see [54].

The complete spectrum eq. (2.54) of the $\mathrm{SL}(2,\mathbb{R})_k$ WZW model consists of the current-algebra representations built on the lowest-weight discrete-series representations $D_j^+ \otimes D_j^+$ for $\frac{1}{2} < j < \frac{k-1}{2}$ and on the continuous-series representations $C_{j,\alpha} \otimes C_{j,\alpha}$ for $j \in \frac{1}{2} + i\mathbb{R}_+$, as well as their associated spectral-flowed representations for all $w \in \mathbb{Z}$. Note that the spectrum does not explicitly list both the lowest-weight and highest-weight discrete-series representations $\widehat{D}_j^{\pm,w} \otimes \widehat{D}_j^{\pm,w}$. These representations are not independent. Rather, one has the following isomorphism, which exchanges lowest and highest weights, shifts the spectral flow by one unit, and reflects $j \to \frac{k}{2} - j$ [54]:

$$\widehat{D}_j^{-,w} \simeq \widehat{D}_{\frac{k}{2}-j}^{+,w-1}. \tag{2.58}$$

JHEP10(2022)195

Note that the interval $j \in \left(\frac{1}{2}, \frac{k-1}{2}\right)$ is mapped to itself under the reflection $j \to \frac{k}{2} - j$, so that if j lies in the interval then so does $\frac{k}{2} - j$ and vice-versa.

The $\mathrm{SL}(2,\mathbb{R})_k/\mathrm{U}(1)$ spectrum eq. (2.14) then follows from eq. (2.54) by the coset construction [54]. The time translation symmetry being generated by $J_0^3 + \bar{J}_0^3$, the Virasoro primaries of $\mathrm{SL}(2,\mathbb{R})_k/\mathrm{U}(1)$ descend from those $\mathrm{SL}(2,\mathbb{R})_k$ states which are (i) Virasoro primary, (ii) J^3 and $\bar{J}^3$ primary, and (iii) satisfy the projection $J_0^3 + \bar{J}_0^3 = 0$. These are of the form

$$\left| j_N, m = \frac{-kw+n}{2}, \bar{m} = \frac{-kw-n}{2}; w \right\rangle \in \begin{cases} \widehat{D}^{+,w}_{j_N} \otimes \widehat{D}^{+,w}_{j_N} & w < 0 \\ \widehat{D}^{-,w}_{j_N} \otimes \widehat{D}^{-,w}_{j_N} & w > 0, \end{cases} \tag{2.59}$$

and

$$\left| j = \frac{1}{2}(1+is), m = \frac{-kw+n}{2}, \bar{m} = \frac{-kw-n}{2}; w \right\rangle \in \widehat{C}^{w}_{j,\alpha} \otimes \widehat{C}^{w}_{j,\alpha}. \tag{2.60}$$

Here, $m + \bar{m} = -kw$ is the projection condition $J_0^3 + \bar{J}_0^3 = 0$, the respective eigenvalues being $m + kw/2$ and $\bar{m} + kw/2$. $m - \bar{m} = n$ is the eigenvalue of $J_0^3 - \bar{J}_0^3$, i.e. the angular momentum around the AdS_3 cylinder, which is therefore integer quantized. In eq. (2.59), $j_N = \frac{1}{2}(k|w| - |n|) - N$ is as in eq. (2.14b), with $N \in \mathbb{N}$, determined in this context by the requirement that the states with the necessary values of m, $\bar{m}$ indeed fit into discrete-series representations. Namely, for $w < 0$ one finds $j_N - m, j_N - \bar{m} \in -\mathbb{N}$ corresponding to a lowest-weight representation, while for $w > 0$, $j_N + m, j_N + \bar{m} \in -\mathbb{N}$ giving a highest-weight representation. In eq. (2.60), there is no relation between j and $m, \bar{m}$, and one simply chooses the appropriate value of α to identify the relevant state in the continuous series.

As mentioned above, spectral-flowed current-algebra primaries $|j, m, \bar{m}; w\rangle \equiv |j, m; w\rangle \otimes |j, \bar{m}; w\rangle$ are Virasoro primary, and from eq. (2.55) they are primary with respect to $J^3, \bar{J}^3$ as well. Thus, the states eq. (2.59)–(2.60) indeed satisfy the necessary conditions, and descend to Virasoro primaries of $\mathrm{SL}(2,\mathbb{R})_k/\mathrm{U}(1)$. The quantum number j, related to the linear-dilaton momentum in the asymptotic cylinder of the cigar or sine-Liouville backgrounds, descends from the $\mathfrak{sl}(2,\mathbb{R})$ spin. The quantized momentum n around the asymptotic cylinder corresponds to the angular momentum around AdS_3. And the winding number $-w$ follows from the spectral-flow parameter of the $\widehat{\mathfrak{sl}}_k(2,\mathbb{R})$ representations.

The conformal weights of these states with respect to the coset stress tensor are as in eq. (2.15), obtained from the $\mathrm{SL}(2,\mathbb{R})_k$ weights eq. (2.57b) less the $\mathrm{U}(1)$ contribution. Note that in writing eq. (2.59) we have applied the isomorphism eq. (2.58) to convert current-algebra descendent states from lowest-weight representations in eq. (2.54) to spectral-flowed primaries from highest-weight representations. This identification is important in the infinitesimal interpretation of the FZZ duality discussed in section 2.3.

Finally, we point out that the components $\mathcal{W}_\pm = \mathcal{O}_{j=\frac{k}{2}-1, n=0, w=\mp 1}$ of the sine-Liouville operator $\mathcal{O}_{\mathrm{sL}} = \mathcal{W}_+ + \mathcal{W}_-$ (eq. (2.29)) descend from the states [41]

$$\mathcal{W}_\pm = \left| \frac{k}{2} - 1, \pm\frac{k}{2}, \pm\frac{k}{2}; \mp 1 \right\rangle \in \widehat{D}^{\pm,\mp 1}_{\frac{k}{2}-1} \otimes \widehat{D}^{\pm,\mp 1}_{\frac{k}{2}-1}. \tag{2.61}$$

In fact, since the $J_0^3, \bar{J}_0^3$ eigenvalues of these states independently vanish (as opposed to merely their sum), the coset states and $\mathrm{SL}(2,\mathbb{R})_k$ states are identical, there being no $\mathrm{U}(1)$

JHEP10(2022)195

factors to strip away. Thus the weights eqs. (2.15) and (2.57b) are identical — namely, $(1,1)$ — and $\mathcal{O}_{\text{sL}}$ defines a marginal operator of both $\text{SL}(2,\mathbb{R})_k$ and $\text{SL}(2,\mathbb{R})_k/\text{U}(1)$. This fact will be important in the next sub-section when we uplift the FZZ duality to AdS_3, and again in section 2.3 when we discuss the infinitesimal versions of these dualities.

2.2.2 Uplifting the duality

Now we would like to lift the FZZ duality from the $\text{SL}(2,\mathbb{R})_k/\text{U}(1)$ coset CFT to its Euclidean AdS_3 parent $\text{SL}(2,\mathbb{C})_k/\text{SU}(2)$, and the associated asymptotic EAdS_3 black hole $\mathbb{Z}\backslash\text{SL}(2,\mathbb{C})_k/\text{SU}(2)$.

The cigar topology, being obtained from EAdS_3 by gauging the translation isometry along the length of the cylinder, may be thought of as a disk sliced from the cylinder (figure 4a). In the FZZ dual description, the disk topology of the cigar is replaced by the annulus topology of the sine-Liouville cylinder, plus the condensate of winding strings. The two descriptions share the same free linear-dilaton $\times$ S^1 limit in the weak-coupling region. Whereas the cigar geometry terminates at the origin of the disk $r = 0$, the sine-Liouville cylinder continues into the strong-coupling region $\hat{r} \to -\infty$, the potential wall instead taking responsibility for reflecting strings away.

It is natural to wonder if there exists a similar duality of the $\text{SL}(2,\mathbb{C})_k/\text{SU}(2)$ CFT in which the solid cylinder target space of eq. (2.44) with its semi-infinite radial coordinate $r \in [0,\infty)$ is replaced by a fully infinite radial direction $\hat{r} \in (-\infty,\infty)$ and a condensate of winding strings that wrap the resulting non-contractible cycle (figure 4b). If such a description existed, such that gauging the translation symmetry reproduced the sine-Liouville sigma-model, one would obtain a three-dimensional uplift of the FZZ duality.

The interpretation of the cigar as a Euclidean black hole followed upon identifying its angular coordinate with Euclidean time. One is likewise free to continue EAdS_3 with respect to its contractible angular direction $\theta = iT$, as opposed to ordinary AdS_3 which was obtained by continuing $\xi = it$. The result is a Lorentzian wedge with a coordinate horizon, which we will refer to as AdS_3-Rindler:

$$\text{d}s^2_{\text{AdS-Rindler}} = l^2_{\text{AdS}} \left(-\sinh^2(r)\text{d}T^2 + \text{d}r^2 + \cosh^2(r)\text{d}\xi^2 \right). \tag{2.62}$$

AdS_3-Rindler is an analogue of ordinary Rindler spacetime, the latter obtained from $\mathbb{R}^2$ by continuing with respect to angular Euclidean time, yielding the right wedge of a two-sided decomposition of Minkowski spacetime separated by a coordinate horizon (figure 8). The coordinates of eq. (2.62) likewise cover a patch of AdS_3 up to a coordinate horizon at $r = 0$, where the coefficient $\sinh^2(r)$ of $\text{d}T^2$ vanishes.

One may furthermore obtain the asymptotic AdS_3 black hole by compactifying $\xi \sim \xi + 4\pi^2/\beta_{\text{BH}}$, where β_{BH} is the inverse Hawking temperature of the black hole, as we review in section 3.2.3 [23, 24]. Thus, the continuation of the would-be uplifted duality likewise relates a connected black hole to a disconnected spacetime. The Euclidean duality will apply both to $\text{SL}(2,\mathbb{C})_k/\text{SU}(2)$ and the quotient $\mathbb{Z}\backslash\text{SL}(2,\mathbb{C})_k/\text{SU}(2)$ that compactifies ξ, and so for the purposes of the present discussion it makes little difference whether ξ is compact or not.

One immediately encounters a problem with the above proposal, however, on examining the $\text{SL}(2,\mathbb{C})_k/\text{SU}(2)$ action (eq. (2.48)). Whereas the cigar and sine-Liouville Lagrangians

JHEP10(2022)195

approach the same free theory at infinity, which may then be deformed by either the cigar-capping or sine-Liouville operators, the EAdS$_3$ Lagrangian is singular at $r \to \infty$.

This singular asymptotic behavior may be remedied by applying the first-order formalism.[37] Classically, one has the identity of Lagrangians

$$f\partial\bar{W}\bar{\partial}W = \chi\bar{\partial}W + \bar{\chi}\partial\bar{W} - \frac{1}{f}\chi\bar{\chi}, \tag{2.63}$$

the auxiliary equations of motion for $\chi, \bar{\chi}$ setting $\chi = f\partial\bar{W}$ and $\bar{\chi} = f\bar{\partial}W$, which recover the left-hand-side upon substitution. Quantum mechanically, the change of variables introduces a dilaton $\log\sqrt{f}$ from the transformation of the functional integral measure. Thus, the action eq. (2.48) may be replaced by

$$S = \frac{k}{2\pi}\int \mathrm{d}^2z \left\{\partial r\bar{\partial}r + \partial\xi\bar{\partial}\xi + \chi(\bar{\partial}\xi + i\bar{\partial}\theta) + \bar{\chi}(\partial\xi - i\partial\theta) - \frac{1}{\sinh^2(r)}\chi\bar{\chi}\right\}, \tag{2.64}$$

together with a dilaton $\Phi = -\log\sinh r + \Phi_0$. This is the cylinder version of the standard Wakimoto form of the action eq. (2.47) in Poincarè coordinates [28].[38] χ is a $(1,0)$ form, set to $\chi = \sinh^2(r)\partial\bar{W}$ by the equations of motion, where $W = \xi + i\theta$ is the complex coordinate on the asymptotic cylinder, $W \sim W + 2\pi i$.

Gauging the ξ translation symmetry in eq. (2.48) produced the cigar action at leading order (eq. (2.51)). In the form eq. (2.64), the current for ξ translations is $J^3(z) = \partial\xi + \chi$, which coincides with eq. (2.50) when evaluated on the auxiliary solution. The gauged first-order action becomes

$$S \to S + \frac{k}{2\pi}\int \mathrm{d}^2z \left(J^3\bar{A} + \bar{J}^3A + A\bar{A}\right). \tag{2.65}$$

Classically integrating out $A, \bar{A}$ yields a first-order description of the cigar,[39]

$$S_{\text{cigar}} = \frac{k}{2\pi}\int \mathrm{d}^2z \left(\partial r\bar{\partial}r + i\chi\bar{\partial}\theta - i\bar{\chi}\partial\theta - \coth^2(r)\chi\bar{\chi}\right), \tag{2.66}$$

and integrating out $\chi, \bar{\chi}$ again reproduces the cigar action.

[37] See e.g. [63, 64] for reviews.

[38] We use χ and W to denote the cylinder-valued first-order coordinates rather than the typical β and γ to avoid confusion with the first-order formalism in Poincarè coordinates.

[39] In this description one has contributions to the dilaton both from the first-order formalism and from integrating out $A, \bar{A}$. Further integrating out $\chi, \bar{\chi}$ eliminates the former contribution, leaving the dilaton profile eq. (2.2b) of the cigar.

JHEP10(2022)195

The presentation eq. (2.64) is advantageous because it is non-singular at $r \to \infty$, where the potential $\chi\bar{\chi}/\sinh^2(r)$ goes to zero. In that limit, the gauged action after classically integrating out the gauge fields is then as in eq. (2.66) but with $\coth^2(r) \to 1$, and further integrating out the auxiliaries yields the expected asymptotic cylinder background,

$$S_{\text{cigar}} \overset{r\to\infty}{\longrightarrow} \frac{k}{2\pi}\int \mathrm{d}^2 z \left(\partial r\bar{\partial} r + \partial\theta\bar{\partial}\theta\right). \tag{2.67}$$

Thus, eq. (2.64) is a preferable description of $\mathrm{SL}(2,\mathbb{C})_k/\mathrm{SU}(2)$ for the purposes of uplifting the FZZ duality because the free theory it approaches at $r \to \infty$ is transparently the uplift of the same limit of the cigar background.

This large r limit of eq. (2.64) is a linear-dilaton plus first-order cylinder system. One may define canonically normalized fields

$$\hat{r} = \frac{1}{Q}r, \qquad \hat{W} = \sqrt{\alpha' k}W, \qquad \hat{\chi} = \sqrt{\alpha' k}\left(\chi + \frac{1}{2}\partial\xi\right), \tag{2.68}$$

such that the asymptotic action appears

$$S_{\mathrm{LD}\times\mathcal{F}(\mathbb{C}/\mathbb{Z})} = \frac{1}{2\pi\alpha'}\int \mathrm{d}^2 z \left(\partial\hat{r}\bar{\partial}\hat{r} + \hat{\chi}\bar{\partial}\hat{W} + \hat{\bar{\chi}}\partial\hat{\bar{W}}\right), \quad \Phi(\hat{r}) = -Q\hat{r}. \tag{2.69}$$

We denote by $\mathcal{F}(X)$ the first-order system valued in X; in this case $X = \mathbb{C}/\mathbb{Z}$ is the cylinder $\hat{W} \sim \hat{W} + 2\pi i\sqrt{\alpha' k}$. As before, $Q = 1/\sqrt{\alpha'(k-2)}$ after accounting for quantum corrections. The asymptotic potential $e^{-2r}\chi\bar{\chi}$ in eq. (2.64) is the leading correction to the free theory at finite r, analogous to $e^{-2r}\partial\theta\bar{\partial}\theta$ in the cigar.

It is important to understand once more how the gauging of the translation symmetry along the length of the EAdS_3 boundary cylinder is implemented in the description eq. (2.69). The holomorphic current $\partial\xi + \chi$ in the unhatted variables becomes $J^3(z) = \hat{\chi} + \frac{1}{4}(\partial\hat{W} + \partial\hat{\bar{W}})$ (after rescaling by $\sqrt{\alpha' k}$ for convenience).[40] Gauging this symmetry of the free linear-dilaton $\times\, \mathcal{F}(\mathbb{C}/\mathbb{Z})$ system is then implemented by

$$S_{\mathrm{LD}\times\mathcal{F}(\mathbb{C}/\mathbb{Z})} \to S_{\mathrm{LD}\times\mathcal{F}(\mathbb{C}/\mathbb{Z})} + \frac{1}{2\pi\alpha'}\int \mathrm{d}^2 z \left(J^3\bar{A} + \bar{J}^3 A + A\bar{A}\right), \tag{2.70}$$

[40] Note that the appropriate current is not simply $\hat{\chi}$, as might be suggested from the coefficient of $\bar{\partial}\hat{W}$ in eq. (2.69). In writing eq. (2.69), we have dropped a term $-\frac{i}{2}(\partial\hat{\xi}\bar{\partial}\hat{\theta} - \bar{\partial}\hat{\xi}\partial\hat{\theta})$, which is total derivative in EAdS_3, though one should include it in EBTZ where it contributes a non-trivial B-field. It does not contribute to the equations of motion, but it does contribute $\frac{i}{2}\partial\hat{\theta} = \frac{1}{4}(\partial\hat{W} - \partial\hat{\bar{W}})$ to the holomorphic current for translations in $\hat{\xi} = \mathrm{Re}(\hat{W})$. The correction is important in order to identify the appropriate current whose gauging reproduces the linear-dilaton $\times\, \mathrm{S}^1$ background.

The same subtlety arises in the ordinary complex boson, $\partial X\bar{\partial}X + \partial Y\bar{\partial}Y = \partial\bar{Z}\bar{\partial}Z - i(\partial X\bar{\partial}Y - \bar{\partial}X\partial Y)$, where $Z = X + iY$. The usual holomorphic current for translations in X is ∂X. In the complex description, the corresponding current including the contribution from the exact B-field is $\partial\bar{Z} + i\partial Y = \frac{1}{2}(\partial Z + \partial\bar{Z}) = \partial X$, as desired.

Note that the current in the hatted variables, $\frac{1}{\sqrt{\alpha' k}}\left(\hat{\chi} + \frac{i}{2}\partial\hat{\theta}\right) = \chi + \frac{1}{2}\partial W$, differs from the current $\chi + \partial\xi = \chi + \frac{1}{2}(\partial W + \partial\bar{W})$ in the unhatted variables by $\frac{1}{2}\partial\bar{W}$, which vanishes by the equations of motion. The discrepancy arises because the change of variables eq. (2.68) shifts χ by $\partial\xi$, preserving the translational symmetry of ξ under which both χ and $\hat{\chi}$ are invariant, while producing currents that differ by irrelevant terms proportional to the equations of motion.

JHEP10(2022)195

which is invariant under $\hat{W} \to \hat{W} + \varepsilon$, $\hat{\bar{W}} \to \hat{\bar{W}} + \varepsilon$, $A \to A - \partial\varepsilon$, $\bar{A} \to \bar{A} - \bar{\partial}\varepsilon$, $\hat{\chi} \to \hat{\chi} + \frac{1}{2}\partial\varepsilon$, and $\hat{\bar{\chi}} \to \hat{\bar{\chi}} + \frac{1}{2}\bar{\partial}\varepsilon$. Integrating out $A, \bar{A}$ and $\chi, \bar{\chi}$, we recover the linear-dilaton $\times$ S^1 background eq. (2.18) as expected.

The $\hat{\chi}\hat{W}$ system is the familiar ($c = 2$) bosonic ghost "$\beta\gamma$" system, except that $\hat{W} \sim \hat{W} + 2\pi i\sqrt{\alpha' k}$ is cylinder-valued. The holomorphic stress tensor is

$$T(z) = -\frac{1}{\alpha'}(\partial\hat{r})^2 - Q\partial^2\hat{r} - \frac{1}{\alpha'}\hat{\chi}\partial\hat{W}, \tag{2.71}$$

whose central charge $3 + 6\alpha' Q^2$ reproduces the exact central charge $3k/(k-2)$ of $\mathrm{SL}(2,\mathbb{C})_k/\mathrm{SU}(2)$. $\hat{\chi}(z)$ carries conformal weight $(1,0)$ and $\hat{W}(z)$ is dimensionless, where the equations of motion imply $\bar{\partial}\hat{W} = \bar{\partial}\hat{\chi} = 0$. Their OPE is

$$\hat{W}(z)\hat{\chi}(0) \sim \frac{\alpha'}{z}, \tag{2.72}$$

with $\hat{W}(z)\hat{W}(0)$ and $\hat{\chi}(z)\hat{\chi}(0)$ non-singular. The anti-holomorphic sector is analogous.

Having obtained the free-field limit eq. (2.69) at the conformal boundary of EAdS_3, we now follow FZZ and attempt to define a dual description by taking the free theory over the infinite $\hat{r}$ line and deforming it by an appropriate uplift of the sine-Liouville potential. As explained following eq. (2.61), $\mathrm{SL}(2,\mathbb{R})_k$ and $\mathrm{SL}(2,\mathbb{R})_k/\mathrm{U}(1)$ contain an identical marginal operator $\mathcal{O}_{\mathrm{sL}}$, whose weak-coupling limit in the coset is the sine-Liouville potential (eq. (2.28)). One may identify the same operator in the continued space of $\mathrm{SL}(2,\mathbb{C})_k/\mathrm{SU}(2)$ operators. We wish to find the asymptotic form of this operator in the linear-dilaton $\times$ $\mathcal{F}(\mathbb{C}/\mathbb{Z})$ description of the EAdS_3 boundary. We will therefore search for a marginal operator of the free theory that carries unit winding around $\mathrm{Im}(\hat{W})$ and no momentum, such that it reduces to the familiar sine-Liouville potential upon gauging the symmetry.

The winding operators of the first-order cylinder system are less familiar than those of the ordinary compact boson [65]. From eq. (2.72) one obtains

$$\hat{W}(z)e^{\mp\sqrt{\frac{k}{\alpha'}}\int^0 \mathrm{d}z'\,\hat{\chi}+\mathrm{d}\bar{z}'\hat{\bar{\chi}}} \sim \pm\sqrt{\alpha' k}\log(z)e^{\mp\sqrt{\frac{k}{\alpha'}}\int^0 \mathrm{d}z'\,\hat{\chi}+\mathrm{d}\bar{z}'\hat{\bar{\chi}}}, \tag{2.73}$$

and likewise for $\hat{\bar{W}}(\bar{z})$. Thus, $e^{\mp\sqrt{\frac{k}{\alpha'}}\int^0 \mathrm{d}z'\,\hat{\chi}+\mathrm{d}\bar{z}'\hat{\bar{\chi}}}$ carries winding ± 1 with respect to $\hat{\theta} = \frac{1}{2i}(\hat{W} - \hat{\bar{W}})$, while $\hat{\xi} = \frac{1}{2}(\hat{W} + \hat{\bar{W}})$ is single-valued. The integral $\int^0 \mathrm{d}z'\,\hat{\chi} + \mathrm{d}\bar{z}'\hat{\bar{\chi}}$ is evaluated along a contour ending at the origin, where the winding operator is inserted. Demanding that observables be independent of the choice of contour constrains the spectrum of the CFT, such that the integrated expression defines a local operator [65].

This winding operator alone is not annihilated by the current $J^3 = \hat{\chi} + \frac{1}{4}(\partial\hat{W} + \partial\hat{\bar{W}})$, however:[41]

$$\left(\hat{\chi}(z) + \frac{1}{4}\partial\hat{W}(z)\right)e^{\mp\sqrt{\frac{k}{\alpha'}}\int^0 \mathrm{d}z'\,\hat{\chi}+\mathrm{d}\bar{z}'\hat{\bar{\chi}}} \sim \pm\frac{\sqrt{\alpha' k}}{4z}e^{\mp\sqrt{\frac{k}{\alpha'}}\int^0 \mathrm{d}z'\,\hat{\chi}+\mathrm{d}\bar{z}'\hat{\bar{\chi}}}. \tag{2.74}$$

[41] The last term $\partial\hat{\bar{W}}$ in the current is trivial by the equations of motion, and does not contribute to any OPEs.

JHEP10(2022)195

To obtain a winding operator with no momentum along the cylinder one must append the factor $e^{\pm\frac{1}{4}\sqrt{\frac{k}{\alpha'}}(\hat{W}+\hat{\bar{W}})}$, which cancels against the OPE eq. (2.74). The OPE of $\hat{W}$ with itself being non-singular, the inclusion of this factor preserves the winding OPE eq. (2.73).

Thus, the combination

$$e^{\pm\frac{1}{4}\sqrt{\frac{k}{\alpha'}}\left(\hat{W}+\hat{\bar{W}}\right)}e^{\mp\sqrt{\frac{k}{\alpha'}}\int \mathrm{d}z'\,\hat{\chi}+\mathrm{d}\bar{z}'\hat{\bar{\chi}}}, \tag{2.75}$$

or more simply $e^{\mp k\int \mathrm{d}z'\chi+\mathrm{d}\bar{z}'\bar{\chi}}$ in the unhatted variables, carries zero momentum and winding ± 1, as desired. Its conformal weight is $k/4$ on the left and right due to the double-contraction with the stress tensor eq. (2.71), just as for the ordinary winding operators $e^{\pm i\sqrt{\frac{k}{\alpha'}}(\hat{\theta}_{\mathrm{L}}-\hat{\theta}_{\mathrm{R}})}$ of the two-dimensional cylinder (eq. (2.34)).

In fact, eq. (2.75) is precisely the dimensional uplift of these ordinary winding operators. Gauging the translation symmetry as in eq. (2.70) and solving the auxiliary equations of motion, one finds $\hat{\chi}=\frac{1}{2}\partial\hat{\xi}-i\partial\hat{\theta}$. Evaluating eq. (2.75) on this solution yields

$$e^{\pm\frac{1}{2}\sqrt{\frac{k}{\alpha'}}\hat{\xi}}e^{\mp\frac{1}{2}\sqrt{\frac{k}{\alpha'}}\int\left(\mathrm{d}z'\partial\hat{\xi}+\mathrm{d}\bar{z}'\bar{\partial}\hat{\xi}\right)}e^{\pm i\sqrt{\frac{k}{\alpha'}}\int\left(\mathrm{d}z'\partial\hat{\theta}-\mathrm{d}\bar{z}'\bar{\partial}\hat{\theta}\right)}=e^{\pm i\sqrt{\frac{k}{\alpha'}}\left(\hat{\theta}_{\mathrm{L}}-\hat{\theta}_{\mathrm{R}}\right)}, \tag{2.76}$$

the equations of motion of the gauged action implying $\partial\bar{\partial}(\hat{W}-\hat{\bar{W}})=0$ and therefore $\hat{\theta}(z,\bar{z})=\hat{\theta}_{\mathrm{L}}(z)+\hat{\theta}_{\mathrm{R}}(\bar{z})$.

Finally, to this unit winding operator we append the same linear-dilaton primary $e^{-\sqrt{\frac{k-2}{\alpha'}}\hat{r}}$ as in eq. (2.36) to obtain a marginal operator. The three-dimensional sine-Liouville potential is then $W_+ + W_-$, where

$$W_{\pm}(z,\bar{z})=e^{-\sqrt{\frac{k-2}{\alpha'}}\hat{r}(z,\bar{z})}e^{\pm\frac{1}{4}\sqrt{\frac{k}{\alpha'}}\left(\hat{W}(z)+\hat{\bar{W}}(\bar{z})\right)}e^{\mp\sqrt{\frac{k}{\alpha'}}\int^{z,\bar{z}}\mathrm{d}z'\,\hat{\chi}+\mathrm{d}\bar{z}'\hat{\bar{\chi}}}, \tag{2.77}$$

and which reduces to the original two-dimensional sine-Liouville potential upon gauging.

The proposal is that the deformation of the linear-dilaton $\times\,\mathcal{F}(\mathbb{C}/\mathbb{Z})$ background (eq. (2.69)) by V_{sL} yields a dual description of $\mathrm{SL}(2,\mathbb{C})_k/\mathrm{SU}(2)$, which is a better description of the CFT when $k-2$, and therefore the linear-dilaton momentum, is small. If one further identifies $\hat{W}\sim\hat{W}+4\pi^2\sqrt{\alpha' k}/\beta_{\mathrm{BH}}$ (corresponding to compactifying $\xi\sim\xi+4\pi^2/\beta_{\mathrm{BH}}$), the same deformation of the linear-dilaton $\times\,\mathcal{F}(\mathbb{C}/(\mathbb{Z}\times\mathbb{Z}))$ yields a dual description of the Euclidean black hole CFT $\mathbb{Z}\backslash\mathrm{SL}(2,\mathbb{C})_k/\mathrm{SU}(2)$.

For string theory in $\mathrm{SL}(2,\mathbb{C})_k/\mathrm{SU}(2)$ and $\mathbb{Z}\backslash\mathrm{SL}(2,\mathbb{C})_k/\mathrm{SU}(2)$, the natural vertex operators are labeled by points on the spacetime conformal boundary cylinder or torus, where they correspond to an insertion of a local operator of the boundary CFT. In the dual description, such an operator behaves asymptotically as a linear-dilaton primary times a delta-function primary of the first-order CFT at that point, plus a sub-leading contribution due to reflection off the sine-Liouville potential in the interior.

Eq. (2.77) gives the limiting form of the components $\mathcal{W}_{\pm}$ of the $\mathrm{SL}(2,\mathbb{C})_k/\mathrm{SU}(2)$ sine-Liouville operator near the conformal boundary of EAdS_3. Recall from eq. (2.61) that $\mathcal{W}_{\pm}$ is obtained from the primary $|k/2-1,\pm k/2,\pm k/2\rangle$ by applying $w=\mp 1$ units of spectral flow. The asymptotic limit of the former is $e^{-(k-2)r}e^{\pm k\xi}$. Spectral flow is

JHEP10(2022)195

meanwhile implemented by the operator $e^{kw\int^z \mathrm{d}z' J^3 + \mathrm{d}\bar{z}'\bar{J}^3} = e^{kw\xi} e^{kw\int^z \mathrm{d}z'\chi + \mathrm{d}\bar{z}'\bar{\chi}}$, where $J^3(z) = \partial\xi + \chi$ [66]. Together, one obtains $\mathcal{W}_\pm \to e^{-(k-2)r} e^{\mp k\int \mathrm{d}z'\chi + \mathrm{d}\bar{z}'\bar{\chi}}$, which is identical to eq. (2.77) with the coordinate transformation Eq. (2.68).

In summary, the proposed duality of $\mathrm{SL}(2,\mathbb{C})_k/\mathrm{SU}(2)$, or its asymptotic EAdS_3 black hole quotient $\mathbb{Z}\backslash\mathrm{SL}(2,\mathbb{C})_k/\mathrm{SU}(2)$, is as follows. On the one hand one has the familiar description, weakly coupled for large k, of a string propagating in a solid cylinder or torus supported by a B-field:

$$S_{\mathrm{EAdS}_3} = \frac{k}{4\pi}\int_\Sigma \mathrm{d}^2\sigma\sqrt{h}\,\Big\{(\nabla r)^2 + \cosh^2(r)(\nabla\xi)^2 + \sinh^2(r)(\nabla\theta)^2 - 2\epsilon^{ab}\sinh^2(r)\nabla_a\xi\nabla_b\theta + \frac{\Phi_0}{k}\mathcal{R}[h]\Big\}, \tag{2.78}$$

where $\sqrt{h}\epsilon^{z\bar{z}} = -\sqrt{h}\epsilon^{\bar{z}z} = -i$. In first-order variables (eq. (2.64)), this background approaches a free linear-dilaton times first-order cylinder system in the $r \to \infty$ limit (eq. (2.69)). The dual sine-Liouville description is given by the same free theory, defined now with an infinite linear-dilaton direction extending into the strong-coupling region, deformed by the marginal potential with unit winding and zero momentum,

$$S_{\mathrm{sL}} = \frac{1}{4\pi\alpha'}\int_\Sigma \mathrm{d}^2\sigma\sqrt{h}\,\Big\{(\nabla\hat{r})^2 + 2h^{ab}(\hat{\chi}_a\nabla_b\hat{W} + \hat{\bar{\chi}}_a\nabla_b\hat{\bar{W}}) + 4\pi\lambda(W_+ + W_-) - \alpha' Q\mathcal{R}[h]\hat{r}\Big\}. \tag{2.79}$$

Gauging the translation symmetry in the two descriptions recovers the cigar and two-dimensional sine-Liouville backgrounds, reproducing the original FZZ duality and strongly suggesting the validity of this three-dimensional proposal. We expect there is an analogous supersymmetric duality given by the uplift of the supersymmetric FZZ duality of Hori and Kapustin [22].

This three-dimensional sine-Liouville background shares many similarities with its two-dimensional counterpart. For example, by integrating over the zero-mode one obtains a relation analogous to eq. (2.41), where now $\mathcal{S}_N$ denote operators of the first-order system rather than the compact boson. In particular, the correlation functions obey the scaling relation λ^κ, where κ is given in eq. (2.40). The same type of scaling is predicted by the dual Wakimoto description of the $\mathrm{SL}(2,\mathbb{C})_k/\mathrm{SU}(2)$ CFT [67–69]. Once again the lack of analyticity is due to the freedom to rescale λ by field redefinitions up to shifts of the dilaton zero-mode. In an action with a given coefficient λ and zero-mode Φ_0, the latter may always be eliminated with the former rescaled to $e^{-2b_{\mathrm{sL}}\Phi_0/Q}\lambda$.

The $\mathrm{SL}(2,\mathbb{C})_k/\mathrm{SU}(2)$ CFT may alternatively be described in Poincarè coordinates by the linear-dilaton $\times\,\mathcal{F}(\mathbb{C})$ system deformed by the Wakimoto potential $\beta\bar{\beta}e^{-2\sigma}$ [28]. We relabel here the linear-dilaton field as σ and the first-order fields as β and γ to be consistent with the notation in eq. (2.47), which is reproduced upon integrating out $\beta,\bar{\beta}$. If one were to quotient $\gamma \sim \gamma + 2\pi i$ in this description, i.e. replacing $\mathcal{F}(\mathbb{C})$ by $\mathcal{F}(\mathbb{C}/\mathbb{Z})$, one would obtain a singular background with a cusp at $\sigma \to -\infty$ where the transverse Poincarè metric $e^{2\sigma}\mathrm{d}\gamma\mathrm{d}\bar{\gamma}$ shrinks. Continuing with respect to the compact Euclidean time $\mathrm{Im}(\gamma)$ would then yield a thermal state in the Poincarè patch at inverse temperature 2π.

JHEP10(2022)195

If one deforms this cusp theory by the spectral flow of the Wakimoto operator around the compactified cycle, it is natural to conjecture that an RG flow is initiated back to the $\mathrm{SL}(2,\mathbb{C})_k/\mathrm{SU}(2)$ CFT. The spectral flow in this case preserves the marginal conformal weight of the operator, and introduces winding one around $\mathrm{Im}(\gamma)$. One may further deform the cusp theory by any number of such spectral-flowed operators with any values of spectral flow without changing the endpoint of the RG flow. These flows are reminiscent of discussions of closed string tachyon condensation in string theory [70–77]. By adding all the spectral-flowed operators with particular coefficients, one expects to obtain another description of the $\mathrm{SL}(2,\mathbb{C})_k/\mathrm{SU}(2)$ CFT, as a condensate of winding strings on the thermal Poincarè orbifold. In principle, smoothness of the interior, as encoded in conformal invariance of the worldsheet theory, would determine the coefficients of all of the spectral-flowed operators.

2.3 Infinitesimal dualities

Finally, we describe an infinitesimal interpretation of the FZZ duality and its three-dimensional uplift described in the previous sub-sections. This interpretation is based on the isomorphism eq. (2.58) that relates the spectral-flowed components $\mathcal{W}_\pm$ of the sine-Liouville operator to unflowed current-algebra descendents, as identified by the authors of [41]. We apply their identification of these vertex operators to discuss an infinitesimal version of each duality in the sense of conformal perturbation theory around the $\mathrm{SL}(2,\mathbb{R})_k/\mathrm{U}(1)$ or $\mathbb{Z}\backslash\mathrm{SL}(2,\mathbb{C})_k/\mathrm{SU}(2)$ CFTs: there are two semi-classical descriptions of perturbations by the sine-Liouville operator which shift the mass of the black hole. In the unflowed description of the perturbation, the value of the dilaton zero-mode is shifted. In the flowed description, the perturbation introduces a condensate of strings that wrap the horizon.

As reviewed in sections 2.1.2 and 2.2.1, the $\mathrm{SL}(2,\mathbb{R})_k$ and $\mathrm{SL}(2,\mathbb{R})_k/\mathrm{U}(1)$ CFT spectra share a marginal operator $\mathcal{O}_{\mathrm{sL}} = \mathcal{W}_+ + \mathcal{W}_-$, normalizable[42] for $k > 3$ and non-normalizable for $2 < k < 3$. One may likewise identify $\mathcal{O}_{\mathrm{sL}}$ in the continued spectrum of $\mathrm{SL}(2,\mathbb{C})_k/\mathrm{SU}(2)$ operators, again (delta-function) normalizable for $k > 3$. The sine-Liouville potential is the limiting form of $\mathcal{O}_{\mathrm{sL}}$ near the weak-coupling boundary in the various sigma-model descriptions of these CFTs.

The sine-Liouville Lagrangians for these CFTs make evident that a conformal perturbation by $\mathcal{O}_{\mathrm{sL}}$ is trivial at the CFT level. The deformation merely shifts the coefficient λ of the sine-Liouville potential, which may be undone by a field redefinition that shifts $\hat{r}$ by a constant. Then the perturbation leaves the same sine-Liouville background, except that the dilaton has been shifted by a constant, resulting from the linear-dilaton in $\hat{r}$. The latter is a trivial improvement term of the CFT, the only effect being to multiply the functional integral by $e^{-\delta\Phi_0\chi}$, where χ is the worldsheet Euler characteristic.[43]

In the string theory, however, $e^{-2\Phi_0}\lambda^{\frac{2}{k-2}}$ controls the mass of the black hole, which is deformed under the perturbation. That the perturbation is normalizable for $k > 3$ implies that the black hole mass may fluctuate [78, 79].[44]

[42] Delta-function normalizable in the $\mathrm{SL}(2,\mathbb{R})_k$ case.

[43] Not to be confused with the first-order auxiliary field.

[44] For $2 < k < 3$ the CFTs likely no longer admit a black hole interpretation [80].

JHEP10(2022)195

Consider the $\mathrm{SL}(2,\mathbb{R})_k/\mathrm{U}(1)$ case. The infinitesimal duality will equate two descriptions of the perturbation by $\mathcal{O}_{\mathrm{sL}}$ in the cigar sigma-model at large k. In one description, the deformation shifts the value Φ_0 of the dilaton at the tip of the cigar, and in the other it introduces a condensate of strings that wrap the tip.

The latter description follows from the asymptotic conditions eq. (2.32) that characterize insertions of $\mathcal{W}_\pm$ in the cigar. In conformal perturbation theory, a deformation by $\varepsilon \int \mathrm{d}^2 z\, \mathcal{O}_{\mathrm{sL}}$ is expanded in powers of ε:

$$e^{-\varepsilon \int (\mathcal{W}_+ + \mathcal{W}_-)} = \sum_{N_1,N_2=0}^{\infty} \frac{(-\varepsilon)^{N_1+N_2}}{N_1! N_2!} \left(\int \mathcal{W}_+\right)^{N_1} \left(\int \mathcal{W}_-\right)^{N_2} . \tag{2.80}$$

At large k, $\mathcal{W}_\pm \propto \mathrm{sech}^k(r)$ is a heavy operator that changes the behavior of the saddles of the functional integral. In the neighborhood of each $\mathcal{W}_\pm$ insertion, the asymptotic condition implies that the image of the string worldsheet asymptotically wraps the tip of the cigar with winding ± 1 (figure 11a). In this way, the conformal perturbation by $\mathcal{O}_{\mathrm{sL}}$ introduces a condensate of strings that wrap the horizon.

To understand the dual semi-classical description of the perturbation, recall from eq. (2.61) that $\mathcal{W}_\pm$ correspond to the states $|j = k/2-1, m = \bar{m} = \pm k/2; w = \mp 1\rangle$ in the $\widehat{\mathfrak{sl}}_k(2,\mathbb{R})_{\mathrm{L}} \oplus \widehat{\mathfrak{sl}}_k(2,\mathbb{R})_{\mathrm{R}}$ representations $\widehat{D}^{\pm,\mp 1}_{\frac{k}{2}-1} \otimes \widehat{D}^{\pm,\mp 1}_{\frac{k}{2}-1}$. By eq. (2.58), $\widehat{D}^{\pm,\mp 1}_{\frac{k}{2}-1}$ is isomorphic to $\widehat{D}^{\mp}_1$, under which the spectral-flowed primaries $\mathcal{W}_\pm$ are identified with unflowed descendents at level one [41]:

$$\left|\frac{k}{2}-1, \pm\frac{k}{2}, \pm\frac{k}{2}; \mp 1\right\rangle \simeq J^{\pm}_{-1} \bar{J}^{\pm}_{-1} \left|1, \mp 1, \mp 1; 0\right\rangle . \tag{2.81}$$

For example, $J^-_{-1}\left|j=1, m=1; w=0\right\rangle$ carries zero J^3_0 charge, is of holomorphic conformal weight one, and is a lowest-weight state of $\mathfrak{sl}(2,\mathbb{R})_{\mathrm{L}}$, consistent with the properties of $|k/2-1, -k/2; 1\rangle$. The latter belongs to the normalizable spectrum for $k > 3$, such that $j = k/2-1$ satisfies the lower bound $j > 1/2$. The former likewise belongs to the spectrum for $k > 3$, such that $j = 1$ satisfies the upper bound $j < \frac{k-1}{2}$, the spectral-flow isomorphism $j \to k/2 - j$ exchanging the upper and lower bounds.

The sine-Liouville operator $\mathcal{O}_{\mathrm{sL}}$ is the sum of the $w = \mp 1$ operators on the left of eq. (2.81). Let us denote by $\mathcal{O}_\Phi$ the sum on the right.[45] The isomorphism identifies the two. On a flat worldsheet, the vertex operator for $\mathcal{O}_\Phi$ in the cigar description is, at large k [22],

$$\mathcal{O}_\Phi(z,\bar{z})\big|_{\mathrm{flat}} = \frac{k}{2\pi} \mathrm{sech}^2(r) \left(\partial r \bar{\partial} r + \tanh^2(r) \partial\theta\bar{\partial}\theta\right) . \tag{2.82}$$

Recalling the cigar metric eq. (2.2a), this operator is evidently a metric deformation. Namely, adding to the cigar action $\varepsilon \int \mathrm{d}^2 z\, \mathcal{O}_\Phi$ results in a sigma-model with shifted metric

$$\mathrm{d}s^2[\varepsilon] = \alpha' k \left(\mathrm{d}r^2 + \tanh^2(r) \mathrm{d}\theta^2\right) \left(1 + \varepsilon \mathrm{sech}^2(r)\right) . \tag{2.83}$$

[45] One could also consider the marginal operator defined by the differences of these operators, but this deformation breaks worldsheet parity [22].

JHEP10(2022)195

The deformed metric is in fact related to the original metric by a reparameterization $\tilde{r} = r + \frac{1}{2}\varepsilon \tanh(r)$:

$$\mathrm{d}s^2[\varepsilon] = \alpha' k \left(\mathrm{d}\tilde{r}^2 + \tanh^2(\tilde{r})\mathrm{d}\theta^2\right) + \mathcal{O}\left(\varepsilon^2\right). \tag{2.84}$$

On a curved worldsheet, the deformation by $\mathcal{O}_\Phi$ must simultaneously transform the dilaton $\Phi \to \Phi[\varepsilon] = -\log\cosh(\tilde{r}) + \tilde{\Phi}_0 + \mathcal{O}(\varepsilon^2)$ so as to preserve the conformal symmetry of the background:

$$\Phi[\varepsilon] = -\log\cosh(r) + \Phi_0 - \frac{1}{2}\varepsilon \tanh^2(r) + \varepsilon\delta\Phi_0 + \mathcal{O}\left(\varepsilon^2\right). \tag{2.85}$$

We have also allowed for the deformation to shift the zero-mode $\Phi_0 \to \tilde{\Phi}_0 = \Phi_0 + \varepsilon\delta\Phi_0$, eq. (2.7) placing no constraint on the constant mode of the dilaton. Since the operator is normalizable at large k, one expects the deformation to vanish at large r, from which we infer that $\delta\Phi_0 = \frac{1}{2}$. Then the vertex operator for $\mathcal{O}_\Phi$ is given by

$$\mathcal{O}_\Phi(z,\bar{z}) = \operatorname{sech}^2(r)\left(\frac{k}{2\pi}\left(\partial r\bar{\partial}r + \tanh^2(r)\partial\theta\bar{\partial}\theta\right) + \frac{1}{16\pi}\mathcal{R}[h]\right). \tag{2.86}$$

The deformation of the cigar sigma-model by $\varepsilon\int \mathrm{d}^2z\,\mathcal{O}_\Phi$ is thus again almost trivial. By the field redefinition $r \to \tilde{r}$ one may undo the deformation, up to a shift $\Phi_0 \to \Phi_0 + \frac{\varepsilon}{2}$ of the value of the dilaton at the tip. This is a trivial improvement term from the perspective of the CFT. In the string theory, however, Φ_0 sets the mass of the black hole (eq. (2.13)), which is shifted under the perturbation, $\delta M = -\varepsilon M$.

Thus, the identification eq. (2.81) leads to an infinitesimal form of the FZZ duality, relating superficially different marginal deformations of the cigar that shift the mass of the black hole. One description simply shifts the value of the dilaton at the tip of the cigar, while the dual description introduces a condensate of winding strings that wrap the tip.

For a black hole of a given mass M, one may formally apportion the mass between the value of the dilaton at the tip and the strength of the condensate — as for Φ_0 and λ in the sine-Liouville description, neither of the two parameters is independently meaningful. One may always trade away the contribution from the condensate in favor of a shifted value of the dilaton by applying the duality. The black hole may therefore be described by the pure cigar background eq. (2.2) of mass eq. (2.13) with the condensate turned off, just as one may set the constant mode of the dilaton to zero in the sine-Liouville background eq. (2.35). Alternatively, one may trade Φ_0 in favor of the condensate. Then as in the sine-Liouville description one may think of the black hole as being made up of winding strings. The conformal perturbation adds additional strings and so increases the black hole mass.

The same isomorphism eq. (2.81) between $\mathcal{O}_{\mathrm{sL}}$ and $\mathcal{O}_\Phi$ holds in three dimensions, and therefore the duality of $\mathrm{SL}(2,\mathbb{C})_k/\mathrm{SU}(2)$ and its black hole quotient $\mathbb{Z}\backslash\mathrm{SL}(2,\mathbb{C})_k/\mathrm{SU}(2)$ admits a similar infinitesimal interpretation. The black hole mass is given by [23, 24]

$$M = \frac{1}{8G_{\mathrm{N}}}\frac{R_{\mathrm{s}}^2}{l_{\mathrm{AdS}}^2}, \tag{2.87}$$

JHEP10(2022)195

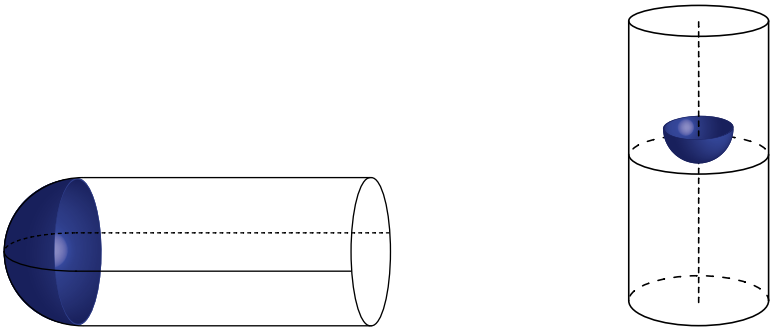

(a) (b)

Figure 11. *Sine-Liouville Asymptotic Conditions.* The spacetime image of the string worldsheet in the neighborhood of a $\mathcal{W}_+$ insertion is shown in the cigar description of $\mathrm{SL}(2,\mathbb{R})_k/\mathrm{U}(1)$ (left) and the cylinder description of $\mathrm{SL}(2,\mathbb{C})_k/\mathrm{SU}(2)$ (right).

where the horizon radius is related to the inverse Hawking temperature by $\beta_{\mathrm{BH}} = 2\pi l_{\mathrm{AdS}}/R_{\mathrm{s}}$. In three-dimensional gravity, $G_{\mathrm{N}} \propto l_{\mathrm{p}} \propto g_{\mathrm{s}}^2 l_{\mathrm{s}}$. Thus, $M \propto e^{-2\Phi_0}$ as in the two-dimensional black hole. A conformal perturbation by $\mathcal{O}_\Phi$ again shifts the constant mode of the dilaton, and in turn the mass. To understand the dual interpretation, one needs the asymptotic conditions for $\mathcal{W}_\pm$ in EAdS_3. The asymptotic conditions eq. (2.32) in the cigar followed from the $\rho \to -\infty$ limit of the cigar-wrapping saddle $r = \sinh^{-1}(e^\rho)$, $\theta = \pm\phi$ [40]. This configuration may be uplifted to a solution of the $\mathrm{SL}(2,\mathbb{C})_k/\mathrm{SU}(2)$ equations of motion with

$$\xi = \pm\frac{1}{2}\log\left(1 + e^{2\rho}\right). \tag{2.88}$$

We conjecture that the asymptotic condition for $\mathcal{W}_\pm$ in EAdS_3 and the Euclidean black hole is then as in eq. (2.32), together with $\xi \to \pm\frac{1}{2}e^{2\rho}$, up to shifts by a constant. Then the perturbation by $\mathcal{O}_{\mathrm{sL}}$ again introduces a condensate of horizon-crossing strings, the horizon now corresponding to the one-dimensional locus $r = 0$ (figure 11b).

This completes our discussion of the Euclidean dualities of the $\mathrm{SL}(2,\mathbb{R})_k/\mathrm{U}(1)$, $\mathrm{SL}(2,\mathbb{C})_k/\mathrm{SU}(2)$, and $\mathbb{Z}\backslash\mathrm{SL}(2,\mathbb{C})_k/\mathrm{SU}(2)$ CFTs. Our goal in the remainder of the paper is to understand the Lorentzian string dualities that follow by analytic continuation in the sense of the target time coordinate. In the next section we discuss how such continuations define Lorentzian string theories in various spacetime states, before finally applying this machinery to describe the ER = EPR string dualities in section 4.

3 State dependence of string perturbation theory

String perturbation theory is often phrased as an expansion around a Lorentzian spacetime solution. However, this is not entirely precise. Even in the non-linear sigma-model approximation at leading order in α', the target space time direction has wrong-sign kinetic terms, and so the definition of the worldsheet functional integral requires the specification of an appropriate contour in a complexification of the target space. Such contours are string theory analogues of the Schwinger-Keldysh contours familiar from field theory. They consist

JHEP10(2022)195

of Euclidean caps that specify the spacetime state, with the Lorentzian background glued between them. In this section, we describe this formulation of string perturbation theory, emphasizing in particular string perturbation theory around the thermofield-double and Hartle-Hawking states that appear in the ER = EPR dualities we propose in section 4.

3.1 Schwinger-Keldysh contours for Lorentzian string theory

Suppose one wishes to construct a string perturbation theory around a Lorentzian geometry M. Roughly speaking, one often thinks of the worldsheet CFT as a sigma-model[46] into M, but this is imprecise for two related reasons. First, the Lorentzian signature of M implies that the kinetic term for the target time coordinate has the wrong sign. Then the sigma-model action on a Euclidean worldsheet is unbounded below, and the functional integral over the real target fields diverges.[47,48] Second, a string perturbation theory is not in general defined by choosing a target geometry M alone; one must also choose a state of semi-classical quantum gravity in spacetime around which one wishes to construct the perturbation theory.[49]

For example, suppose $M = \mathrm{AdS}_3$, on which we will focus in this section because it is one of the simplest and best understood examples. In constructing string perturbation theory in AdS_3, one can choose from a variety of states, such as the global AdS vacuum, an excited state above the vacuum, a thermal state, the thermofield-double (TFD) state in two copies of AdS_3, and so on.

The divergence of the functional integral over Lorentzian target fields and the ambiguity in the choice of state are closely related. The functional integral should instead be defined by continuation from a sigma-model with Euclidean target. Such a continuation is not unique, and the choice one makes encodes the state around which the perturbation theory is defined. Thus, the divergence of the functional integral and the necessity of choosing a state are reconciled by defining the functional integral along a contour in a complexification of the

[46] Combined with background fields to support conformal symmetry, and a unitary internal CFT to cancel the conformal anomaly.

[47] In this section, we always choose a Euclidean metric on the worldsheet. When we speak of continuing between Lorentzian and Euclidean signatures, we mean with respect to the time coordinate of the target space M. We will describe the continuation of the worldsheet metric that is appropriate for computing Lorentzian string amplitudes in the next section. We argue, there, that in the vicinity of a Euclidean time winding operator insertion, the Euclidean worldsheet (or, more precisely, the string moduli space) should be continued to Lorentzian signature in the sense of angular quantization. This prescription generalizes that of [38] for ordinary momentum operators, whose neighborhood is continued in the sense of radial quantization when integrating over the moduli.

[48] The functional integral over real spatial directions can also diverge, such as along the asymptotic linear-dilaton directions present in several of the backgrounds we consider in this paper [40, 61, 81]. Along such directions the functional integral should again be defined over a complex cycle in the target space. But that issue is separate from the divergence of the functional integral over the time coordinate in Lorentzian backgrounds.

[49] When computing the string S-matrix in Minkowski spacetime, it is usually implicit that one has chosen the vacuum state. But one could also consider, for example, string perturbation theory in Minkowski spacetime in a thermal state [82, 83], or the HH state of a black hole in asymptotic Minkowski spacetime, and so on.

JHEP10(2022)195

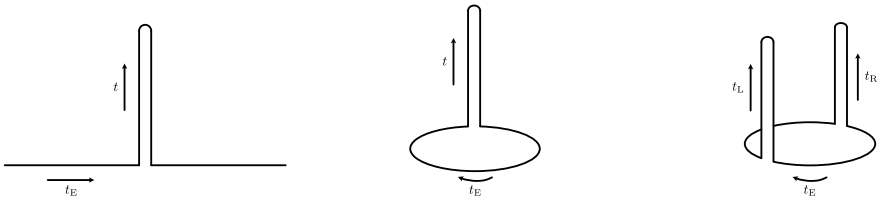

(a) (b) (c)

Figure 12. *Schwinger-Keldysh Contours.* A Schwinger-Keldysh contour is a contour in the complex time plane that consists of Euclidean caps joined to Lorentzian excursions. The functional integral defined along such a contour computes the expectation value of operators inserted on the Lorentzian section between the initial and final states specified by the Euclidean caps. In field theory, the contour defines the domain on which the fields are defined. In string theory, it is the contour in target space over which the worldsheet functional integral is to be performed. The first contour pictured computes expectation values in a pure state such as the vacuum. The second computes expectation values in a thermal state, and the third in a TFD state.

target space. The contour consists of Euclidean caps at either end, which ensure convergence of the functional integral, joined along a Lorentzian excursion in the middle [84–87].

Several such contours in the complex target time plane are pictured in figure 12. The first computes expectation values in a pure state such as the vacuum, the second in a thermal state, and the third in a TFD state. They share a common Lorentzian section (with two copies thereof in the last example), but correspond to different complexifications of the target time $t_E + it$, t_E being non-compact in the first and compact in the second and third. Moreover, the periodicity $t_E \sim t_E + \beta$ in the latter cases is an additional choice, specifying the inverse temperature of the thermal state.[50]

The continuation is real when the Lorentzian geometry has a Z_2 time-reflection isometry. Moreover the Euclidean and Lorentzian sections share a common zero-time slice — the fixed-point locus of the symmetry — along which they may be glued together to define the contour.

Complex time contours of this form are familiar from ordinary field theory, where they are known as Schwinger-Keldysh contours. In that context, they are contours in the base spacetime, rather than in the target space. Then the contour specifies the domain on which the fields are defined, and the functional integral computes expectation values between the states specified by the caps. The functional integral over the incoming Euclidean cap prepares a state in the Hilbert space of the quantum field theory on the spatial slice to which it is glued. Then the state is evolved forward in Lorentzian time and any desired local operators are inserted. Finally, the Lorentzian segment is reversed and glued to the outgoing Euclidean cap which prepares the outgoing state.

Such complexified functional integrals may be computed by starting from a Euclidean correlation function and moving the operators to the Lorentzian section by continuing the insertion times in the Euclidean answer. One thinks of cutting open the Euclidean manifold

[50]For a black hole geometry, the periodicity of the Euclidean continuation is fixed to obtain a smooth geometry. Then the black hole in the HH state has a fixed temperature. However, a thermal state in e.g. AdS can have any temperature (at least, until the Hagedorn limit).

JHEP10(2022)195

on one or more constant Euclidean time slices and gluing in the Lorentzian excursion. Moreover, one need not continue all of the operator insertions to the Lorentzian section. Operators left on the Euclidean caps prepare different states in which the expectation value is computed.

In string theory, the Schwinger-Keldysh contour becomes a contour in the target space, over which the functional integral that defines the worldsheet CFT is to be performed. Again, one may proceed by starting from a worldsheet correlation function with the Euclidean target and then continuing the vertex operator insertions to the Lorentzian section. Of course, it is not the location of the vertex operator insertion on the worldsheet that one wishes to continue in this case, but rather the quantum numbers that label how the operator transforms under the spacetime symmetries. The Euclidean caps define the state in which the string perturbation theory is constructed, and in AdS/CFT, the string amplitudes compute expectation values of the boundary CFT in the dual state associated to the caps.[51] One may also construct string theories with different initial and final states, e.g. by fixing different operator insertions on the incoming and outgoing Euclidean sections.

In fact, regarded as a deformation of the Euclidean integration contour in target space, the Lorentzian excursion is contractible. It does not alter the homology cycle of the Euclidean functional integral, and therefore inserting the excursion does not change the integral. One merely takes the Euclidean answer and continues the labels to Lorentzian time.

Although we have phrased the above discussion in the sigma-model approximation, which is convenient for visualizing the target geometry as a complex contour for the functional integral, it is not necessary to resort to a Lagrangian description of the worldsheet CFT. One may begin from an abstract definition of the CFT by its three-point function and OPE, and continue the operator labels to define the Lorentzian string theory. As we review now, string theory in AdS_3 in various states is constructed by continuation from the unitary $\mathrm{SL}(2,\mathbb{C})_k/\mathrm{SU}(2)$ coset CFT, and various orbifolds thereof, without requiring any reference to a Lagrangian.

3.2 States in AdS_3

Let us make this discussion concrete for strings in AdS_3 and related examples. In eqs. (2.42) and (2.44) we defined EAdS_3 by the continuation $\xi = it$ from AdS_3, with $\xi \in (-\infty, \infty)$. The Lorentzian metric is time-independent, and so one may cut it along any spatial slice and glue in a Euclidean cap to prepare a state. Cutting and gluing the two cylinders at $\xi = t = 0$ prepares the global AdS_3 vacuum state.

Alternatively, one could define the Euclidean continuation with compact $\xi \sim \xi + \beta$. The resulting manifold is known as thermal AdS_3 ($\mathrm{TAdS}_3|_\beta = \mathrm{EAdS}_3/\beta\mathbb{Z}$), and has the topology of a solid torus whose non-contractible cycle is parameterized by ξ. Cutting the torus at $\xi = 0$ and gluing in the Lorentzian cylinder prepares a thermal state in AdS_3 at inverse temperature β. More generally, one may slice the torus in half by making cuts at both $\xi = 0$ and $\xi = \beta/2$, and then glue a copy of AdS_3 at each cut. The result is the TFD

[51] More precisely, the string amplitudes compute contributions to the boundary CFT expectation values. Depending on whether or not the background is the dominant bulk saddle for a given boundary CFT observable, the corresponding string amplitudes will be the dominant contribution or a sub-dominant correction.

JHEP10(2022)195

(a) (b)

Figure 13. *TFD and Factorized Vacuum States in* $\mathrm{AdS}_3 \cup \mathrm{AdS}_3$. Thermal AdS_3, obtained from Euclidean AdS_3 by compactifying the global time coordinate $\xi \sim \xi + \beta$, has the topology of a solid torus. Cutting the torus in half at $\xi = 0$ and $\xi = \beta/2$ and gluing a copy of Lorentzian AdS_3 at each prepares the TFD state in two disconnected copies of AdS_3 (left). By contrast, the factorized vacuum (right) is an unentangled state prepared by cutting EAdS_3 in half and gluing it to each copy of AdS_3. In the figure, the EAdS_3 half-cylinder has been compactified to a half-ball.

state in two disconnected copies of AdS_3 (figure 13a). Tracing over one slice returns the thermal state on the other, corresponding to sewing one of the cuts back up. Figure 13b shows the same two copies of AdS_3, now with each in its vacuum state. In the figure we have compactified the half-cylinder to the half-ball.

As reviewed in section 2.2.1, AdS_3 is equivalent to $\mathrm{SL}(2,\mathbb{R})$, and to describe a bosonic string in AdS_3 it is natural to take the $\mathrm{SL}(2,\mathbb{R})_k$ WZW model for the worldsheet CFT [28–31, 54, 55]. The $\mathrm{SL}(2,\mathbb{R})_k$ WZW action is an inadequate definition of the worldsheet CFT, however, for the reasons explained above. Instead one must choose a state, and define the theory by the corresponding continuation from a unitary CFT. The simplest choice is the vacuum state, corresponding to continuation from $\mathrm{EAdS}_3 = \mathrm{SL}(2,\mathbb{C})/\mathrm{SU}(2)$. The $\mathrm{SL}(2,\mathbb{C})_k/\mathrm{SU}(2)$ coset was studied in [32, 56, 57]. Its continuation to Lorentzian signature, constructed in [31, 54, 55], defines string perturbation theory in AdS_3 in the spacetime vacuum state, as we review now in some detail. We then describe string perturbation theories with other choices of the spacetime state.

3.2.1 Vacuum state

Consider the theory of a string in AdS_3 in the spacetime vacuum state. As reviewed in section 2.2.1, the isometry algebra of $\mathrm{AdS}_3 = \mathrm{SL}(2,\mathbb{R})$ is $\mathfrak{sl}(2,\mathbb{R})_{\mathrm{L}} \oplus \mathfrak{sl}(2,\mathbb{R})_{\mathrm{R}} \simeq \mathfrak{so}(2,2)$, which is extended to an $\widehat{\mathfrak{sl}}_k(2,\mathbb{R})_{\mathrm{L}} \oplus \widehat{\mathfrak{sl}}_k(2,\mathbb{R})_{\mathrm{R}}$ current algebra of the worldsheet CFT. As usual in AdS/CFT, the isometry algebra of the bulk is identified with the global conformal algebra of the dual CFT (BCFT) defined on the spacetime conformal boundary. Namely, the BCFT global conformal generators[52] $\{\mathsf{L}_0, \mathsf{L}_{\mp 1}\} \cup \{\bar{\mathsf{L}}_0, \bar{\mathsf{L}}_{\mp 1}\}$ satisfy the same algebra as the current zero-modes $\{J_0^3, J_0^{\pm}\} \cup \{\bar{J}_0^3, \bar{J}_0^{\pm}\}$ (eq. (2.52)): $[\mathsf{L}_0, \mathsf{L}_{\mp 1}] = \pm \mathsf{L}_{\mp 1}$, $[\mathsf{L}_{-1}, \mathsf{L}_1] = -2\mathsf{L}_0$, and similarly for the anti-holomorphic sector.

Likewise, the $\mathrm{SL}(2,\mathbb{C})_k/\mathrm{SU}(2)$ coset is equipped with an $\widehat{\mathfrak{sl}}_k(2,\mathbb{C})$ current algebra, whose global sub-algebra $\mathfrak{sl}(2,\mathbb{C}) \simeq \mathfrak{so}(1,3)$ is the isometry algebra of EAdS_3 and the global

[52] We denote the worldsheet Virasoro generators by L_n and the BCFT Virasoro generators by L_n.

JHEP10(2022)195

conformal algebra of the BCFT in Euclidean signature.[53] The two current algebras share a common complexification, $\widehat{\mathfrak{sl}}_k(2,\mathbb{C})_{\rm L} \oplus \widehat{\mathfrak{sl}}_k(2,\mathbb{C})_{\rm R}$. The complexified global sub-algebra $\mathfrak{sl}(2,\mathbb{C})_{\rm L} \oplus \mathfrak{sl}(2,\mathbb{C})_{\rm R}$ is the standard complexification of the global conformal algebra from the perspective of the BCFT, wherein the complex coordinate x and its complex-conjugate $\bar{x}$ on the boundary sphere are promoted to independent complex coordinates, on which the holomorphic and anti-holomorphic dual Virasoro generators act independently.

Whereas string amplitudes in asymptotically flat space compute S-matrix elements, string amplitudes in AdS compute correlation functions of local operators of the BCFT, or expectation values thereof in Lorentzian signature. The spectrum of the BCFT is organized in unitary representations of its Virasoro algebra,

$$[\mathsf{L}_n, \mathsf{L}_m] = (n-m)\mathsf{L}_{n+m} + \frac{\mathsf{c}}{12}\left(n^3 - n\right)\delta_{n+m}, \tag{3.1}$$

and similarly for $\bar{\mathsf{L}}_n$, with $[\mathsf{L}_n, \bar{\mathsf{L}}_m] = 0$. The central charge is, at large k, [89]

$$\mathsf{c} = \frac{3}{2}\frac{l_{\rm s}}{l_{\rm p}}\sqrt{k}. \tag{3.2}$$

The representations are built on Virasoro primary states labeled by their spins $(J, \bar{J})$, which are positive real numbers. Focusing on the holomorphic factor, a Virasoro primary state $|J, M = J\rangle$ is annihilated by the positive modes $\mathsf{L}_{n>0}$ and is an eigenstate of L_0 with eigenvalue $M = J$. Being annihilated by L_1, it sits at the bottom of a lowest-weight discrete-series representation $D_J^+ = \{|J, M\rangle : M \in J + \mathbb{N}\}$ of the global conformal algebra $\mathfrak{sl}(2,\mathbb{C})_{\rm L}$, the descendent states being obtained by action of L_{-1}, $|J, M\rangle \propto (\mathsf{L}_{-1})^{M-J}|J, J\rangle$.

To each global representation D_J^+, one associates by the state-operator map a primary operator $\mathcal{O}_J(x)$ that transforms under $\mathfrak{sl}(2,\mathbb{C})_{\rm L}$ according to

$$[\mathsf{L}_{-1}, \mathcal{O}_J(x)] = \partial\mathcal{O}_J(x) \tag{3.3a}$$

$$[\mathsf{L}_0, \mathcal{O}_J(x)] = (x\partial + J)\,\mathcal{O}_J(x) \tag{3.3b}$$

$$[\mathsf{L}_1, \mathcal{O}_J(x)] = \left(x^2\partial + 2Jx\right)\mathcal{O}_J(x). \tag{3.3c}$$

$\mathcal{O}_J(x)$ prepares the lowest-weight state when inserted at the origin, $\mathcal{O}_J(0)|0\rangle = |J, J\rangle$. By the AdS/CFT dictionary, there is a dual state of a string in AdS_3, which likewise transforms as a lowest-weight state in D_J^+, now with respect to the global $\mathfrak{sl}(2,\mathbb{C})_{\rm L}$ sub-algebra of the worldsheet current algebra. The descendent states $|J, M\rangle \in D_J^+$ are prepared in the boundary by inserting derivatives of $\mathcal{O}_J(x)$, which are dual to excited string states in the bulk.

Similarly, when inserted at the point-at-infinity, $\lim_{x\to\infty} x^{2J}\mathcal{O}_J(x)$ prepares a highest-weight state $|J, M = -J\rangle \in D_J^-$. Thus, lowest-weight states may be interpreted as in-states and highest-weight states as out-states.

[53] Prior to the quotient, one has an $\widehat{\mathfrak{sl}}_k(2,\mathbb{C})_{\rm L} \oplus \widehat{\mathfrak{sl}}_k(2,\mathbb{C})_{\rm R}$ current algebra corresponding to the independent symmetries $g \to \Omega_{\rm L} g \Omega_{\rm R}^\dagger$ on the left and right. After the quotient, one is left with a single copy of the symmetry to preserve Hermiticity, $g \to \Omega g \Omega^\dagger$.

JHEP10(2022)195

The string amplitudes, which compute correlation functions of such BCFT operators, are defined by continuation from the $\mathrm{SL}(2,\mathbb{C})_k/\mathrm{SU}(2)$ coset CFT. The spectrum of the latter is organized in representations of its $\widehat{\mathfrak{sl}}_k(2,\mathbb{C})$ current algebra. These are standard current-algebra representations, built upon a spin-j representation of the global $\mathfrak{sl}(2,\mathbb{C})$ sub-algebra that is primary with respect to the positive current modes.[54] The primaries appearing in the coset Hilbert space are the continuous-series representations with $j \in \frac{1}{2} + i\mathbb{R}_+$ [32, 56, 57]. j may be continued away from this line, however [31, 32]. Indeed, these are not the representations of interest for string theory in AdS_3 — they correspond to the bosonic string tachyon, and would map to dual representations with complex conformal weights.

As in the two-dimensional BCFT context recalled above, the spin-j representation of $\mathfrak{sl}(2,\mathbb{C})$ may be described in a function space basis, with the generators implemented by differential operators acting on functions of a complex coordinate x [32, 57]:

$$\mathcal{D}^3 = x\frac{\partial}{\partial x} + j, \qquad \mathcal{D}^+ = \frac{\partial}{\partial x}, \qquad \mathcal{D}^- = x^2\frac{\partial}{\partial x} + 2jx. \tag{3.4}$$

The primary operators of the worldsheet $\widehat{\mathfrak{sl}}_k(2,\mathbb{C})$ current algebra may then be written $\Phi_j(z,\bar{z};x,\bar{x})$, where $(z,\bar{z})$ are worldsheet coordinates and $(x,\bar{x})$ parameterize the representation. Their OPEs with the currents are

$$J^a(z)\,\Phi_j(z',\bar{z}';x,\bar{x}) \sim \frac{\mathcal{D}^a\Phi_j(z',\bar{z}';x,\bar{x})}{z-z'} \qquad a = 3,\pm. \tag{3.5}$$

They are worldsheet scalars of conformal weight

$$h_j = -\frac{j(j-1)}{k-2}. \tag{3.6}$$

h_j is a real number for $j \in \frac{1}{2} + i\mathbb{R}$, as well as for $j \in \mathbb{R}$. In the former case it is always positive, while in the latter it is positive only in the window $0 < j < 1$. Note also that h_j is symmetric under $j \to 1-j$, a reflection about $j = \frac{1}{2}$.

In the asymptotic region, the vertex operators behave for large k as [29, 32]

$$\Phi_j(z,\bar{z};x,\bar{x}) \overset{\sigma\to\infty}{\longrightarrow} e^{-2(1-j)\sigma}\delta^2(\gamma-x) + \frac{1}{\pi}(2j-1)e^{-2j\sigma}|\gamma-x|^{-4j}. \tag{3.7}$$

Accounting for the measure factor $\sqrt{g} = l_{\mathrm{AdS}}^2 e^{2\sigma}$ from the metric eq. (2.45), observe that the target wavefunction is delta-function normalizable only for $\mathrm{Re}(j) = \frac{1}{2}$, consistent with the preceding statement that the $\mathrm{SL}(2,\mathbb{C})_k/\mathrm{SU}(2)$ Hilbert space contains only the complex branch states.

For $\mathrm{Re}(j) < \frac{1}{2}$, the second exponential dominates, and the operator is spread over the boundary sphere. For $\mathrm{Re}(j) > \frac{1}{2}$, however, the first term dominates, and the non-normalizability of the wavefunction is localized at $\gamma = x$, interpreted as a source for an operator of the BCFT on the boundary S^2. eq. (3.7) is the standard asymptotic expansion of a solution to the AdS_3 wave equation for a scalar of mass $l_{\mathrm{AdS}}^2 m^2 = \Delta(\Delta-2)$, with a

[54] As in section 2.2.1, we denote the $\mathfrak{sl}(2,\mathbb{C})$ spin j and J_0^3 eigenvalue m by lower-case letters for unflowed representations, and capital J, M for spectral-flowed representations.

JHEP10(2022)195

delta-function source at $(x, \bar{x})$ for the dual operator of dimension $\Delta = 2j$. The leading term inserts the source and the sub-leading term is $e^{-2j\sigma}/(2\Delta - d)$ times the two-point function of the dual operator [90].

Thus, for $j > \frac{1}{2}$ one has a map from the worldsheet vertex operator $\Phi_j(z, \bar{z}; x, \bar{x})$ to a primary scalar BCFT operator $\hat{\Phi}_j(x, \bar{x})$ of real conformal weight (j, j) inserted at $(x, \bar{x})$, the transformation of the vertex operator under the global sub-algebra (eq. (3.5)) matching the global conformal transformation of the boundary operator (eq. (3.3)).[55] A string amplitude with many insertions $\Phi_{j_i}(z_i, \bar{z}_i; x_i, \bar{x}_i)$ computes a BCFT correlation function on S^2 with operator insertions at $(x_i, \bar{x}_i)$ of dual conformal weights (j_i, j_i).[56] The vertex operators with $j > \frac{1}{2}$ are non-normalizable from the perspective of the $SL(2, \mathbb{C})_k/SU(2)$ coset, as appropriate for operators that insert delta-function sources on the boundary of Euclidean AdS, and are defined by analytic continuation in j [31, 32]. String amplitudes of two, three, and four primaries were studied in this way in [31].

From BCFT correlation functions on S^2, the boundary insertion points $(x, \bar{x})$ may be continued in the usual way from the Euclidean sphere to the Lorentzian cylinder in order to define expectation values of the BCFT in the vacuum state (figure 14). The conformal transformation $(x = e^{\xi + i\theta}, \bar{x} = e^{\xi - i\theta})$ maps the sphere to the Euclidean cylinder, and continuing $\xi \to it$ yields the Lorentzian cylinder $(x = e^{i(t+\theta)}, \bar{x} = e^{i(t-\theta)})$. In doing so, one has continued $(x, \bar{x})$ to independent complex coordinates, and in turn the vertex operator $\Phi_j(z, \bar{z}; x, \bar{x})$ is continued to a representation of the complexified current algebra $\widehat{\mathfrak{sl}}_k(2, \mathbb{C})_{\mathrm{L}} \oplus \widehat{\mathfrak{sl}}_k(2, \mathbb{C})_{\mathrm{R}}$. The original boundary S^2 and the Lorentzian cylinder correspond to two real sections of the complexification. On the worldsheet, one interpolates between vertex operators for insertions on the Euclidean sphere or Lorentzian cylinder by restricting the complexified primary $\Phi_j(z, \bar{z}; x, \bar{x})$ to the appropriate section.

For example, the two-point amplitude of $\Phi_j(z, \bar{z}; x, \bar{x})$ is [31]

$$\left\langle \hat{\Phi}_j(x_1, \bar{x}_1) \hat{\Phi}_j(x_2, \bar{x}_2) \right\rangle = \frac{1}{V_{\mathrm{conf}}} \left\langle \Phi_j(z = 0; x_1, \bar{x}_1) \Phi_j(z = 0; x_2, \bar{x}_2) \right\rangle \propto |x_{12}|^{-4j}, \tag{3.8}$$

as appropriate for a BCFT scalar of dimension $2j$. Making the boundary conformal transformation $\Phi_j(z, \bar{z}; x, \bar{x}) \to e^{-2j\xi} \Phi_j(z, \bar{z}; \xi, \theta)$, one obtains the standard CFT two-point function for a scalar on the cylinder:

$$\left\langle \hat{\Phi}_j(\xi_1, \theta_1) \hat{\Phi}_j(\xi_2, \theta_2) \right\rangle \propto (\cosh(\xi_{12}) - \cos(\theta_{12}))^{-2j} . \tag{3.9}$$

As expected for a Euclidean correlation function, this expression is non-singular as long as the two insertions are not coincident.

To obtain a Lorentzian expectation value, one slides each insertion to the zero-time slice and then onto the Lorentzian section:

$$\langle 0 | \, \hat{\Phi}_j(t_1, \theta_1) \hat{\Phi}_j(t_2, \theta_2) \, | 0 \rangle \propto (\cos(t_{12}) - \cos(\theta_{12}))^{-2j} . \tag{3.10}$$

[55] More precisely, one has a map from $\Phi_j(z, \bar{z}; x, \bar{x}) \otimes \mathcal{O}_h(z, \bar{z})$, where $\mathcal{O}_h$ is a primary of the internal CFT such that the combined vertex operator is marginal. The construction of the full BCFT Virasoro algebra was discussed in [28–30].

[56] In fact, the string partition function is related to the BCFT generating functional in an ensemble in which the BCFT central charge fluctuates. To obtain a standard CFT with fixed central charge one must perform a Legendre transform of the string partition function, as explained in [69].

JHEP10(2022)195

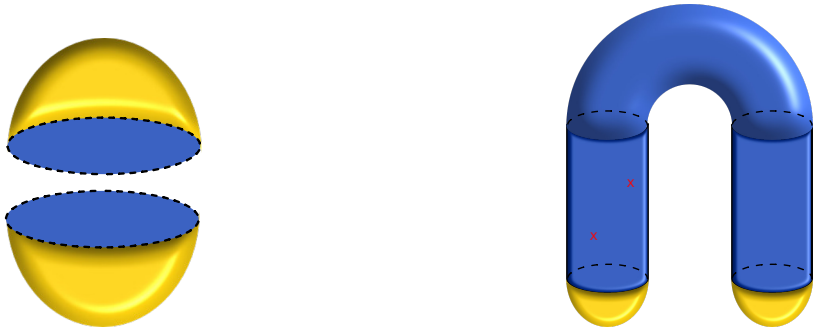

(a) (b)

Figure 14. AdS_3 *Vacuum Schwinger-Keldysh Contour*. String amplitudes for AdS_3 in the spacetime vacuum state compute vacuum expectation values of the dual CFT and are defined by continuation from $SL(2,\mathbb{C})_k/SU(2)$. The Euclidean amplitudes compute BCFT correlation functions on the S^2 conformal boundary of $EAdS_3$, with insertions at the points $(x,\bar{x})$ which labeled the worldsheet vertex operators. The spacetime is complexified and the insertions continued to the Lorentzian section to obtain vacuum expectation values. Though the procedure does not rely on a Lagrangian, one may think of these amplitudes as defined by a worldsheet functional integral along the Schwinger-Keldysh contour in target space shown. A Euclidean cap (in yellow) prepares the AdS_3 vacuum, which is glued to a Lorentzian excursion (in blue) that flows forward and backward in time, and is then glued to the outgoing vacuum cap. String vertex operators insert dual operators on the conformal boundary, indicated by the red $\times$'s. Operators may also be left on the Euclidean caps to define string perturbation theory in AdS_3 in different excited pure states.

In doing so, one encounters singularities when one operator hits the lightcone of the other, $t_{12} = \pm\theta_{12}$. Following the usual $i\varepsilon$ prescription to avoid the singularity and obtain a time-ordered expectation value, one replaces $t \to t(1-i\varepsilon)$. We mostly suppress the $i\varepsilon$'s for notational simplicity.

The perturbative string states of eq. (2.54) may be identified with the modes of the boundary position basis vertex operators. For example, the vertex operators $\Phi_{jm\bar{m}}(z,\bar{z})$ for the string states $|j,m,\bar{m}\rangle$ are formally given by the spacetime Fourier transform of $\Phi_j(z,\bar{z};t,\theta)$:

$$\Phi_{jm\bar{m}}(z,\bar{z}) \propto \int_{-\infty}^{\infty} \mathrm{d}t \int_{0}^{2\pi} \mathrm{d}\theta\, e^{-i(m+\bar{m})t} e^{-i(m-\bar{m})\theta} \Phi_j(z,\bar{z};t,\theta), \tag{3.11}$$

where $m+\bar{m}$ is the spacetime energy and $m-\bar{m}$ is the angular momentum, and similarly for the spectral-flowed operators reviewed below. One may likewise compute string amplitudes of such momentum-basis insertions [31].

When inserted at the origin of the Euclidean section, $\Phi_j(z,\bar{z};x,\bar{x})$ prepares the lowest-weight state $|j,j,j\rangle$ in the representation $D_j^+ \otimes D_j^+$ of the global sub-algebra:

$$\Phi_j(z=0;x=0)\,|0\rangle = |j,j,j\rangle\,. \tag{3.12}$$

This is the bulk string state dual to the BCFT Virasoro primary state of conformal weight (j,j), the latter prepared by the dual operator $\hat{\Phi}_j(x=0)$, both transforming as lowest-

JHEP10(2022)195

weight states of $\mathfrak{sl}(2,\mathbb{C})_{\rm L}\oplus\mathfrak{sl}(2,\mathbb{C})_{\rm R}$.[57] The global descendent states $|j,m,\bar m\rangle\in D_j^+\otimes D_j^+$, related to the lowest-weight state by the action of $J_0^+,\bar J_0^+$, are prepared by inserting x derivatives of $\Phi_j(z,\bar z;x,\bar x)$, and are dual to the global conformal descendents of the BCFT Virasoro primary. In the bulk effective field theory, $|j,j,j\rangle$ is the lowest-energy state of a scalar field of mass[58] $l_{\rm AdS}^2m^2=\Delta(\Delta-2)$ dual to the BCFT scalar primary operator of dimension $\Delta=2j$.

Of course, the Virasoro primaries of the dual CFT are not all scalars. In addition to the current-algebra primaries $\Phi_j(z,\bar z;x,\bar x)$ that prepare lowest-weight states $|j,j,j\rangle\in\widehat D_j^+\otimes\widehat D_j^+$, one has vertex operators denoted $\Phi_{jw}^{J\bar J}(z,\bar z;x,\bar x)$ that prepare the spectral-flowed states of eq. (2.54) [31]:

$$\Phi_{jw}^{J\bar J}(z=0;x=0)\,|0\rangle=\Big|j,m=J-kw/2,\bar m=\bar J-kw/2;w\Big\rangle\,,\qquad w>0. \tag{3.13}$$

These operators are worldsheet Virasoro — but not current-algebra — primaries of conformal weights as in eq. (2.57b):

$$h_{jw}^{J\bar J}=-\frac{j(j-1)}{k-2}-wJ+\frac14kw^2,\qquad \bar h_{jw}^{J\bar J}=-\frac{j(j-1)}{k-2}-w\bar J+\frac14kw^2. \tag{3.14}$$

They carry the additional labels[59] $(J,\bar J)$ specifying their spins with respect to the global $\mathfrak{sl}(2,\mathbb{C})_{\rm L}\oplus\mathfrak{sl}(2,\mathbb{C})_{\rm R}$, as well as the spectral-flow label w.

Recall from section 2.2.1 that, for $w>0$, the spectral flow $|j,m,\bar m;w\rangle$ of a current-algebra primary carries J_0^3 weight $M=m+\frac k2w$ and transforms as a lowest-weight state $|J,M=J\rangle\in D_J^+$ with respect to $\mathfrak{sl}(2,\mathbb{C})_{\rm L}$, and similarly for $\mathfrak{sl}(2,\mathbb{C})_{\rm R}$ with $\bar M=\bar J=\bar m+\frac k2w$. Thus, each spectral-flowed primary $|j,m,\bar m;w\rangle$ with $w>0$ sits at the bottom of a discrete-series representation[60] $D_J^+\otimes D_{\bar J}^+$ of the global sub-algebra, and is dual to a BCFT Virasoro primary state of spin $(J,\bar J)$.[61] Associated to each such lowest-weight string state one has a vertex operator $\Phi_{jw}^{J\bar J}(z,\bar z;x,\bar x)$ that prepares it. The global descendent states $(J_0^+)^N(\bar J_0^+)^{\bar N}\,|j,m,\bar m;w\rangle$ are as before prepared by insertions with derivatives.[62]

For $w<0$, on the other hand, $|j,m,\bar m;w\rangle$ transforms as a highest-weight state $|J',-J'\rangle\otimes\Big|\bar J',-\bar J'\Big\rangle\in D_{J'}^-\otimes D_{\bar J'}^-$ of spin $J'=-\Big(m+\frac k2w\Big)$, $\bar J'=-\Big(\bar m+\frac k2w\Big)$. As recalled earlier, a lowest-weight state is interpreted as an in-state in the dual CFT, prepared by a

[57] Again, once combined with an internal operator such that the Virasoro constraints are satisfied.

[58] It is hopefully clear from context when we use m to refer to the mass as opposed to the J_0^3 eigenvalue.

[59] For unflowed operators one has $\Phi_j=\Phi_{j,w=0}^{J=\bar J=j}$.

[60] Note that, with respect to the global sub-algebra, one obtains a lowest-weight discrete-series representation regardless of whether $|j,m,\bar m;w\rangle$ came from a spectral-flowed discrete-series $\widehat D_j^{+,w}\otimes\widehat D_j^{+,w}$ or continuous-series $\widehat C_{j,\alpha}^w\otimes\widehat C_{j,\alpha}^w$ representation of the current algebra, as appropriate for a primary of the BCFT. In a continuous-series representation, J and j (and $\bar J$ and j) are unrelated, whereas in a lowest-weight discrete-series representation they are related by $j=J-\frac k2w-\mathbb{N}$.

[61] Once combined with the internal CFT and subjected to the constraints. In particular, $J=m+\frac k2w$ is not guaranteed to be positive on the spectrum of the $\mathrm{SL}(2,\mathbb{R})_k$ WZW model. It is only after applying the Virasoro constraints that one obtains a physical state of positive $J,\bar J$, which maps to a primary of the BCFT.

[62] Note that $(J_0^+)^N(\bar J_0^+)^{\bar N}\,|j,m,\bar m;w\rangle=(J_{-w}^+[w])^N(\bar J_{-w}^+[w])^{\bar N}\,|j,m,\bar m;w\rangle$ transforms as a current-algebra descendent with respect to the unflowed generators, and should not be confused with the state $\Big|j,m+N,\bar m+\bar N;w\Big\rangle$. The latter is the lowest-weight state of its own discrete-series representation, and carries a different worldsheet conformal weight besides.

JHEP10(2022)195

spin $(J,\bar{J})$ primary insertion at the origin, whereas a highest-weight state is interpreted as an out-state, prepared by an insertion at infinity. $\Phi^{J\bar{J}}_{jw}(z,\bar{z};x,\bar{x})$, which likewise transforms as a local operator of spin $(J,\bar{J})$ in x-space with respect to the global sub-algebra, also prepares a lowest-weight in-state, and should therefore be labeled by $w>0$ as in eq. (3.13). When inserted at infinity, it prepares the highest-weight out-state $\left|j,-\left(J-\frac{k}{2}w\right),-\left(\bar{J}-\frac{k}{2}w\right);-w\right\rangle$ in $D^-_J\otimes D^-_{\bar{J}}$.

The complete spectrum of the $\mathrm{SL}(2,\mathbb{R})_k$ WZW model given in eq. (2.54), when combined with a unitary internal CFT and subjected to the Virasoro constraints, yields the unitary spectrum of strings in AdS_3 in the vacuum state [54]. The upper bound on the real branch, $j<\frac{k-1}{2}$, is required to obtain a unitary on-shell spectrum, and ensures compatibility with the spectral-flow isomorphism, which exchanges the upper and lower bounds under $j\to\frac{k}{2}-j$. The spectrum also includes the unflowed complex branch representations $\widehat{C}_{j=\frac{1}{2}(1+is),\alpha}$, whose vertex operators $\Phi_j(z,\bar{z};x,\bar{x})$ do not map to well-defined local operators of the BCFT. These are the bosonic string tachyons, whose spacetime mass $l^2_{\mathrm{AdS}}m^2=-1-s^2$ falls below the tachyonic BF bound $l^2_{\mathrm{AdS}}m^2<-1$ for a scalar in AdS_3 [54, 91].[63]

String amplitudes with spectral-flowed vertex operators were also computed in [31], and may similarly be continued to BCFT expectation values by continuing the boundary insertion points to the Lorentzian cylinder.

For a Virasoro primary $\Phi^{J\bar{J}}_{jw}\otimes\mathcal{O}_{h\bar{h}}$, with $\mathcal{O}_{h\bar{h}}$ a contribution from the internal CFT, the Virasoro constraint $L_0-1=0$ may be written

$$J=\frac{1}{4}kw+\frac{1}{w}\left(-\frac{j(j-1)}{k-2}+h-1\right). \tag{3.15}$$

On the complex branch, j and J are unrelated, and this equation gives a continuous spectrum of spacetime conformal weights parameterized by $\mathrm{Im}(j)$.[64] These are known as "long string" states. They are heavy in the semi-classical limit, J being of order k, and are believed to be a peculiarity of the pure NS background. For the real branch, on the other hand, j and J are related by $j=J-\frac{k}{2}w-N$, with $N\in\mathbb{N}$. Solving the on-shell condition for J then yields a discrete spectrum of spacetime conformal weights [54],

$$J=N+w+\frac{1}{2}+\sqrt{\frac{1}{4}+(k-2)\left(h-1-Nw-\frac{1}{2}w(w+1)\right)}. \tag{3.16}$$

These, by constrast, are known as "short string" states, and are the more typical vertex operators.

[63] We point out that below $k=3$, at which point it has been argued that the $\mathrm{SL}(2,\mathbb{R})_k$ WZW model undergoes a phase transition [21, 80], the real branch spectrum $\frac{1}{2}<j<\frac{k-1}{2}$ falls within the BF window $-1<l^2_{\mathrm{AdS}}m^2<0$ in which two normalizable fall-offs are admissible.

[64] The constraint guarantees J is positive, $-j(j-1)\geq\frac{1}{4}$ being bounded below on the complex branch and $h\geq 0$ being positive by unitarity of the internal CFT. Then eq. (3.15) is positive with $k>2$ and $w>0$. Note that the constraint, $m+\frac{k}{2}w=\frac{1}{4}kw+\frac{1}{w}\left(-\frac{j(j-1)}{k-2}+h-1\right)$, is invariant under $w\to-w$ and $m\to-m$. Namely, if $\Phi^{J\bar{J}}_{jw}(z,\bar{z};x,\bar{x})\otimes\mathcal{O}_{h,\bar{h}}(z,\bar{z})$ prepares a physical lowest-weight in-state $\left|j,J-\frac{k}{2}w,\bar{J}-\frac{k}{2}w;w\right\rangle\otimes\left|h,\bar{h}\right\rangle$ when inserted at the origin, then the highest-weight out-state $\left|j,-\left(J-\frac{k}{2}w\right),-\left(\bar{J}-\frac{k}{2}w\right);-w\right\rangle\otimes\left|h,\bar{h}\right\rangle$ obtained by inserting the operator at infinity is likewise physical.

JHEP10(2022)195

Next we describe how string perturbation theory in AdS_3 is defined for other choices of the state. Note first of all that one need not continue all the operator insertions in x-space to the Lorentzian section. Leaving an insertion on the Euclidean cap prepares the associated state on the cylinder from the perspective of the BCFT, and defines string perturbation theory in an excited pure state from the perspective of the worldsheet theory.

3.2.2 Thermal state

Suppose now that one wishes to study string perturbation theory in AdS_3 in a thermal state. In the BCFT, thermal expectation values are obtained by continuation from Euclidean correlation functions on T^2, the periodicity of the Euclidean time circle fixing the inverse temperature of the state. One constructs the Schwinger-Keldysh contour by cutting the torus at a single time-slice and gluing in the Lorentzian cylinder, or by cutting the torus in half to prepare the TFD state in two copies of the BCFT Hilbert space on a circle. In the bulk, this BCFT state is dual to the Hartle-Hawking wavefunctional defined by the gravitational functional integral with thermal boundary conditions at infinity and ending on a spatial slice bounded by two circles. Below the Hawking-Page temperature, this wavefunctional is sharply peaked on two disconnected copies of the AdS_3 metric, and above the Hawking-Page temperature it is peaked on the zero-time slice of the two-sided, asymptotically AdS_3 black hole [10].

Thus, one may think of the bulk dual to the BCFT TFD state as either the bulk TFD state in two disconnected copies of AdS_3 or the Hartle-Hawking (HH) state in the AdS_3 black hole. At the Hawking-Page temperature $T_{\rm HP} = \frac{1}{2\pi}$ (in AdS units) there is a first-order phase transition between the two [9, 10, 12]. At lower temperatures, the dominant bulk Euclidean saddle is $TAdS_3$, whose Euclidean time circle is non-contractible, while at higher temperatures the bulk saddle is the Euclidean black hole, which has the same solid-torus topology but whose Euclidean time direction is now identified with the contractible cycle.

The worldsheet theory for a string in $TAdS_3|_\beta$ is the $J_0^3+\bar{J}_0^3$ orbifold $\beta\mathbb{Z}\backslash \mathrm{SL}(2,\mathbb{C})_k/\mathrm{SU}(2)$ that compactifies the cylinder, $\xi \sim \xi + \beta$. String perturbation theory in a thermal state in AdS_3 is defined by continuation from this quotient. Its string amplitudes compute the dominant contribution to BCFT T^2 correlation functions below the Hawking-Page temperature. Above the Hawking-Page temperature, a thermal gas of strings in AdS_3 collapses to a black hole, which becomes the dominant contribution thereafter.[65] We discuss the black hole in the next sub-section.

The quotient preserves two of the six isometries of $EAdS_3$, corresponding to ξ and θ translations. The orbifold projection is

$$e^{i\beta\left(J_0^3+\bar{J}_0^3\right)}\Phi_j\left(z,\bar{z};x,\bar{x}\right)e^{-i\beta\left(J_0^3+\bar{J}_0^3\right)} = \Phi_j\left(z,\bar{z};x,\bar{x}\right). \tag{3.17}$$

[65] Until one reaches the Hagedorn temperature, where the theory becomes unstable. Of course, the bosonic string theory is already unstable because of the tachyon. But as the temperature is increased, the thermal circle becomes small and the modes that wind it become lighter. At the Hagedorn temperature, the circle becomes so small that the lightest winding mode becomes tachyonic [21, 82].

JHEP10(2022)195

After the boundary conformal transformation $x = e^{\xi+i\theta}$ which sends $\Phi_j(z,\bar{z};x,\bar{x}) \to e^{-2j\xi}\Phi_j(z,\bar{z};\xi,\theta)$, the projection condition simply enforces periodicity in ξ:

$$\Phi_j(z,\bar{z};\xi,\theta) = \Phi_j(z,\bar{z};\xi+\beta,\theta). \tag{3.18}$$

Each unflowed primary Φ_j of $\mathrm{SL}(2,\mathbb{C})_k/\mathrm{SU}(2)$ may be projected to an operator in the untwisted sector of the orbifold by summing over images,

$$\Phi_j(z,\bar{z};\xi,\theta) \to \sum_{n\in\mathbb{Z}} \Phi_j(z,\bar{z};\xi+\beta n,\theta). \tag{3.19}$$

For spectral-flowed operators, one may likewise sum over images of $\Phi^{J\bar{J}}_{jw}(z,\bar{z};x,\bar{x}) \to e^{-J(\xi+i\theta)}e^{-\bar{J}(\xi-i\theta)}\Phi^{J\bar{J}}_{jw}(z,\bar{z};\xi,\theta)$ to obtain a projection-invariant operator:

$$\Phi^{J\bar{J}}_{jw}(z,\bar{z};\xi,\theta) \to \sum_{n\in\mathbb{Z}} \Phi^{J\bar{J}}_{jw}(z,\bar{z};\xi+\beta n,\theta). \tag{3.20}$$

We emphasize that the projection acts on the Euclidean $\mathrm{SL}(2,\mathbb{C})_k/\mathrm{SU}(2)$ vertex operators and not on the spectrum of Lorentzian string states $|j,m,\bar{m};w\rangle \otimes \left|h,\bar{h}\right\rangle$. The string states are particle-like excitations on top of the AdS_3 background — whether the background is in the vacuum or thermal state does not affect the spectrum of particles.

The correlation functions of the projected primaries eqs. (3.19)–(3.20) in the orbifold are obtained by summing over images in the original $\mathrm{SL}(2,\mathbb{C})_k/\mathrm{SU}(2)$ correlators, and their amplitudes produce the T^2 correlation functions of the BCFT for $\beta > 2\pi$. Correspondingly, the BCFT local operators and correlation functions on T^2 may independently be obtained from the cylinder by summing over images.

The continuation to Lorentzian expectation values in the thermal state is as before. If one cuts the torus at $\xi = 0$ and continues the operators to the Lorentzian section, one obtains string amplitudes in AdS_3 in the thermal state at inverse temperature β. If one makes cuts at both $\xi = 0$ and $\xi = \beta/2$, one can continue the operator labels to either $\xi = it_{\mathrm{R}}$ or $\xi = \frac{\beta}{2} + it_{\mathrm{L}}$. The resulting string amplitudes compute expectation values of the continued insertions in two copies of AdS_3 in the TFD state. The corresponding Schwinger-Keldysh contour is obtained by gluing together two copies of figure 13a. One may also leave insertions on the T^2 Euclidean section to define perturbation theory in a thermal or TFD state deformed by sources.

For example, the two-point amplitude of Φ_j is obtained by summing over images in eq. (3.9),[66]

$$\left\langle \hat{\Phi}_j(\xi_1,\theta_1)\hat{\Phi}_j(\xi_2,\theta_2)\right\rangle \propto \sum_{n\in\mathbb{Z}} \left\{\cosh(\xi_{12}+n\beta) - \cos(\theta_{12})\right\}^{-2j}. \tag{3.21}$$

By cutting the torus at $\xi = 0$ and continuing both insertions to the Lorentzian cylinder one obtains the amplitude in a thermal state, [10, 92, 93]

$$\mathrm{tr}\left(e^{-\beta H}\hat{\Phi}_j(t_1,\theta_1)\hat{\Phi}_j(t_2,\theta_2)\right) \propto \sum_{n} \left\{\cos(t_{12}+in\beta) - \cos(\theta_{12})\right\}^{-2j}, \tag{3.22}$$

[66] Note that by simply replacing each operator by its sum over images, e.g. $\sum_{n,m\in\mathbb{Z}}\langle\mathcal{O}(\xi+n\beta)\mathcal{O}(\xi'+m\beta)\rangle = \sum_{\substack{n-m\in\mathbb{Z}\\ n+m\in\mathbb{Z}}}\langle\mathcal{O}(\xi-\xi'+(n-m)\beta)\mathcal{O}(0)\rangle$, one obtains an extraneous divergent sum $\sum_{n+m}$, which should be discarded.

JHEP10(2022)195

again suppressing the $i\varepsilon$'s. Alternatively, one could cut the torus at both $\xi = 0$ and $\xi = \beta/2$ preparing the TFD state, and e.g. continue one operator to each side

$$\begin{aligned} &\langle \mathrm{TFD}| \left(1_{\mathrm{L}} \otimes \hat{\Phi}_j(t_{\mathrm{R},1}, \theta_1)\right)\left(\hat{\Phi}_j(t_{\mathrm{L},2}, \theta_2) \otimes 1_{\mathrm{R}}\right) |\mathrm{TFD}\rangle \\ &\propto \sum_{n\in\mathbb{Z}} \left\{\cos\left(t_{\mathrm{R},1} - t_{\mathrm{L},2} + i\left(n - 1/2\right)\beta\right) - \cos(\theta_{12})\right\}^{-2j}. \end{aligned} \tag{3.23}$$

One may also consider twisted-sector operators of the orbifold, but these are not expected to map to local operators of the BCFT.

3.2.3 Hartle-Hawking state

Above the Hawking-Page temperature, the asymptotic AdS_3 black hole, known also as BTZ, is the dominant contribution to thermal BCFT expectation values [10, 12, 23, 24]. BTZ is a particularly simple black hole because it is a quotient of AdS_3, performed with respect to the $J_0^2 + \bar{J}_0^2$ isometry. The parameterization eq. (2.43) diagonalized the action of $J_0^3 \pm \bar{J}_0^3$. To describe the BTZ orbifold, it is more natural to diagonalize $J_0^2 \pm \bar{J}_0^2$ via

$$g = e^{i\left(\tilde{\Theta}+\tilde{T}\right)\mathrm{T}_2} e^{2i\tilde{R}\mathrm{T}_1} e^{i\left(\tilde{\Theta}-\tilde{T}\right)\mathrm{T}_2} \in \mathrm{SL}\left(2,\mathbb{R}\right), \tag{3.24}$$

on which the group metric evaluates to

$$\mathrm{d}s^2_{\text{AdS-Rindler}} = l^2_{\mathrm{AdS}}\left(-\sinh^2\left(\tilde{R}\right)\mathrm{d}\tilde{T}^2 + \mathrm{d}\tilde{R}^2 + \cosh^2\left(\tilde{R}\right)\mathrm{d}\tilde{\Theta}^2\right). \tag{3.25}$$

We recognize in eq. (3.25) the AdS_3-Rindler metric (eq. (2.62)), where $\tilde{T}, \tilde{\Theta} \in (-\infty, \infty)$ and $\tilde{R} \in (0, \infty)$. These coordinates cover only a wedge of AdS_3, up to the coordinate horizon at $\tilde{R} = 0$ where the coefficient of $\mathrm{d}\tilde{T}^2$ vanishes.

$\tilde{T}$ translations are implemented in eq. (3.24) by $g \to e^{i\delta\tilde{T}\mathrm{T}_2} g e^{-i\delta\tilde{T}\mathrm{T}_2}$, and $\tilde{\Theta}$ translations by $g \to e^{i\delta\tilde{\Theta}\mathrm{T}_2} g e^{i\delta\tilde{\Theta}\mathrm{T}_2}$. These isometries are therefore generated in $\mathrm{SL}(2,\mathbb{R})_k$ by $J_0^2 - \bar{J}_0^2$ and $J_0^2 + \bar{J}_0^2$, respectively. The (non-rotating) BTZ black hole of radius R_{s} is defined by the $J_0^2 + \bar{J}_0^2$ orbifold that compactifies

$$\tilde{\Theta} \sim \tilde{\Theta} + 2\pi R_{\mathrm{s}}/l_{\mathrm{AdS}}. \tag{3.26}$$

In $\mathrm{SL}(2,\mathbb{R})$, this is the identification $g \sim hgh$, with $h = e^{2\pi i R_{\mathrm{s}}\mathrm{T}_2/l_{\mathrm{AdS}}} = \mathrm{Diag}(e^{\pi R_{\mathrm{s}}/l_{\mathrm{AdS}}}, e^{-\pi R_{\mathrm{s}}/l_{\mathrm{AdS}}})$. h is a hyperbolic element of $\mathrm{SL}(2,\mathbb{R})$, meaning that $\mathrm{tr}(h) = 2\cosh(\pi R_{\mathrm{s}}/l_{\mathrm{AdS}}) > 2$. The quotient preserves the translation isometries in $\tilde{T}$ and $\tilde{\Theta}$.

The more familiar form of the BTZ metric is obtained by the coordinate transformation

$$R = R_{\mathrm{s}}\cosh(\tilde{R}), \qquad T = \frac{l_{\mathrm{AdS}}}{R_{\mathrm{s}}}\tilde{T}, \qquad \Theta = \frac{l_{\mathrm{AdS}}}{R_{\mathrm{s}}}\tilde{\Theta}, \tag{3.27}$$

in terms of which eq. (3.25) becomes

$$\mathrm{d}s^2_{\mathrm{BTZ}} = -\left(R^2 - R_{\mathrm{s}}^2\right)\mathrm{d}T^2 + \frac{l^2_{\mathrm{AdS}}}{R^2 - R_{\mathrm{s}}^2}\mathrm{d}R^2 + R^2\mathrm{d}\Theta^2, \tag{3.28}$$

with the BTZ identification $\Theta \sim \Theta + 2\pi$. These Schwarzschild-like coordinates cover the right wedge $R > R_{\mathrm{s}}$ of the black hole, which may as usual be extended to a two-sided

JHEP10(2022)195

geometry with left and right asymptotic AdS_3 regions separated by the horizon (figure 15a). The black hole mass was given in eq. (2.87).

The states of a string in BTZ are given by the $J_0^2+\bar{J}_0^2$ orbifold of the $SL(2,\mathbb{R})_k$ spectrum (eq. (2.54)) with the projection $e^{2\pi i R_s/l_{AdS}(J_0^2+\bar{J}_0^2)}=1$, combined with the twisted sectors that wind the compactified Θ cycle [33–35]. As in eq. (3.24), one therefore chooses a basis of $SL(2,\mathbb{R})_k$ that diagonalizes $J_0^2, \bar{J}_0^2$, which have continuous spectrum. The spectrum of the Hamiltonian $\frac{R_s}{l_{AdS}}(J_0^2-\bar{J}_0^2)$ with respect to the Schwarzschild time T is likewise continuous, as is expected from the bulk effective field theory in the black hole background in the $M_p\to\infty$ limit.

Note that in BTZ there is no simple relationship between the perturbative string states and BCFT primary operators, in contrast to the vacuum theory. In the latter case, for example, the lowest-weight string state $|j,j,j\rangle\in\widehat{D}_j^+\otimes\widehat{D}_j^+$ is prepared on the worldsheet by inserting $\Phi_j(z=0;x=0)$ (eq. (3.12)). It is dual to the BCFT Virasoro primary state $|j,j,j\rangle\in D_j^+\otimes D_j^+$, likewise transforming in the lowest-weight discrete-series representation of the boundary global conformal algebra, and itself prepared by inserting the dual operator $\hat{\Phi}_j(x=0)$ at the origin of the boundary hemisphere. Both states are eigenstates of the respective bulk and boundary Hamiltonians, global AdS_3 time translations being generated by $J_0^3+\bar{J}_0^3$, which maps to $\mathsf{L}_0+\bar{\mathsf{L}}_0$ in the dual. In BTZ, by contrast, a boundary local operator insertion does not prepare an eigenstate of the bulk Hamiltonian $J_0^2-\bar{J}_0^2$, and one should not expect a simple relationship between bulk string states and BCFT primaries.

The BTZ string theory is again defined by continuation from its Euclidean counterpart. Setting $\tilde{T}_E=i\tilde{T}$ in eq. (3.25) defines the Euclidean BTZ black hole (EBTZ):

$$\mathrm{d}s^2_{EBTZ}=l^2_{AdS}\left(\sinh^2\left(\tilde{R}\right)\mathrm{d}\tilde{T}_E^2+\mathrm{d}\tilde{R}^2+\cosh^2\left(\tilde{R}\right)\mathrm{d}\tilde{\Theta}^2\right). \tag{3.29}$$

Near $\tilde{R}=0$, the metric $\tilde{R}^2\mathrm{d}\tilde{T}_E^2+\mathrm{d}\tilde{R}^2+\mathrm{d}\tilde{\Theta}^2+\cdots$ describes the plane in polar coordinates times a circle, and the angle $\tilde{T}_E$ must be 2π periodic to obtain a smooth solution; the near-horizon Lorentzian geometry is then Rindler $\times\,S^1$. eq. (3.24) is likewise invariant under $\tilde{T}\to\tilde{T}+2\pi i$, as $e^{\pm 2\pi \mathrm{T}_2}=-1_{2\times 2}$. The Euclidean Schwarzschild time T_E is periodic in $\beta=2\pi l_{AdS}/R_s$, which is identified as the inverse Hawking temperature of the black hole in AdS units.

EBTZ at inverse temperature β is therefore a solid torus, with contractible cycle $\tilde{T}_E\sim\tilde{T}_E+2\pi$ and non-contractible cycle $\tilde{\Theta}\sim\tilde{\Theta}+4\pi^2/\beta$. It is identical to the $TAdS_3|_{\tilde{\beta}}$ solid torus at inverse temperature $\tilde{\beta}=2\pi R_s/l_{AdS}=4\pi^2/\beta$. When referring to $TAdS_3$, however, it is the non-contractible cycle that one identifies with the Euclidean time as in the previous sub-section. Whereas cutting the solid torus in half across its non-contractible cycle prepared the TFD state in two disconnected copies of AdS_3 (figure 13a), cutting across its contractible cycle produces a Euclidean cap in the shape of a halved bagel, which prepares the HH state in the connected black hole (figures 15b and 1a) [7, 8, 10].

The zero-time slice of the two-sided black hole is a wormhole passing between the left and right asymptotic AdS_3 regions. Topologically, it is an annulus, with the two circle boundaries corresponding to slices of the two AdS_3 boundary cylinders. The black hole is Z_2 symmetric with respect to this zero-time slice, and in preparing the HH state the annulus is glued to the halved EBTZ torus, whose annular boundary is identical.

JHEP10(2022)195

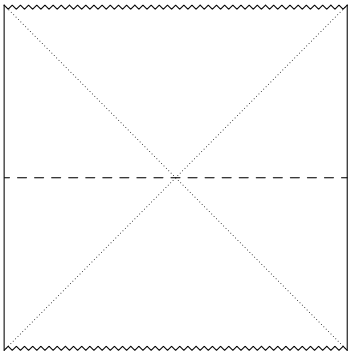

(a) *The BTZ Black Hole.* The BTZ black hole is the two-sided, asymptotically AdS_3 solution of three-dimensional gravity with negative cosmological constant. It is a quotient of AdS_3, obtained by compactifying $\tilde{\Theta} \sim \tilde{\Theta} + 2\pi R_s/l_{AdS}$ in the coordinates of eq. (3.24). The $\tilde{\Theta}$ circle is suppressed in the figure. The geometry is time-dependent, but Z_2 symmetric with respect to the dashed line. This line is the wormhole between the left and right causally disconnected regions. It has the topology of an annulus, with the two circle boundaries corresponding to slices of the asymptotic AdS_3 boundaries.

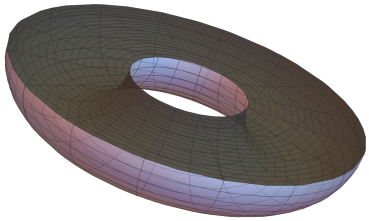

(b) *The Hartle-Hawking Cap.* The Euclidean continuation of the BTZ black hole is a solid torus, whose contractible cycle is identified with the Euclidean time. Slicing the torus in half across this cycle produces a manifold in the shape of a halved bagel. Its annular boundary is identical to the zero-time slice of the Lorentzian black hole, indicated by the dashed line on the left. Gluing the Euclidean cap to this slice prepares the Hartle-Hawking state in the black hole background (figure 1a), whose reduced density matrix in a single wedge is a thermal state of inverse temperature $2\pi l_{AdS}/R_s$. The purple boundary of the torus prepares the TFD state of the BCFT on the two circle boundaries of the annulus (figure 1b).

Figure 15. The Lorentzian and Euclidean BTZ Black Hole.

Alternatively, the HH state may be thought of as a TFD state with respect to the left and right wedges of the black hole, entangled by the Euclidean cap that evolves between them in angular time (figure 16a). The reduced density matrix in a single wedge is a thermal state at inverse temperature $\beta = 2\pi l_{AdS}/R_s$. In this sense, both slicings of the $TAdS_3$/EBTZ solid torus prepare TFD states, the distinction being that in the first case the spacetime is disconnected while in the second it is connected.

The worldsheet theory for a string in BTZ in the HH state is then similarly obtained by continuation from the $\frac{4\pi^2}{\beta}\mathbb{Z}\backslash SL(2,\mathbb{C})_k/SU(2)$ orbifold, but with the continuation now performed with respect to the contractible cycle [33–35]. The equivalence of $EBTZ|_\beta$ and $TAdS|_{4\pi^2/\beta}$ shows that the $J_0^3 + \bar{J}_0^3$ and $J_0^2 + \bar{J}_0^2$ orbifolds are identical in the Euclidean case, and we may proceed as in the previous sub-section but with the temperature inverted.

Thus, the projection to the untwisted sector of the orbifold is

$$e^{i\frac{4\pi^2}{\beta}\left(J_0^3+\bar{J}_0^3\right)}\Phi_j\left(z,\bar{z};x,\bar{x}\right)e^{-i\frac{4\pi^2}{\beta}\left(J_0^3+\bar{J}_0^3\right)} = \Phi_j\left(z,\bar{z};x,\bar{x}\right). \tag{3.30}$$

After the boundary conformal transformation $x = e^{\frac{2\pi}{\beta}(\Theta+iT_E)}$, the projection demands periodicity in Θ,

$$\Phi_j\left(z,\bar{z};T_E,\Theta+2\pi\right) = \Phi_j\left(z,\bar{z};T_E,\Theta\right), \tag{3.31}$$

JHEP10(2022)195

and likewise for $\Phi^{J\bar{J}}_{jw}(z,\bar{z};T_{\rm E},\Theta)$. Their correlation functions in the orbifold are again obtained by summing over images, and their string amplitudes compute T^2 correlation functions of the BCFT for $\beta < 2\pi$. For example,

$$\begin{aligned}&\langle\hat{\Phi}_j(T_{\rm E,1},\Theta_1)\hat{\Phi}_j(T_{\rm E,2},\Theta_2)\rangle \\ &\propto \sum_{n\in\mathbb{Z}}\left\{\cosh\left(\frac{2\pi}{\beta}\left(\Theta_{12}+2\pi n\right)\right)-\cos\left(\frac{2\pi}{\beta}T_{\rm E,12}\right)\right\}^{-2j}.\end{aligned} \tag{3.32}$$

Cutting the torus at $T_{\rm E}=0$ and gluing in the Lorentzian cylinder prepares the thermal state. Continuing both operators gives their thermal expectation value [10, 92, 93]

$$\begin{aligned}&\mathrm{tr}\left(e^{-\beta H}\hat{\Phi}_j(T_1,\Theta_1)\hat{\Phi}_j(T_2,\Theta_2)\right) \\ &\propto \sum_{n\in\mathbb{Z}}\left\{\cosh\left(\frac{2\pi}{\beta}\left(\Theta_{12}+2\pi n\right)\right)-\cosh\left(\frac{2\pi}{\beta}T_{12}\right)\right\}^{-2j}.\end{aligned} \tag{3.33}$$

Or, making cuts at both $T_{\rm E}=0$ and $\beta/2$ and e.g. continuing an operator to each side,[67]

$$\begin{aligned}&\langle\mathrm{TFD}|\left(1_{\rm L}\otimes\hat{\Phi}_j\left(T_{\rm R,1},\Theta_1\right)\right)\left(\hat{\Phi}_j\left(T_{\rm L,2},\Theta_2\right)\otimes 1_{\rm R}\right)|\mathrm{TFD}\rangle \\ &\propto \sum_{n\in\mathbb{Z}}\left\{\cosh\left(\frac{2\pi}{\beta}\left(\Theta_{12}+2\pi n\right)\right)+\cosh\left(\frac{2\pi}{\beta}\left(T_{\rm R,1}+T_{\rm L,2}\right)\right)\right\}^{-2j}.\end{aligned} \tag{3.34}$$

As in eq. (3.11), one may Fourier transform the boundary position space basis of vertex operators to obtain operators of definite BTZ energy and angular momentum. For example,

$$\Phi_{jK\bar{K}}(z,\bar{z})\propto\int_{-\infty}^{\infty}\mathrm{d}T\int_0^{2\pi}\mathrm{d}\Theta\, e^{-i\frac{2\pi}{\beta}(K-\bar{K})T}e^{-i\frac{2\pi}{\beta}(K+\bar{K})\Theta}\sum_{n\in\mathbb{Z}}\Phi_j(z,\bar{z};T,\Theta+2\pi n), \tag{3.35}$$

where $\frac{2\pi}{\beta}(K\mp\bar{K})$ are the energy and angular momentum. Examples of string amplitudes in this basis are computed in [35]. Absent the sum over images n, one would instead obtain a mode of AdS_3-Rindler.

3.3 The two-dimensional black hole

Finally, we briefly discuss string perturbation theory in the two-dimensional black hole in the HH state. The two-dimensional Euclidean black hole (eq. (2.2)) followed from $\mathrm{SL}(2,\mathbb{R})_k$ (or $\mathrm{SL}(2,\mathbb{C})_k/\mathrm{SU}(2)$) by gauging the $J^3_0+\bar{J}^3_0$ isometry that generates translations along the length of the cylinder (eq. (2.51)). The Lorentzian black hole is then obtained by continuing in the compact coordinate $\theta=it$ (eq. (2.10)). Alternatively, recalling the BTZ coordinates on $\mathrm{SL}(2,\mathbb{R})$ describe an AdS_3-Rindler patch (eqs. (3.24)–(3.25)), likewise related to EAdS_3 by continuation in the compact cycle, one may arrive directly at the two-dimensional Lorentzian black hole by gauging the $J^2_0+\bar{J}^2_0$ symmetry of $\mathrm{SL}(2,\mathbb{R})_k$ that generates translations in Θ. Then whereas the two-dimensional Euclidean black hole spectrum (eq. (2.14)) followed

[67] We flip the sign of $T_{\rm L}$ here because the Schwarzschild time Killing vector points in opposite directions on the left and right sides of the black hole.

JHEP10(2022)195

from the $\mathrm{SL}(2,\mathbb{R})_k$ spectrum (eq. (2.54)) by the coset construction that gauged $J_0^3 + \bar{J}_0^3$, the Lorentzian spectrum is obtained by the coset construction with respect to $J_0^2 + \bar{J}_0^2$.

String perturbation theory in the two-dimensional black hole in the HH state is again defined by continuation from the Euclidean black hole. For example, continuing the Euclidean vertex operators $\mathcal{O}_{jn,w=0}$ with $j = \frac{1}{2}(1+is)$ by sending $n \to iE$ yields scattering states in the right wedge.[68] From eq. (2.24) one obtains

$$\mathcal{O}_{jE} \overset{r\to\infty}{\longrightarrow} \left(e^{-2(1-j)r} + R(j,E)e^{-2jr}\right) e^{-iEt}, \tag{3.36}$$

with wavefunction

$$\Psi_{jE} \underset{\propto}{\overset{r\to\infty}{\longrightarrow}} \left(e^{isr} + R(j,E)e^{-isr}\right) e^{-iEt}, \tag{3.37}$$

describing an incoming particle in the right wedge that scatters off the black hole horizon. One may likewise construct by continuation vertex operators describing outgoing modes, as well as similar modes in the left wedge, and modes behind the past and future horizons [25].

In the Euclidean theory, one found normalizable bound states at poles of the reflection coefficient. Now $R(j,E)$ is non-singular on the real branch, and one finds only these delta-function normalizable scattering states on the complex branch.[69] These modes do not form a complete set, however. The reason is tied to non-unitarity of the scattering matrix — strings can fall behind the horizon. One can close the OPE by including additional modes, including the operators with $w \neq 0$, but at the cost of sacrificing mutual locality of the vertex operators.

String amplitudes of such scattering operators in the HH state may be obtained by continuation from the corresponding Euclidean amplitudes. The Schwinger-Keldysh contour consists of the two Euclidean caps obtained by halving the cigar (figure 5b), glued to the zero-time slice of the Lorentzian black hole (figure 5a), which evolves forward and backward in Lorentzian time. The continuation is more technically challenging than in AdS_3 where one simply continued the boundary insertion point in x-basis worldsheet vertex operators. In momentum basis, one instead computes the Euclidean amplitude as a function of the discrete Matsubara frequencies n, and then continues the result to continuous Lorentzian energies E [25]. The analogous objects in three dimensions are the Fourier modes eqs. (3.11), (3.35).

4 Stringy ER = EPR

Having described the formulation of Lorentzian string perturbation theory in various states by continuation from unitary CFTs, we now consider the string theories obtained by continuation from the dual descriptions of the $\mathrm{SL}(2,\mathbb{C})_k/\mathrm{SU}(2)$, $\mathbb{Z}\backslash\mathrm{SL}(2,\mathbb{C})_k/\mathrm{SU}(2)$, and $\mathrm{SL}(2,\mathbb{R})_k/\mathrm{U}(1)$ CFTs. Each of the three Euclidean dualities shares the essential feature that the Euclidean time circle is contractible in one description and non-contractible in the

[68] Here E is the energy measured in units of $1/\sqrt{\alpha' k}$, and is conjugate to $t = -i\theta$. The proper time in the large r limit of the metric (eq. (2.10)) is $-\alpha' k \mathrm{d}t^2$.

[69] As in Rindler, the modes are singular at the horizon, $\Psi_{jE} \propto r^{-iE} e^{-iEt}(1 + \mathcal{O}(r^2))$.

JHEP10(2022)195

other, with Euclidean time winding conservation violated in the latter case by a condensate of winding strings. Upon continuation then, each gives a string duality realizing ER = EPR. On one side is string theory in a connected spacetime with a horizon in its Hartle-Hawking state, and on the other is string theory in a disconnected union of entangled spacetimes in the thermofield-double state. The principal remaining challenge in formulating these continuations is the Lorentzian interpretation of the Euclidean time winding operators that play a critical role in each of the examples. We will argue that these insertions should be treated in angular quantization on the worldsheet — with a corresponding deformation of the moduli space integration contour where necessary — giving rise to a condensate of pairs of entangled, folded strings emanating from the strong-coupling region.

4.1 Two-dimensional Dilaton-Gravity

We begin with the $\mathrm{SL}(2,\mathbb{R})_k/\mathrm{U}(1)$ CFT. As we have reviewed in the previous sections, for large k this CFT admits a weakly-coupled description given by a string in the cigar-shaped Euclidean black hole of two-dimensional dilaton-gravity, with an asymptotically linear dilaton (eq. (2.3)). Cutting the cigar across its contractible θ cycle and continuing yields the conventional description of a string in the 2D Lorentzian black hole in the HH state [25]. String amplitudes computing the S-matrix of particles scattering off the black hole horizon may be obtained by continuation from the Euclidean amplitudes of vertex operators $\mathcal{O}_{jn,w=0}$ under $n \to iE$, where n is the discrete Matsubara frequency of the mode around the compact Euclidean time circle and E is the continuous Lorentzian energy. This is the ER description of the string theory.

We now turn to the EPR description, corresponding to the string background obtained by continuation from the dual, sine-Liouville description of $\mathrm{SL}(2,\mathbb{R})_k/\mathrm{U}(1)$ (eq. (2.35)). The sine-Liouville background consists of the free linear-dilaton $\times\,\mathrm{S}^1$ background (eq. (2.18)) plus the sine-Liouville potential $4\pi\lambda(W_+ + W_-)$, where $W_\pm$ are the marginal linear-dilaton $\times\,\mathrm{S}^1$ operators with winding ± 1 (eq. (2.36)). It is a strongly-coupled description of the CFT at large k.

In the asymptotic region $r, \hat{r} \to \infty$ of the cigar and sine-Liouville, the two backgrounds are identical, with the coordinates related by eq. (2.16). In that limit, the $\mathrm{SL}(2,\mathbb{R})_k/\mathrm{U}(1)$ Virasoro primaries $\mathcal{O}_{jnw}$ behave as the superposition of linear-dilaton $\times\,\mathrm{S}^1$ primaries given in eq. (2.24). To compute an $\mathrm{SL}(2,\mathbb{R})_k/\mathrm{U}(1)$ correlation function of such operators in the sine-Liouville description, one would insert the corresponding free-field superpositions in the sine-Liouville functional integral.

Let us consider the sine-Liouville potential as a large deformation of the linear-dilaton $\times$ S^1 background, expanding the condensate in powers of the winding operators,

$$\begin{aligned} &\left\langle e^{-\frac{\lambda}{2\alpha'}\int \mathrm{d}^2 z\,(W_+ + W_-)} \cdots \right\rangle_{\mathrm{LD}\times\mathrm{S}^1} \\ &= \sum_{N=0}^{\infty} \frac{1}{(N!)^2} \left(\frac{\lambda}{2\alpha'}\right)^{2N} \left\langle \left(\int \mathrm{d}^2 z\, W_+(z,\bar{z})\right)^N \left(\int \mathrm{d}^2 z'\, W_-(z',\bar{z}')\right)^N \cdots \right\rangle_{\mathrm{LD}\times\mathrm{S}^1}, \end{aligned} \tag{4.1}$$

where the ellipses stand for additional operator insertions $\prod_i e^{-2Q(1-j_i)\hat{r}} e^{in_i\theta}$. Note that the winding conservation law of the free background demands that an equal number of W_+

JHEP10(2022)195

and W_- factors contribute in each term.[70] We wish to understand the Lorentzian string theory defined by continuation from each term in this expansion, which we refer to as the EPR microstate string backgrounds.[71]

Note that eq. (4.1) is not a perturbative expansion around the linear-dilaton $\times$ S^1 background, however. As recalled in section 2.1.3, because λ may be rescaled by field redefinitions, there is no sense in which it is a small parameter. As a result, sine-Liouville correlation functions are not in general analytic in λ, but rather scale with λ^κ as in eq. (2.41), where κ is the function of the primary momenta $\{j_i\}$ given in eq. (2.40). In the special case that $\kappa \in 2\mathbb{N}$, however, one does obtain an analytic function[72] proportional to $\lambda^\kappa \Gamma(-\kappa) \langle (\int W_+)^{\kappa/2} (\int W_-)^{\kappa/2} \cdots \rangle_{\mathrm{LD}\times\mathrm{S}^1,\emptyset}$.

Correspondingly, for compatible values of the momenta $\{j_i\}$, one finds in eq. (4.1) a single term consistent with the anomalous momentum conservation law of the linear dilaton (eq. (2.21)),

$$2Nb_{\mathrm{sL}} + Q\sum_i (1-j_i) = \frac{1}{2}Q\chi. \tag{4.2}$$

This is simply the condition that $\kappa = 2N$, reproducing the preceding result. The zero-mode integral collapses to $\int \mathrm{d}\hat{r}_0$, which diverges with the volume of the target and is reflected in the pole of the gamma function. The free-theory correlators therefore compute the residues of sine-Liouville correlation functions at these poles [94]. In principle the correlation functions for general momenta could be obtained by "continuation" from these residues computed from the free theory, by determining the meromorphic function with the corresponding pole structure, as in Liouville [60, 95–97].

For generic values of $\{j_i\}$, including the scattering states of interest for the black hole, the anomalous conservation law need never be satisfied, and each linear-dilaton $\times$ S^1 correlation function on the right-hand-side of eq. (4.1) appears to vanish. Yet sine-Liouville admits no such anomalous conservation law, the translation symmetry of the target linear-dilaton direction being completely broken by the potential, and exact CFT correlation functions of operators that violate eq. (4.2) certainly need not vanish.

This puzzle is familiar from analogous manipulations in Liouville CFT [60, 95, 96]. The source of the trouble is the strong-coupling region. Namely, eq. (4.1) should be interpreted as defining a perturbative expansion of the sine-Liouville measure in powers of $\lambda e^{-2b_{\mathrm{sL}}\hat{r}_0}$, where $\hat{r}_0$ is the zero-mode of $\hat{r}$. Whereas λ itself is not a small parameter, the combination is invariant under $\hat{r}_0 \to \hat{r}_0 + \delta$, $\lambda \to e^{2b_{\mathrm{sL}}\delta}\lambda$, and gives a perturbative expansion about the weak-coupling region.

To proceed more carefully, one should introduce a regulator that controls the strong-coupling region. In the zero-mode integral eq. (2.39) that lead to eq. (2.41), one could introduce a hard cut-off $\hat{r}_{\mathrm{c}}$ on the lower bound of the integral and attempt to understand

[70] We restrict our attention here to non-winding S^1 primaries that, with $j = \frac{1}{2}(1+is)$, continue to ordinary scattering states of the black hole.

[71] Note, however, that these continued backgrounds describe the thermally entangled microstates. We will not discuss string backgrounds for the pure EPR microstates, though it would be interesting to do so.

[72] Or, rather, the residue at the pole of the gamma function is an analytic function of λ.

JHEP10(2022)195

the limit as $\hat{r}_c \to -\infty$. The regulator will break the anomalous momentum conservation law of the free background, eliminating the spurious constraint eq. (4.2). Alternatively, rather than this hard cut-off step function $\Theta(\hat{r}_0 - \hat{r}_c)$, one could employ a soft cut-off by inserting $\exp\left(-e^{-2b_{sL}(\hat{r}_0-\hat{r}_c)}\right)$ in the integral, which behaves similarly but varies smoothly. Then eq. (2.39) becomes

$$\int_{-\infty}^{\infty} \mathrm{d}\hat{r}_0 \; e^{2b_{sL}\kappa\hat{r}_0 - \left(\frac{\lambda}{\alpha'}V_{sL}\left[\hat{r}',\hat{\theta}\right] + e^{2b_{sL}\hat{r}_c}\right)e^{-2b_{sL}\hat{r}_0}} = \frac{1}{2b_{sL}}\left(\frac{\lambda}{\alpha'}V_{sL}\left[\hat{r}',\hat{\theta}\right] + e^{2b_{sL}\hat{r}_c}\right)^{\kappa}\Gamma\left(-\kappa\right). \quad (4.3)$$

Writing $\varepsilon = e^{2b_{sL}\hat{r}_c}$, such that $\varepsilon \to 0$ when $\hat{r}_c \to -\infty$ meaning that the regulator is removed, the regulated version of eq. (2.41) is

$$\begin{aligned} &\left\langle \prod_N e^{-2Q(1-j_N)\hat{r}}\mathcal{S}_N \right\rangle_{sL,\varepsilon} \\ &= \frac{1}{2b_{sL}}\Gamma\left(-\kappa\right)\left\langle \left(\frac{\lambda}{\alpha'}V_{sL}\left[\hat{r},\hat{\theta}\right] + \varepsilon\right)^{\kappa}\prod_N e^{-2Q(1-j_N)\hat{r}}\mathcal{S}_N \right\rangle_{LD\times S^1,\emptyset}. \end{aligned} \quad (4.4)$$

One may now attempt to expand the free-field correlator in powers of $\frac{1}{\varepsilon}$ by writing

$$\left(\frac{\lambda}{\alpha'}V_{sL} + \varepsilon\right)^{\kappa} = \varepsilon^{\kappa}\sum_{M=0}^{\infty}\binom{\kappa}{M}\left(\frac{\lambda}{\alpha'}\frac{V_{sL}}{\varepsilon}\right)^{M}, \quad (4.5)$$

where $\binom{\kappa}{M}$ is the generalized binomial coefficient. In this way, one more properly obtains as in eq. (4.1) an expansion for sine-Liouville correlation functions as a sum over free-theory correlators with integer powers of the integrated potential inserted. This expansion may diverge, in general. The situation is similar to conformal perturbation theory, where one expands an exactly marginal deformation $e^{-\lambda\int\mathcal{O}}$, obtaining a series with finite radius of convergence. In that case the expansion is suppressed by factors of $\frac{1}{M!}$, whereas the binomial coefficients in eq. (4.5) fall off less rapidly. Thus, the above expansion may only be an asymptotic series, which we speculate may be Borel resummable. We have not attempted to verify this, however.

We will not pursue further the explicit implementation of the regulator here. Our goal is not to offer a new computational framework for obtaining string amplitudes in the black hole, but to give an abstract understanding of the string backgrounds corresponding to the thermal EPR microstates. To that end, we now consider the Lorentzian continuation of the string background defined by each term in eq. (4.1).

Consider first the free linear-dilaton $\times\,\mathrm{S}^1$ itself, i.e. $N = 0$. This is the flat space solution of the dilaton-gravity equations of motion (eq. (2.9)). The target cylinder has the topology of an annulus, which, when halved and glued to its Lorentzian continuation with respect to the S^1, prepares a Schwinger-Keldysh contour for the disconnected union of two copies of linear-dilaton $\times$ time in the TFD state (figure 6a).

As in the Euclidean background, each Lorentzian spatial slice extends from a weak-string-coupling limit at $\hat{r} \to \infty$ to a strong-coupling region $\hat{r} \to -\infty$. The two asymptotic weak-coupling regions are identical to the left and right asymptotic regions of the two-sided

JHEP10(2022)195

black hole. But whereas the left and right regions of the black hole are connected in the interior at the horizon, the two copies of linear-dilaton × time are disconnected, with strong-coupling boundaries in their interiors instead of horizons.

Each remaining term in the expansion eq. (4.1) inserts N pairs of W_+, W_- operators on top of the linear-dilaton × S^1 background. Thus, upon continuation they will introduce deformations of the TFD state in the disconnected union of linear-dilaton × time. Because the $W_\pm$ are winding operators around the Euclidean time circle, however, the Lorentzian interpretation of these deformations is not immediately obvious.

Moreover, there is a problem of mutual locality that arises in attempting to continue $n \to iE$ in the insertions represented by the ellipses in eq. (4.1). Namely, the winding and momentum operators of the compact boson obey an OPE

$$e^{in\theta(z,\bar{z})}e^{\pm ik\tilde{\theta}(0)} \sim \left(\frac{z}{\bar{z}}\right)^{\pm n/2} e^{in\theta(0)\pm ik\tilde{\theta}(0)}. \tag{4.6}$$

When the momentum operator circles the winding insertion at the origin ($z \to e^{2\pi i}z, \bar{z} \to e^{-2\pi i}\bar{z}$), the OPE coefficient transforms by a factor $e^{\pm 2\pi i n}$. Then the operator algebra is well-defined only for $n \in \mathbb{Z}$, which is of course the expected momentum quantization of the compact boson. It follows that by continuing the momentum labels $n \to iE$ in a linear-dilaton × S^1 correlator with a given number of $W_\pm$ insertions, one will in general obtain a multi-valued function on the worldsheet. In order to define string perturbation theory in the EPR microstates obtained by continuation from each term in the expanded background, we must establish how to compute a well-defined string amplitude by integrating such an apparently multi-valued expression over the moduli space.

We address these questions in the following two sub-sections. We first show that each pair of W_+, W_- insertions introduces on top of the disconnected linear-dilaton × S^1 background a pair of strings in a TFD state in the sense of angular quantization on the worldsheet (figure 7a). Each string is folded, with its ends in the strong-coupling region, and each folded string is entangled with its pair, with one in the left and one in the right copy of the spacetime (figure 6a). We then argue that the multi-valued correlation functions obtained by continuation from the linear-dilaton × S^1 should be integrated over a deformed contour in a complexification of the string moduli space on which they are single-valued in order to obtain amplitudes in the background of such entangled, folded strings.

4.1.1 Angular quantization

As recalled in the introduction, one sometimes obtains a target space picture in string theory by adopting the "static" gauge after choosing a flat metric on the worldsheet, in order to fix the residual conformal gauge redundancy that remains within the full diffeomorphism × Weyl gauge redundancy of the functional integral. In static gauge, the target Euclidean time coordinate is fixed to the worldsheet time coordinate ρ in the sense of radial quantization, where $z = e^{\rho+i\phi}$. This choice is unacceptable in the background of Euclidean time winding operators, however. For example, in the neighborhood of a winding ±1 insertion at the origin on the worldsheet, the target Euclidean time $\theta \sim \theta + 2\pi$

JHEP10(2022)195

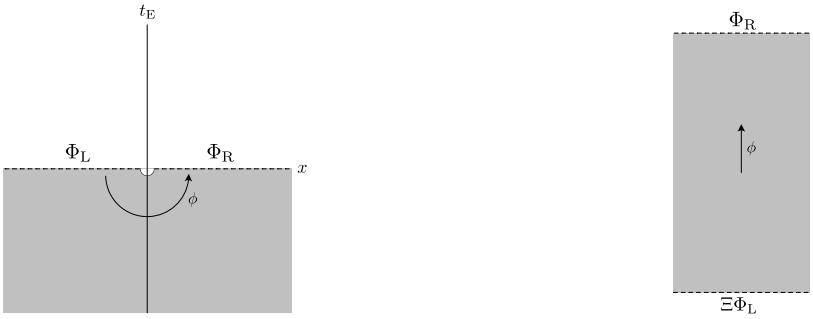

(a) (b)

Figure 16. *The Minkowski Vacuum and the Rindler TFD.* The Euclidean functional integral over the lower-half plane prepares the Minkowski vacuum state on the $t_E = 0$ slice (left). The same functional integral may be interpreted as a Euclidean transition amplitude between states on the negative and positive x-axis, with the angular direction ϕ interpreted as Euclidean time (right). Then the Minkowski vacuum is equivalent to the TFD state in the angularly quantized Hilbert space $\mathcal{H}_L \otimes \mathcal{H}_R$. In the same way, the HH state for the two-sided black hole may be interpreted as a TFD state with respect to the left and right wedges. The reduced density matrix in a single wedge is a thermal state of inverse Hawking temperature β_{BH}.

should obey

$$\theta \overset{\rho\to-\infty}{\longrightarrow} \pm\phi. \tag{4.7}$$

Rather than the static gauge $\theta = \rho$, one may instead adopt an angular gauge condition $\theta = \pm\phi$, in which the compact coordinate ϕ is viewed as the worldsheet Euclidean time direction.

We are therefore motivated to treat the neighborhood of Euclidean time winding insertions on the worldsheet in angular rather than the usual radial quantization. In this section we elaborate on this quantization scheme. In fact, the following is a pure CFT discussion, independent of the application to Lorentzian string theory that we ultimately have in mind, and which we return to at the end of the section.

The basic idea of angular quantization is familiar[73] from the functional integral derivation of the Unruh effect in Rindler spacetime [100]. Consider a field theory on $\mathbb{R}^2$, with the flat metric $ds^2 = dt_E^2 + dx^2$. The functional integral over the lower-half plane prepares the Minkowski vacuum state $|\Omega\rangle$ in the Hilbert space of the theory on the x-axis (figure 16a). It is a wavefunctional, $\Psi_\Omega[\Phi(x)] = \langle\Phi|\Omega\rangle$, that takes field data $\Phi(x)$ on the fixed t_E slice and returns the value of the functional integral over the lower-half plane with that boundary condition.

Let $x = e^\rho \cos(\phi)$, $t_E = e^\rho \sin(\phi)$ define cylinder coordinates, in terms of which $ds^2 = e^{2\rho}(d\rho^2 + d\phi^2)$. The lower-half plane may be foliated by radial lines at fixed ϕ, rather than horizontal lines at fixed t_E. Then the same functional integral admits an alternative Hilbert space interpretation as a transition amplitude between a state on the negative x-axis and a state on the positive x-axis, with Euclidean time evolution given by

[73] See e.g. [98, 99] for useful reviews.

JHEP10(2022)195

rotation in ϕ (figure 16b):

$$\langle\Phi|\Omega\rangle = \langle\Phi_{\rm R}|\, e^{-\pi R}\Xi\,|\Phi_{\rm L}\rangle\,. \tag{4.8}$$

We have divided the field data $\Phi(x)$ into $\Phi_{\rm L}(x)$ on the negative x-axis and $\Phi_{\rm R}(x)$ on the positive x-axis. R generates rotations in ϕ, and Ξ is the CPT operator which maps the Hilbert space on the left to the Hilbert space on the right.

Inserting a complete set of eigenstates of R, the transition amplitude may be written

$$\langle\Phi_{\rm R}|\, e^{-\pi R}\Xi\,|\Phi_{\rm L}\rangle = \langle\Phi_{\rm L}|\otimes\langle\Phi_{\rm R}|\left(\sum_i e^{-\pi\omega_i}\,|i^*\rangle\otimes|i\rangle\right), \tag{4.9}$$

where $|i^*\rangle = \Xi^\dagger\,|i\rangle$. Thus, the Minkowski vacuum $|\Omega\rangle$ on the slice $t_{\rm E}=0$ is equivalent to the TFD state in $\mathcal{H}_{\rm L}\otimes\mathcal{H}_{\rm R}$:

$$|\Omega\rangle = \sum_i e^{-\pi\omega_i}\,|i^*\rangle\otimes|i\rangle\,. \tag{4.10}$$

More precisely, the Hilbert space on the line does not factorize into a product of left and right Hilbert spaces due to divergences associated to degrees of freedom in the neighborhood of the origin. The vacuum in the full spacetime does define a state on the von Neumann operator algebra in both Rindler wedges.

When $\mathbb{R}^2$ is continued with respect to $t_{\rm E} = it$, one obtains standard coordinates on Minkowski space, with metric $\mathrm{d}s^2 = -\mathrm{d}t^2 + \mathrm{d}x^2$. Then expectation values in the vacuum state may be computed by cutting the Euclidean functional integral on $\mathbb{R}^2$ at $t_{\rm E}=0$, gluing in the Minkowski plane, and continuing operator insertions to the Lorentzian section.

Instead continuing with respect to $\phi = i\mathfrak{t}$, one obtains the right wedge of the Rindler decomposition of Minkowski spacetime (figure 8b). In particular, $x = e^\rho\cosh(\mathfrak{t})$ and $t = e^\rho\sinh(\mathfrak{t})$, and therefore the coordinates ρ and $\mathfrak{t}$ cover the region $x > |t|$, bounded by the Rindler horizon. The relation between the Rindler coordinates on the right wedge and the full Minkowski spacetime is analogous to the relation between Schwarzschild coordinates on the right wedge of a black hole and the extended two-sided black hole. One may similarly define Rindler coordinates in the remaining wedges. Lines of constant ρ are hyperbolas $x^2 - t^2 = \text{const.}$, and lines of constant $\mathfrak{t}$ are straight lines through the origin, $t/x = \text{const.}$ Translation in $\mathfrak{t}$ is an isometry, timelike in the right and left wedges (though with opposite orientations), and spacelike in the top and bottom wedges. It corresponds to the boost isometry in the original Minkowski coordinates.

Because ϕ is 2π periodic, when a Euclidean functional integral on $\mathbb{R}^2$ is cut at $\phi = 0$ (i.e. the positive x-axis) and operator insertions are continued to the right Rindler wedge $\phi \to i\mathfrak{t}$, one obtains an expectation value in a thermal state at inverse temperature 2π. This is the Unruh effect: the reduced density matrix of the Minkowski vacuum in the right (or left) Rindler wedge is a thermal state. Indeed, from eq. (4.10) one obtains $\mathrm{tr}_{\mathcal{H}_{\rm L}}\left(|\Omega\rangle\langle\Omega|\right) = e^{-2\pi R}$. By slicing the Euclidean functional integral at both $\phi = 0$ and $\phi = \pi$, one may continue operators to either the left or right Rindler wedges, and so obtain expectation values in $\mathcal{H}_{\rm L}\otimes\mathcal{H}_{\rm R}$ in the TFD state.

JHEP10(2022)195

(a) (b)

Figure 17. *Radial and Angular Slicings.* The same Euclidean functional integral on a sphere may be assigned different Hilbert space interpretations by choosing different foliations. In radial quantization (left), one slices the sphere into circles centered at the poles. Each circle is a spatial slice, and Euclidean time flows along the radial direction transverse to the slices. Then the functional integral over the sphere computes the inner-product of the states prepared by the operator insertions at the poles in the Hilbert space e.g. on the equatorial circle. In angular quantization, the spatial slices are instead radial lines connecting the poles, and Euclidean time flows along the angular direction. Then the same two-point function on the sphere computes the thermal trace in the angularly quantized Hilbert space on the dashed line. Given a point on the sphere, its spatial slice in radial quantization is the orbit of the rotation generator, and its Euclidean time evolution is the orbit of the dilation generator. In angular quantization, the roles of the two symmetries are exchanged.

The thermal state $e^{-2\pi R}$ and its TFD purification are simple examples of states in an angularly quantized Hilbert space. The angular quantization that we propose in what follows generalizes this construction by allowing operator insertions at one or both asymptotic endpoints of the spatial slices.

CFTs are usually treated in radial quantization. That is, when one refers to the Hilbert space of a 2D CFT, one typically means the Hilbert space $\mathcal{H}(\mathrm{S}^1)$ on a circle, corresponding to a slice of the cylinder $\mathrm{S}^1 \times \mathbb{R}$ with Lorentzian time running along its length. One has an isomorphism between this Hilbert space and the space of local operators at a point. Each local operator is mapped to a state on the circle by the Euclidean functional integral over a hemisphere glued to the circle slice, with the operator inserted at the pole. And each state may be mapped to its corresponding local operator by a conformal transformation that shrinks the circle to a point.

Thus, a Euclidean CFT correlation function on S^2, such as the two-point function illustrated in figure 17a, may be cut, e.g. on the equator, and interpreted as an inner-product in the radially quantized Hilbert space on that circle:

$$\langle \mathcal{O}(0)\mathcal{O}'(\infty)\rangle_{\mathrm{S}^2} = \langle \mathcal{O}'|\mathcal{O}\rangle_{\mathcal{H}(\mathrm{S}^1)}\,. \tag{4.11}$$

The Euclidean functional integral over the southern hemisphere prepares the state associated to the operator insertion at the south pole, and the integral over the northern hemisphere prepares the state associated to the operator at the north pole. By sewing up the cut on the dashed circle, the functional integral on the sphere computes the inner-product of these two states. One may also insert the Lorentzian cylinder at the cut, and by continuing additional operator insertions to the Lorentzian section one may compute their expectation value between the two states.

JHEP10(2022)195

In that continuation, Euclidean time evolution is defined by the dilation symmetry of the CFT, which scales the local complex coordinate $z \to \lambda z$ centered at the operator insertion at the pole (and therefore translates the cylinder time coordinate $\log|z| \to \log|z| + \log\lambda$). The slices of the sphere at fixed Euclidean time are circles centered at the poles. In this foliation, given a point on the sphere, its spatial slice is the orbit of the rotation generator around the poles, and its Euclidean time evolution flows along the orbit of the dilation generator.

This foliation is not unique, however. Let us instead slice the sphere in radial lines connecting the poles as in figure 17b, and define Euclidean time evolution by rotation. In this slicing, the roles of the dilation and rotation generators are exchanged: the spatial slice on which a point lies is its orbit under dilation, and Euclidean time runs along the orbit of rotation.

Then the Euclidean functional integral over the sphere with the radial cut prepares a thermal state $e^{-2\pi R} \in \mathcal{H}_{\mathcal{O}\mathcal{O}'}(\mathbb{R})$ in the Hilbert space of angular quantization on the dashed line, where the subscripts label the operator insertions at the poles. The same two-point function, obtained by sewing up the cut, is therefore assigned a different interpretation in this quantization scheme — it is a thermal trace in $\mathcal{H}_{\mathcal{O}\mathcal{O}'}(\mathbb{R})$:

$$\langle\mathcal{O}'|\mathcal{O}\rangle_{\mathcal{H}(\mathrm{S}^1)} = \mathrm{tr}_{\mathcal{H}_{\mathcal{O}\mathcal{O}'}(\mathbb{R})}\left(e^{-2\pi R}\right). \tag{4.12}$$

One may continue additional operator insertions with respect to $\phi \to i\mathfrak{t}$, corresponding to gluing in a Rindler wedge at the cut, and so obtain expectation values of operators in Rindler spacetime in this thermal state. And one may cut the sphere in half to define the TFD state in two copies of $\mathcal{H}_{\mathcal{O}\mathcal{O}'}(\mathbb{R})$ (figure 7a). By continuing additional operator insertions via $\phi \to i\mathfrak{t}_{\mathrm{R}}$ or $\phi \to \pi + i\mathfrak{t}_{\mathrm{L}}$, one obtains an expectation value in the TFD state in the left and right Rindler wedges.

One way to regulate the UV divergences associated to the left/right split of the Hilbert space here is to end the Rindler wedges at a boundary with appropriate boundary conditions. In the Euclidean functional integral this corresponds to excising a small neighborhood of the insertion point of the operator being treated in angular quantization (figure 18) [101]. In the limit that the regulator is removed, the boundary conditions become the asymptotic conditions associated to the inserted operator. Of course, the regulator breaks conformal symmetry, which is only restored in the limit.

Let us now apply this machinery to the linear-dilaton $\times\,\mathrm{S}^1$ background with insertions of $W_\pm$ operators in order to understand the deformations they introduce on top of the $\mathbb{R}^{1,1} \cup \mathbb{R}^{1,1}$ string theory upon continuation. The Hilbert space $\mathcal{H}_{\mathcal{O}\mathcal{O}'}(\mathbb{R})$ is defined by the asymptotic conditions imposed by the insertions $\mathcal{O}, \mathcal{O}'$ at the ends of the line. For a $W_\pm$ insertion, these asymptotic conditions follow from eq. (2.30) with $\alpha = b_{\mathrm{sL}}$,[74]

$$\hat{r} \overset{\rho\to-\infty}{\longrightarrow} \sqrt{\alpha'(k-2)}\rho, \tag{4.13}$$

[74]When the operator insertion coincides with a curvature singularity, the asymptotic condition is modified by a contribution from the linear-dilaton background charge. But the correction is sub-leading in the large k limit because $Q \sim \frac{1}{\sqrt{k}}$.

JHEP10(2022)195

together with the winding condition eq. (4.7). Note in particular that the neighborhood of the insertion point is mapped to the strong-coupling region $\hat{r} \to -\infty$ in spacetime.[75]

Consider the leading term $N = 1$ on top of the linear-dilaton $\times$ S^1 string background in eq. (4.1), with a pair of winding operators W_+, W_- inserted on CP^1. Let $W_+(0)$ be fixed at the origin and $W_-(\infty)$ at the point-at-infinity using the global conformal redundancy of the string worldsheet (figure 7a). In the neighborhood of each of the two insertions, the string is mapped to the strong-coupling region as it wraps the Euclidean spacetime cylinder with unit winding. In between, the worldsheet extends along the cylinder toward finite string coupling before folding back on itself (figures 6b and 7b).

When the Euclidean spacetime annulus is halved to prepare the TFD state on the two zero-time slices $t_R = 0$ at $\theta = 0$ and $t_L = 0$ at $\theta = \pi$, one finds a pair of entangled folded strings, one on each spatial slice, emanating from the strong-coupling region (figure 6a). The respective folded strings are the images of the worldsheet spatial slices — in the sense of angular quantization — at $\phi = 0$ and $\phi = \pi$. The pre-image of the halved embedded worldsheet that connects the two folded strings across the target Euclidean cap is the halved worldsheet shown in figure 7a, bounded by $\phi = 0$ and π. Thus, the pair of folded strings are prepared in the worldsheet TFD state in two copies of the angularly quantized Hilbert space, $\mathcal{H}_{+-}(\mathbb{R}) \otimes \mathcal{H}_{+-}(\mathbb{R})$.

When the angular gauge condition $\theta = \phi$ is continued with respect to the target and angularly quantized worldsheet (i.e. $\theta = it_R$ and $\phi = i\mathfrak{t}_R$, and $\theta = \pi + it_L$ and $\phi = \pi + i\mathfrak{t}_L$), one may think of the folded strings as evolving along their respective Lorentzian spacetimes, with both ends continuing to asymptote to the strong-coupling boundaries.

The asymptotic conditions can be implemented by a boundary condition on an excised neighborhood of the operator insertion, in the limit that the boundary shrinks away (figure 18). For example, the linear-dilaton $\times$ S^1 with W_+ and W_- insertions at the origin and point-at-infinity is described by the $L \to \infty$ limit of the action[76]

$$S = \frac{1}{4\pi\alpha'} \int_{-L}^{L} \mathrm{d}\rho \int_0^{2\pi} \mathrm{d}\phi \left\{ (\partial_\rho \hat{r})^2 + (\partial_\phi \hat{r})^2 + \left(\partial_\rho \hat{\theta}\right)^2 + \left(\partial_\phi \hat{\theta}\right)^2 \right\} \tag{4.14}$$
$$+ 2\left(b_{sL} - \frac{Q}{2}\right) \int_0^{2\pi} \frac{\mathrm{d}\phi}{2\pi} \left(\hat{r}|_L + \hat{r}|_{-L}\right) + \int_0^{2\pi} \frac{\mathrm{d}\phi}{2\pi} \left\{ \sigma_+ \left(\partial_\phi \hat{\theta}|_L - R\right) + \sigma_- \left(\partial_\phi \hat{\theta}|_{-L} - R\right) \right\}.$$

Then the boundary equations of motion,

$$\partial_\rho \hat{r}|_{\rho=\pm L} = \mp 2\alpha' \left(b_{sL} - \frac{Q}{2}\right) \tag{4.15a}$$
$$\partial_\phi \hat{\theta}|_{\rho=\pm L} = R, \tag{4.15b}$$

[75] More precisely, the asymptotic condition fixes the derivative $\partial_\rho \hat{r}$ in the neighborhood of the operator insertion, and eq. (4.13) may be shifted by a constant. This constant shift may be an imaginary number, since in general the saddles of the functional integral may be complex. The asymptotic condition nevertheless implies $\mathrm{Re}(\hat{r}) \to -\infty$, meaning that the string is sent to the strong-coupling region.

[76] Here we choose the cylinder metric, which is responsible for the background-charge shifts of the boundary terms by $-Q/2$. These terms are unimportant in the large k limit, however. One should also add an L-dependent counterterm to render the on-shell action finite.

JHEP10(2022)195

imply the asymptotic conditions in the $L \to \infty$ limit. $\sigma_\pm$ are Lagrange multipliers that implement the winding condition around S^1.

Similarly, for $N > 1$ each pair of W_+, W_- insertions may be thought of as introducing an additional pair of folded strings to the background in the TFD state of angular quantization (figure 9a). Then the exponentiated sine-Liouville potential amounts in the Lorentzian continuation to a condensate of folded strings emanating from strong coupling on top of the disconnected union of two copies of linear-dilaton $\times$ time.

Angular quantization should be understood as applying to the neighborhood of each pair of winding operators, and a genus-zero string diagram with $2N$ such insertions is analogous to a diagram with $2N$ loops of open strings (i.e. $2N$ holes). The associated process is the amplitude of ordinary closed string scattering states to interact with N pairs of folded strings in a state defined by the associated Euclidean functional integral. This also includes interactions by string exchange between the folded strings.

The folded string worldsheets we describe here are somewhat formal in the sense that there is no such saddle of the linear-dilaton $\times S^1$ functional integral — e.g. the two-point function of W_+ and W_- alone vanishes by the anomalous conservation law. To obtain interesting saddles one must of course insert additional operators, which will connect to the folded string asymptotic conditions at strong coupling and fill in the solution in the interior. As discussed earlier, in general one must also regulate the linear-dilaton to suppress its strong-coupling region.

Alternatively, one may consider the continued sine-Liouville background itself without expanding the condensate. Here it is the sine-Liouville potential that regulates the strong-coupling region. In this context, one may interpret the physics of the condensate by considering the effect of introducing an additional pair of $\mathcal{W}_\pm$ insertions on top of it. Then the asymptotic conditions associated to these insertions must be modified from eqs. (4.7) and (4.13) because those map the string out of the weak-coupling region where the free-field description is no longer valid.[77] However, the free-field asymptotic conditions do show that a string initially found at large $\hat{r}$ will head toward strong coupling at the rate $\sqrt{\alpha'(k-2)}$ and with winding ± 1 as one begins to approach the insertion point on the worldsheet. Then in the weak-coupling regions one will again find a pair of folded strings, with their ends headed toward strong coupling. The state of the pair of strings is again the TFD state of angular quantization on the worldsheet, formally defined by the Euclidean functional integral on a hemisphere with insertions of $\mathcal{W}_+$ and $\mathcal{W}_-$ on its boundary. In other words, one has added another pair of folded strings on top of the full EPR background, whose ends dissolve into the condensate at strong coupling.

To properly define the state of the folded strings, one should include the contribution from the bc gauge-fixing ghost system. Given a weight $(1,1)$ Virasoro primary operator of the matter CFT such as $W_\pm$, one forms a physical operator $W_\pm c\bar{c}$ of the full string background by including a factor $c\bar{c}$ from the ghosts. In radial quantization, this operator prepares the

[77] In the cigar description, the asymptotic conditions for a $\mathcal{W}_\pm$ insertion tell the string to wrap the tip of the cigar with winding ± 1 (eq. (2.32)). We do not know the full asymptotic conditions in the sine-Liouville description, however.

JHEP10(2022)195

BRST invariant state $|W_\pm c\bar{c}\rangle = |W_\pm\rangle \otimes |{\downarrow\downarrow}\rangle \in \mathcal{H}(S^1)$ of the linear-dilaton $\times$ S^1 $\times$ $bc \times \bar{b}\bar{c}$ CFT, where $|{\downarrow}\rangle$ is the bc vacuum state of ghost number $-1/2$ prepared by $c(0)$.

In angular quantization, with $W_+ c\bar{c}$ and $W_- c\bar{c}$ inserted at the poles of CP^1, one obtains the TFD state in two copies of $\mathcal{H}_{+-}(\mathbb{R}) \otimes \mathcal{H}_{cc}(\mathbb{R}) \otimes \mathcal{H}_{\bar{c}\bar{c}}(\mathbb{R})$, where $\mathcal{H}_{cc}(\mathbb{R})$ is the angularly quantized Hilbert space of the bc CFT with c insertions at either end, and likewise for $\mathcal{H}_{\bar{c}\bar{c}}(\mathbb{R})$. To define the latter Hilbert spaces, it is convenient to recall that the $bc \times \bar{b}\bar{c}$ CFT is itself equivalent to a linear-dilaton of complex background charge $Q_X = 3i/\sqrt{2\alpha'}$ [102]. On the one hand, one has the ghost CFT of central charge $c_{bc} = -26$, with holomorphic stress tensor

$$T_{bc}(z) = -(\partial b)c - 2b\partial c, \tag{4.16}$$

and with OPEs

$$b(z)c(0) \sim \frac{1}{z}, \qquad b(z)b(0),\ c(z)c(0) \sim 0, \tag{4.17}$$

and the analogous anti-holomorphic formulas. The dual description is a linear dilaton $X(z,\bar{z}) = X(z) + \bar{X}(\bar{z})$ with holomorphic stress tensor

$$T_X(z) = -\frac{1}{\alpha'}(\partial X)^2 - Q_X \partial^2 X \tag{4.18}$$

and OPE

$$X(z)X(0) \sim -\frac{\alpha'}{2}\log z. \tag{4.19}$$

The fields are related by the identifications

$$b(z) = e^{i\sqrt{\frac{2}{\alpha'}}X(z)}, \qquad c(z) = e^{-i\sqrt{\frac{2}{\alpha'}}X(z)}, \tag{4.20}$$

and similarly for the anti-holomorphic fields. In particular, the linear-dilaton central charge $c_X = 1 + 6\alpha' Q_X^2$ reproduces -26. b and c transform with conformal weights $(2,0)$ and $(-1,0)$ with respect to T_{bc}, and $e^{\pm i\sqrt{\frac{2}{\alpha'}}X}$ carry the same weights with respect to T_X.

To ensure fractional powers of b and c do not appear, X must be compact with periodicity $2\pi\sqrt{\alpha'/2}$ [103]. There is no contradiction with the presence of the linear dilaton, however, because the background charge Q_X is complex; though the dilaton action $-\frac{Q_X}{4\pi}\int \mathrm{d}^2\sigma\sqrt{h}\,\mathcal{R}X$ is not invariant under the shift, its variation is a multiple of $2\pi i$, and therefore the functional integral measure is well-defined.

The bc equations of motion imply the classical conservation of the ghost-number current $J(z) = -bc$, with respect to which c carries ghost number $+1$ and b carries ghost number -1. Then the identifications eq. (4.20), taking care to account for the implied normal ordering, yield $J = -i\sqrt{\frac{2}{\alpha'}}\partial X$. X therefore corresponds to the bosonization of the ghost-number current, the ghost-number symmetry of the bc description mapping to the translation symmetry in X of the linear-dilaton description.

The ghost-number symmetry is anomalous due to the mismatch in the number of c and b zero-modes on a worldsheet of genus g, which, by the Riemann-Roch theorem, is

JHEP10(2022)195

$\dim\{c_0\} - \dim\{b_0\} = 3 - 3g$. Then the functional integral measure $\mathrm{D}c\,\mathrm{D}b \supset \prod\{\mathrm{d}c_0\}\{\mathrm{d}b_0\}$ carries charge $-(3-3g)$ under the symmetry, and the charges of any insertions must sum to $3 - 3g = \frac{3}{2}\chi$ to obtain a non-zero correlation function, where $\chi = 2 - 2g$ is the Euler characteristic of the worldsheet. Correspondingly, the target translation symmetry of X in the linear-dilaton background is anomalous (eq. (2.21)). With $\alpha_b = -i/\sqrt{2\alpha'}$ for a b insertion and $\alpha_c = +i/\sqrt{2\alpha'}$ for a c insertion, the linear-dilaton anomalous conservation law likewise ensures that a correlator with N_c insertions of $e^{-i\sqrt{\frac{2}{\alpha'}}X}$ and N_b insertions of $e^{i\sqrt{\frac{2}{\alpha'}}X}$ may be non-zero only if $N_c - N_b = \frac{3}{2}\chi$.

The anomaly also implies that the ghost-number current is not a Virasoro primary, and therefore under the conformal map $z = e^w$ between the plane and cylinder, the transformed current is given not by $\tilde{J}(w) = zJ(z)$ but by $\tilde{J}(w) = zJ(z) - \frac{3}{2}$. Then the ghost-number charges of a state on the cylinder and a local operator on the plane differ by $-3/2$, accounting for the discrepancy between the ghost-number 1 operator c and the ghost-number $-1/2$ vacuum state $|{\downarrow}\rangle$ it prepares. The corresponding anomaly in the linear-dilaton current is likewise responsible for the shifted momentum of states proportional to the background charge.

The equivalence of the $bc \times \bar{b}\bar{c}$ CFT and the linear-dilaton X makes the construction of the TFD state in two copies of the Hilbert space $\mathcal{H}_{cc}(\mathbb{R}) \otimes \mathcal{H}_{\bar{c}\bar{c}}(\mathbb{R})$ of angular quantization analogous to the TFD in two copies of $\mathcal{H}_{+-}(\mathbb{R})$. The asymptotic condition eq. (4.13) for a $W_\pm$ insertion at the end of the line is replaced by

$$X \overset{\rho\to-\infty}{\longrightarrow} i\sqrt{2\alpha'}\rho, \tag{4.21}$$

or $X \to -i\sqrt{\frac{\alpha'}{2}}\rho$ when combined with the background-charge contribution in the far past on the cylinder. Along with the linear-dilaton $\times\, \mathrm{S}^1$ action eq. (4.14), one has the bosonized ghost action

$$S_X = \frac{1}{4\pi\alpha'} \int_{-L}^{L} \mathrm{d}\rho \int_0^{2\pi} \mathrm{d}\phi \left\{ (\partial_\rho X)^2 + (\partial_\phi X)^2 \right\} + 2\left(\alpha_c - \frac{Q_X}{2}\right) \int_0^{2\pi} \frac{\mathrm{d}\phi}{2\pi} \left(X|_L + X|_{-L} \right). \tag{4.22}$$

The combination $W_\pm c\bar{c}$ is BRST invariant in the operator sense, and prepares a BRST invariant state on the circle in the sense of radial quantization. The thermal (and TFD) state in the Hilbert space of angular quantization is likewise BRST invariant. Indeed, consider the integral of j_{BRST} around the dashed loop shown in figure 18, where $j_{\mathrm{BRST}} = e^{-i\sqrt{\frac{2}{\alpha'}}X}\left(T_{\hat{r}} + T_{\hat{\theta}} + T_X\right)$ [104]. The grey annulus represents the worldsheet with the neighborhood of the origin and point-at-infinity excised and replaced by the asymptotic conditions on their boundaries. The integral around the closed loop vanishes by conservation of the current, and therefore the difference in the charges evaluated along the two radial line segments equals the integrals of the current over the two circular arcs. The latter vanish in the limit $L \to \infty$ because the conformal weight of the excised insertion was zero. That is, when the linear-dilaton $\times\, \mathrm{S}^1$ stress tensor $T_{\hat{r}} + T_{\hat{\theta}}$ (eq. (2.23)) is evaluated on the

JHEP10(2022)195

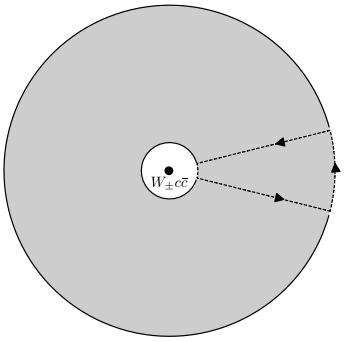

Figure 18. *BRST Invariance.* The physical vertex operator $W_{\pm}c\bar{c}$ is BRST invariant and prepares a BRST invariant state in the sense of radial quantization. The thermal state of angular quantization prepared with an asymptotic insertion of $W_{\pm}c\bar{c}$ is likewise BRST invariant. With the neighborhood of the insertion excised from the worldsheet and replaced by the appropriate asymptotic conditions on the resulting boundary circle, the BRST current vanishes on the circle in the limit that it shrinks away. Because the line integral of the current around the dashed loop shown vanishes by current conservation, it follows that the BRST charges measured on the two radial slices are identical.

asymptotic conditions eqs. (4.7), (4.13) one obtains

$$T_{\hat{r}} + T_{\hat{\theta}} \overset{z\to 0}{\longrightarrow} \frac{1}{z^2}, \tag{4.23}$$

whereas on the ghost asymptotic condition eq. (4.21) one finds

$$T_X \overset{z\to 0}{\longrightarrow} -\frac{1}{z^2}. \tag{4.24}$$

Together therefore, $j_{\text{BRST}} \to 0$. It follows that the BRST charge in the sense of angular quantization commutes with the Hamiltonian (i.e. the rotation generator), and therefore the thermal state of angular quantization associated to $W_{\pm}c\bar{c}$ is BRST invariant.[78]

4.1.2 Mutual locality and the string moduli contour

We now address the question of mutual locality that arises in attempting to continue the labels of vertex operator insertions in a given term in the expansion eq. (4.1) from their Euclidean Matsubara frequencies n to Lorentzian energies E. Namely, the OPE eq. (4.6) of a compact boson primary operator $e^{in\theta(z,\bar{z})}$ of momentum n with a unit-winding operator $e^{\pm ik\tilde{\theta}(z,\bar{z})}$ is single-valued on the z-plane only for integral n. It follows that a correlation function where these insertions approach one another will behave as $(z/\bar{z})^{\pm n/2} = e^{\pm in\phi}$, whose continuation $e^{\mp E\phi}$ is a multi-valued function of ϕ. Thus, a correlation function with a given number of winding operators $W_{\pm}$ and scattering operators $\mathcal{O}_{jn,w=0}|_{\hat{r}\to\infty}$ will generically yield a multi-valued function of z upon continuation. This multi-valuedness

[78] In principle, a trace defined with the BRST invariant density matrix we construct here should be computable by summing over BRST invariant states in the angularly quantized Hilbert space. We leave it for future work to determine this BRST cohomology [105, 106]. In the classical limit, [36] found there were no solutions with vanishing stress energy. However, the $T = 0$ condition in the linear-dilaton theory is not itself a classically conformally invariant equation, necessitating a fully quantum treatment.

JHEP10(2022)195

appears to be an obstacle to defining Lorentzian string perturbation theory for the EPR thermal microstates obtained by continuation from each term of eq. (4.1).

On the one hand, one could evaluate a Lorentzian string amplitude for a given N by first computing the Euclidean amplitude with $n \in \mathbb{Z}$ — i.e. integrating the Euclidean correlation function over the moduli space — and only then continuing $n \to iE$ in the final answer. In principle, this is a satisfactory definition of string perturbation theory in each of the EPR microstates. However, we would like to give a fully Lorentzian prescription for computing EPR string amplitudes directly from the apparently multi-valued correlation functions of winding operators and scattering operators.

The multi-valuedness of the continued linear-dilaton $\times$ S^1 correlation functions is not in and of itself problematic, as these are not the objects of interest in string perturbation theory. Rather, the worldsheet CFT correlation functions serve to produce a measure on the string moduli space, which, when integrated, yields the desired string amplitude. The relevant conditions on the measure are then that it should be single-valued along the integration contour and such that the integral converges.

We will argue that the continued correlation functions should be integrated along a deformed contour in a complexification of the moduli space for which these conditions are satisfied.

The necessity of complexification and deformation of the integration contour is in fact encountered already in ordinary string backgrounds, though it is not always described in that language [38]. The deformation is required to avoid divergences that appear at points in the moduli space corresponding to the collision of two operator insertions on the worldsheet. For example, the Virasoro-Shapiro amplitude for tree-level $2 \to 2$ tachyon scattering in flat spacetime is typically expressed as an integral over the complex plane with three marked points, corresponding to summing over the insertion point $(z, \bar{z})$ of one operator, with the other three being fixed at arbitrary points using the conformal redundancy. The integral over the z-plane diverges whenever the momenta are above the threshold set by the tachyon mass, due to singularities when the integrated operator approaches the fixed insertions [107]. In this example, it so happens that the amplitude may be defined by evaluating the integral over z in an unphysical region where it does converge and then continuing the answer to the physical region. But more generally, the naive integral over the moduli space may never converge, and so a more systematic approach is necessary.

As explained in [38], to obtain a finite string amplitude one complexifies the moduli space, corresponding in the $2 \to 2$ example to treating the coordinates $(z, \bar{z})$ of the integrated operator as independent complex coordinates $(z, \tilde{z})$. The original moduli space is the section $\tilde{z} = \bar{z}$ on which $\tilde{z}$ coincides with the complex conjugate of z. An appropriate integration contour for the sum over moduli may then be taken to be the usual cycle $\tilde{z} = \bar{z}$ almost everywhere, but with a small disk neighborhood of each of the fixed insertions where the original integral diverged replaced by the Lorentzian cylinder of radial quantization. In general one must also ascend to a cover of the complexified moduli space on which the integrand is single-valued.

In the neighborhood of the origin, for example, one continues $(z = e^{\rho + i\phi}, \bar{z} = e^{\rho - i\phi})$ to independent complex coordinates, and replaces the original contour (on which ρ and ϕ

JHEP10(2022)195

were real) by continuing $\rho = \rho_0 + i\mathfrak{t}$ in a small neighborhood $|z| < e^{\rho_0}$ of the insertion. $\mathfrak{t}$ is the worldsheet Lorentzian time in the sense of radial quantization, and so the deformation effectively glues the Lorentzian cylinder at $\mathfrak{t} = 0$ to the z-plane with an excised disk along the boundary circle $|z| = e^{\rho_0}$. The singular neighborhood of the collision point at the origin is thereby removed from the integration contour, and one instead integrates along $\mathfrak{t} \in (-\infty, 0]$. ϕ remains real on this contour.

In a string background with Euclidean time winding operator insertions, we conjecture that Lorentzian string amplitudes should be defined with an analogous angular rather than radial contour deformation. That is, in the neighborhood of a point on the moduli space where a momentum operator and a winding operator collide, the original contour is replaced not with the Lorentzian cylinder of radial quantization, but with a Rindler wedge (or wedges) of angular quantization. In this case it is ρ that remains real while $\phi = i\mathfrak{t}$ is continued.[79] The contour is sketched in figure 9b, referring to the portion of the moduli integral over the insertion point of an ordinary scattering operator. Whereas the radial deformation prevents two scattering insertions from colliding, the angular deformation prevents a scattering insertion from looping around a winding insertion.

With this deformation, the measure obtained from a linear-dilaton $\times$ S^1 correlation function after continuing $n \to iE$, which was multi-valued on the original moduli space $\tilde{z} = \bar{z}$, becomes single-valued on the new contour in the complexification. In particular, the continuation of the problematic OPE coefficient $e^{\mp E\phi}$ that followed from eq. (4.6) is now a single-valued and oscillatory function $e^{\mp iE\mathfrak{t}}$ of $\mathfrak{t}$.

For example, consider the two-point function in the $N = 1$ background of $e^{-2Q(1-j)\hat{r}}e^{in\theta}\mathcal{O}_h$ and $e^{-2Q(1-j)\hat{r}}e^{-in\theta}\mathcal{O}_h$, where $\mathcal{O}_h$ is an internal primary of weight h. Using the conformal gauge redundancy, fix the winding operators at the origin and point-at-infinity, and fix one of the momentum operators at $z = 1$. The insertion point of the remaining momentum operator is to be integrated. To avoid the need for a regulator, let us for simplicity pick $j = \frac{k-1}{2}$, such that eq. (4.2) is satisfied.[80] Continuing $n \to iE$, the internal weight h is chosen to satisfy the on-shell condition,

$$-\frac{j(j-1)}{k-2} - \frac{E^2}{4k} + h = 1. \tag{4.25}$$

The moduli space contour over which the location of the unfixed momentum operator is to be integrated is shown in figure 9b.

4.2 Asymptotic AdS_3 gravity

Next we consider the examples of ER = EPR for asymptotic AdS_3 gravity obtained by continuation from the dual descriptions of the $SL(2,\mathbb{C})_k/SU(2)$ and $\mathbb{Z}\backslash SL(2,\mathbb{C})_k/SU(2)$ CFTs. These examples are in several respects simpler than in two-dimensional dilaton-gravity.

[79] It would also be interesting to understand the appropriate contour deformation when two Euclidean time winding operators collide.

[80] Albeit this is not a scattering operator, for which j would lie on the complex branch. When we discuss the AdS_3 duality in the next section, however, it will be the real branch j's that are of physical interest.

JHEP10(2022)195

For large k, the weakly-coupled description of $\mathrm{SL}(2,\mathbb{C})_k/\mathrm{SU}(2)$ is of a string in a solid cylinder geometry (eq. (2.44)) supported by a B-field (eq. (2.78)). A Virasoro primary operator $\Phi^{J\bar{J}}_{jw}(z,\bar{z};\xi_0,\theta_0)$ is labeled by a point (ξ_0,θ_0) on the spacetime conformal boundary, where a delta-function source for the dual BCFT primary operator of conformal weight $(J,\bar{J})$ is inserted. A Euclidean string amplitude computes a BCFT correlation function of such dual operator insertions.

In the weakly-coupled description of $\mathbb{Z}\backslash\mathrm{SL}(2,\mathbb{C})_k/\mathrm{SU}(2)$, the length $\xi \sim \xi + \tilde{\beta}$ is compactified to form a solid torus geometry. Untwisted vertex operators of the orbifold may be obtained from the primaries $\Phi^{J\bar{J}}_{jw}(z,\bar{z};\xi_0,\theta_0)$ by summing over images in ξ_0 to enforce periodicity, and the string amplitudes of such operators compute BCFT correlation functions on the spacetime boundary T^2.

In the dual description of $\mathrm{SL}(2,\mathbb{C})_k/\mathrm{SU}(2)$ (eq. (2.79)), which is strongly coupled for large k, the EAdS_3 solid cylinder is replaced by the first-order cylinder system $\mathcal{F}(\mathbb{C}/\mathbb{Z})$ and an infinite linear-dilaton direction (eq. (2.69)), deformed by the three-dimensional sine-Liouville potential $4\pi\lambda(W_+ + W_-)$, where $W_\pm$ wind the now non-contractible θ cycle of the $W = \xi + i\theta \in \mathbb{C}/\mathbb{Z}$ cylinder (eq. (2.77)). After writing the EAdS_3 action in first-order form (eq. (2.64)), the two backgrounds coincide in the weak-coupling region, where the vertex operators $\Phi^{J\bar{J}}_{jw}(z,\bar{z};\xi_0,\theta_0)$ asymptote to a superposition of linear-dilaton $\times\, \mathcal{F}(\mathbb{C}/\mathbb{Z})$ operators. For an unflowed operator, for example, transforming eq. (3.7) to cylinder coordinates one finds for $j > 1/2$,[81]

$$\Phi_j(z,\bar{z};\xi_0,\theta_0) \to e^{-2Q(1-j)\hat{r}}\delta(\xi-\xi_0)\sum_{n\in\mathbb{Z}}\delta(\theta-\theta_0-2\pi n) + \text{sub-leading}. \tag{4.26}$$

Inserting these linear-dilaton $\times\, \mathcal{F}(\mathbb{C}/\mathbb{Z})$ operators in the sine-Liouville functional integral, one may in principle compute $\mathrm{SL}(2,\mathbb{C})_k/\mathrm{SU}(2)$ correlation functions in the dual description. The dual description of $\mathbb{Z}\backslash\mathrm{SL}(2,\mathbb{C})_k/\mathrm{SU}(2)$ is the same, but with the first-order cylinder $\mathcal{F}(\mathbb{C}/\mathbb{Z})$ replaced by the torus $\mathcal{F}(\mathbb{C}/(\mathbb{Z}\times\mathbb{Z}))$, corresponding to compactifying $\xi = \mathrm{Re}(W)$.

When the EAdS_3 cylinder is cut and continued with respect to the Euclidean time coordinate ξ along its length, the Schwinger-Keldysh contour prepares the spacetime vacuum state in AdS_3. Then continuing the operator labels $\xi_0 \to it_0$ in the Euclidean string amplitudes yields BCFT expectation values of local operator insertions on the Lorentzian boundary cylinder in the dual vacuum state of radial quantization. When $\xi \sim \xi + \tilde{\beta}$ is compactified, continuing with respect to ξ defines string theory two copies of AdS_3 in the bulk TFD state of inverse temperature $\tilde{\beta}$.

Performing the same continuation in the sine-Liouville background yields a dual description of string perturbation theory in AdS_3 in the vacuum or thermal state. This is the better description of these theories when $k-2$ is a small number.

Our interest in the context of ER = EPR, however, is the continuation with respect to the compact Euclidean time coordinate θ — contractible in the original description and non-contractible in the dual, where the condensate is responsible for breaking the winding symmetry.

[81] Here ξ,θ are sigma-model fields of the first-order system and ξ_0,θ_0 are labels for the boundary insertion point.

JHEP10(2022)195

When the original description of $\mathrm{SL}(2,\mathbb{C})_k/\mathrm{SU}(2)$ is continued with respect to $\theta \to iT$, the Schwinger-Keldysh contour prepares the TFD state in a connected pair of AdS_3-Rindler wedges (eq. (2.62)), and the continued string amplitudes compute expectation values of the BCFT in its TFD state in two copies of the angularly quantized Hilbert space on a line. After the $\xi \sim \xi + \tilde{\beta}$ orbifold, the same continuation of $\mathbb{Z}\backslash\mathrm{SL}(2,\mathbb{C})_k/\mathrm{SU}(2)$ prepares the HH state in the two-sided BTZ black hole of inverse Hawking temperature $\beta = 4\pi^2/\tilde{\beta}$.[82] In both cases, one obtains the theory of a string in a connected, two-sided geometry with a horizon. These are the ER descriptions of string theory in AdS_3-Rindler and BTZ.

The θ continuation of the dual backgrounds defines the EPR description of each of these two string theories. As in eq. (4.1), we treat the sine-Liouville potential as a large deformation of the free theory, now being the linear-dilaton $\times\, \mathcal{F}(\mathbb{C}/\mathbb{Z})$, or $\mathcal{F}(\mathbb{C}/(\mathbb{Z}\times\mathbb{Z}))$, background. At leading order, continuing $\theta = \mathrm{Im}(W)$ yields the Schwinger-Keldysh contour for the TFD state in two copies of linear-dilaton $\times\, \mathcal{F}(\mathbb{R}^{1,1})$ or $\mathcal{F}(\mathbb{R}\times\mathrm{S}^1)$ (figure 6a).

The remaining terms in the expansion insert pairs of W_+, W_- operators on top of the free-field Euclidean background, and in turn introduce deformations of the spacetime TFD state upon continuation. As in the two-dimensional case, we interpret each set as inserting a pair of folded strings emanating from the strong-coupling region in the TFD state of angular quantization on the worldsheet. The asymptotic conditions defining a $W_\pm$ insertion are as in eq. (4.13) in the linear-dilaton direction, and, from eq. (2.73),

$$W(z) \overset{z\to 0}{\longrightarrow} \pm\log(z) \tag{4.27a}$$

$$\bar{W}(\bar{z}) \overset{\bar{z}\to 0}{\longrightarrow} \pm\log(\bar{z}). \tag{4.27b}$$

Or, in terms of $\xi = \frac{1}{2}(W+\bar{W})$ and $\theta = \frac{1}{2i}(W-\bar{W})$,

$$\xi \overset{\rho\to-\infty}{\longrightarrow} \pm\rho \tag{4.28a}$$

$$\theta \overset{\rho\to-\infty}{\longrightarrow} \pm\phi. \tag{4.28b}$$

Thus, with $W_+(0)$ and $W_-(\infty)$ fixed on CP^1, the worldsheet is mapped to the strong-coupling region with unit winding in the neighborhood of each insertion, while $\xi \to \mp\infty$. In between, the string formally extends partway toward finite $\hat{r}$ before folding back toward strong-coupling, while ξ ranges over the real line. When the target is halved to prepare the spacetime TFD state, one finds on the left and right zero-time slices a folded string emanating from the strong-coupling region and extended along the ξ direction (figure 19).

The same asymptotic conditions describe the sine-Liouville potential in the Euclidean black hole. Although eq. (4.28a) may at first appear to be in tension with the compactification of ξ, recall that in these variables the current with respect to which the orbifold is performed is not simply ξ's conjugate variable χ, but $\chi + \partial\xi$, and the second term introduces an additional twist. As a result it is not obvious at a glance that the asymptotic condition

[82] The black hole coordinates from section 3.2.3 are obtained by rescaling $\Theta = \frac{\beta}{2\pi}\xi$, which is the non-contractible cycle of periodicity 2π, and $T_{\mathrm{E}} = \frac{\beta}{2\pi}\theta$, which is the contractible cycle of periodicity β.

JHEP10(2022)195

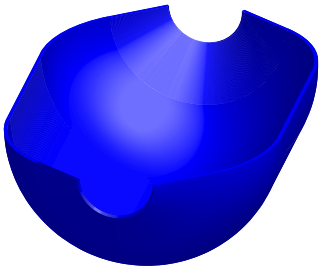

Figure 19. *Folded Strings in* EAdS_3. The spacetime image of the halved worldsheet from figure 7a with a pair of $W_\pm$ insertions is shown. The inner semicircles correspond to the strong-coupling region $\hat{r} \to -\infty$ of the linear-dilaton, the θ direction winds around these circles, and the ξ direction extends along the depth of the figure. The left and right boundaries are folded strings extending from the strong-coupling region partway toward finite $\hat{r}$ before falling back to strong coupling, while ξ ranges from minus infinity to infinity. The folded strings live on the zero-time slices $\theta = t_{\mathrm{R}} = 0, \theta = it_{\mathrm{L}} + \pi = \pi$ of the Lorentzian continuation.

respects the orbifold projection, but one is guaranteed as much because the operators $W_\pm$ are invariant.

Unlike the two-dimensional linear-dilaton $\times$ S^1 background, where the winding and continued scattering operator insertions were mutually non-local (eq. (4.6)) and required the Rindler deformation of the moduli contour discussed in the previous section, the boundary position basis vertex operators admitted by the AdS_3 asymptotics do not suffer from this issue of mutual locality with the winding operators that appear in the expanded background. Indeed, the Euclidean boundary position basis vertex operators are manifestly periodic in Euclidean time, and the Lorentzian vertex operators, being defined by continuation, likewise respect the imaginary time periodicity. Explicitly, the relevant OPE to check is between[83] the winding operators $e^{\mp\sqrt{\frac{k}{\alpha'}}\int^{(z,\bar{z})} \mathrm{d}z'\hat{\chi}(z')+\mathrm{d}\bar{z}'\hat{\bar{\chi}}(\bar{z}')}$ of the first-order system and the delta-function operators

$$\begin{aligned} &\sum_{n\in\mathbb{Z}} \delta^2\left(\hat{W}(z) - \hat{W}_0 - 2\pi i\sqrt{\alpha' k}n\right) \\ &\propto \sum_{n\in\mathbb{Z}} \int \mathrm{d}p\, e^{\frac{i}{2}\left(p - i\frac{n}{\sqrt{\alpha' k}}\right)\left(\hat{W}(z)-\hat{W}_0\right)} e^{\frac{i}{2}\left(p + i\frac{n}{\sqrt{\alpha' k}}\right)\left(\hat{\bar{W}}(\bar{z})-\hat{\bar{W}}_0\right)}, \end{aligned} \tag{4.29}$$

which are conveniently expressed via their inverse Fourier transform. Using eq. (2.72), one finds the OPE

$$\begin{aligned} &e^{\frac{i}{2}\left(p - i\frac{n}{\sqrt{\alpha' k}}\right)\left(\hat{W}(z)-\hat{W}_0\right)} e^{\mp\sqrt{\frac{k}{\alpha'}}\int^0 \mathrm{d}z'\hat{\chi}(z')} \\ &\quad = z^{\pm\frac{i}{2}\sqrt{\alpha' k}\left(p - i\frac{n}{\sqrt{\alpha' k}}\right)} e^{\frac{i}{2}\left(p - i\frac{n}{\sqrt{\alpha' k}}\right)\left(\hat{W}(0)-\hat{W}_0\right)\mp\sqrt{\frac{k}{\alpha'}}\int^0 \mathrm{d}z'\hat{\chi}(z')} \left(1 + \mathcal{O}(z)\right), \end{aligned} \tag{4.30}$$

and similarly for the anti-holomorphic factors. Together, the $z, \bar{z}$ dependence of the pre-

[83] The additional factors of eqs. (2.77) and (4.26) are not relevant to the mutual locality question.

JHEP10(2022)195

factors is

$$z^{\pm\frac{i}{2}\sqrt{\alpha' k}\left(p-i\frac{n}{\sqrt{\alpha' k}}\right)}\bar{z}^{\pm\frac{i}{2}\sqrt{\alpha' k}\left(p+i\frac{n}{\sqrt{\alpha' k}}\right)} = |z|^{\pm i\sqrt{\alpha' k}p}\left(\frac{z}{\bar{z}}\right)^{\pm n/2}, \tag{4.31}$$

which is single-valued and oscillatory, regardless of whether $\hat{W}_0, \hat{\bar{W}}_0$ sit on the Euclidean or Lorentzian section. Then the only $i\varepsilon$ prescription necessary to define Lorentzian string amplitudes with vertex operator insertions in the boundary position basis is the usual prescription that replaces the target Lorentzian time insertion point $T \to T(1 - i\varepsilon)$, as expected from the perspective of the dual CFT, and required to identify the branch of the continued of Euclidean string amplitudes appropriate for time-ordered expectation values.

Of course, if one wishes to compute string amplitudes in the momentum basis rather than the boundary position basis (eqs. (3.11), (3.35)), an analogous mutual locality issue as in the two-dimensional case will arise, and the Rindler deformation of the moduli integration contour will again be necessary.

Unlike the two-dimensional black hole, in AdS_3 the short-string vertex operators of interest include the real branch of j, and the unregulated expansion eq. (4.1) is of greater practical utility. For the two-point function of $\Phi_j(z, \bar{z}; \xi_0, \theta_0)$, for example, the solution of the compatibility condition eq. (4.2) at genus zero is

$$j_N = \frac{1}{2}\left((k-2)N + 1\right). \tag{4.32}$$

In e.g. the $N = 1$ background, one finds a compatible correlator for $j = \frac{k-1}{2}$.[84] Then one could compute

$$\begin{aligned} &\langle \Phi_j(z_0, \bar{z}_0; \xi_0, \theta_0)\Phi_j(z_1, \bar{z}_1; \xi_1, \theta_1)\rangle_{\mathrm{SL}(2,\mathbb{C})_k/\mathrm{SU}(2)} \\ &= \left(\frac{\lambda}{2\alpha'}\right)^2 \left\langle \mathcal{V}_{j,\xi_0,\theta_0}(z_0, \bar{z}_0)\mathcal{V}_{j,\xi_1,\theta_1}(z_1, \bar{z}_1)\int \mathrm{d}^2 z_+ \mathrm{d}^2 z_- W_+(z_+, \bar{z}_+)W_-(z_-, \bar{z}_-)\right\rangle_{\mathrm{LD}\times\mathcal{F}(\mathbb{C}/\mathbb{Z})}, \end{aligned} \tag{4.33}$$

where $\mathcal{V}_{j,\xi_i,\theta_i}$ is given by the right-hand-side of eq. (4.26). To extract the correlator for general j one would, as in Liouville, determine the meromorphic function whose poles coincide with the free-theory correlators of j_N.

To compute the string amplitude obtained from eq. (4.33), one would fix $z_+ = 0$, $z_- = \infty$, and $z_1 = 1$, and integrate over z_0. No contour deformation is necessary in this basis. One must also tensor the operators with an internal CFT scalar primary $\mathcal{O}_h$ of conformal weight h, chosen such that the on-shell condition is satisfied,

$$-\frac{j(j-1)}{k-2} + h = 1. \tag{4.34}$$

4.3 Infinitesimal Lorentzian dualities

Lastly, we briefly consider the Lorentzian continuation of the infinitesimal dualities described in section 2.3. Each infinitesimal duality identifies two equivalent descriptions of the effect of a conformal perturbation by the sine-Liouville operator $\mathcal{O}_{\mathrm{sL}} = \mathcal{W}_+ + \mathcal{W}_-$ (eq. (2.29)) in

[84] Curiously, this coincides with the upper bound of the discrete-series spectrum.

JHEP10(2022)195

the ER description of the respective CFTs. In one description, the deformation introduces a condensate of strings that wrap the Euclidean horizon $r = 0$, and in the other the constant mode of the dilaton is shifted. The black hole mass is in turn shifted under the deformation, in the case of $\mathrm{SL}(2,\mathbb{R})_k/\mathrm{U}(1)$ and $\mathbb{Z}\backslash\mathrm{SL}(2,\mathbb{C})_k/\mathrm{SU}(2)$.

The conformal perturbation deforms the Euclidean background that defines the Lorentzian string theory upon continuation. Expanding the perturbation as in eq. (2.80), a superposition of $\mathcal{W}_\pm$ insertions is introduced on the worldsheet. Note that, in contrast to eq. (4.1), we are now treating the perturbation as an expansion around the exact CFT background as opposed to the free-field background. In particular, the winding number need not be conserved.

In the cigar, the asymptotic conditions eq. (2.32) for $\mathcal{W}_\pm$ map the neighborhood of the insertion point to the tip as pictured in figure 11a. On the $\theta = 0$ fixed-time slice, one finds a string with one end at the tip of the cigar, and likewise on the $\theta = \pi$ slice. When the cigar is cut in half across its θ cycle to prepare the HH state of the black hole, the $\mathcal{W}_\pm$ insertion therefore adds a pair of entangled strings in the TFD state of $\mathcal{H}_{\pm,1}(\mathbb{R}) \otimes \mathcal{H}_{\pm,1}(\mathbb{R})$, one in the left wedge and one in the right, each with one end pinned at the horizon bifurcation point. Or, with a pair of $\mathcal{W}_+, \mathcal{W}_-$ insertions as in figure 7a, one finds on the spacetime zero-time slice a pair of folded strings emanating from the horizon in the TFD state of $\mathcal{H}_{+-}(\mathbb{R}) \otimes \mathcal{H}_{+-}(\mathbb{R})$, as sketched in figure 10a. These folded strings should be compared with those emanating from the strong-coupling region of the EPR background (figure 6a). One may think of the deformation as adding to the condensate of strings that make up the black hole and thus shifting the mass. The dual dilaton-shifting description of course shifts the mass as well.

In $\mathrm{SL}(2,\mathbb{C})_k/\mathrm{SU}(2)$ or $\mathbb{Z}\backslash\mathrm{SL}(2,\mathbb{C})_k/\mathrm{SU}(2)$ the picture is similar. The $\mathcal{W}_\pm$ insertions again add pairs of strings to the AdS_3-Rindler or BTZ backgrounds with one or both ends on the horizon bifurcation locus, the strings now extending in the ξ direction as well due to the additional asymptotic condition $\xi \to \pm\frac{1}{2}e^{2\rho} + \text{const.}$ (eq. (2.88)). The conformal perturbation by $\mathcal{O}_{\mathrm{sL}}$ introduces a condensate of such strings.

Acknowledgments

We would like to thank Nick Agia, Ofer Aharony, Bruno Balthazar, Cindy Keeler, Zohar Komargodski, David Kutasov, Juan Maldacena, Shiraz Minwalla, Victor Rodriguez, Eva Silverstein, Edward Witten, and Xi Yin for stimulating and helpful discussions. This work was supported in part in its inception by NSFCAREER grant PHY-1352084, and then by DOE grant DE-SC0021528.

JHEP10(2022)195

References

[1] M. Van Raamsdonk, *Comments on quantum gravity and entanglement*, arXiv:0907.2939 [INSPIRE].

[2] M. Van Raamsdonk, *Building up spacetime with quantum entanglement*, *Int. J. Mod. Phys. D* **19** (2010) 2429 [arXiv:1005.3035] [INSPIRE].

[3] V.E. Hubeny, M. Rangamani and T. Takayanagi, *A Covariant holographic entanglement entropy proposal*, *JHEP* **07** (2007) 062 [arXiv:0705.0016] [INSPIRE].

[4] J. Maldacena and L. Susskind, *Cool horizons for entangled black holes*, *Fortsch. Phys.* **61** (2013) 781 [arXiv:1306.0533] [INSPIRE].

[5] S. Ryu and T. Takayanagi, *Holographic derivation of entanglement entropy from AdS/CFT*, *Phys. Rev. Lett.* **96** (2006) 181602 [hep-th/0603001] [INSPIRE].

[6] S. Ryu and T. Takayanagi, *Aspects of Holographic Entanglement Entropy*, *JHEP* **08** (2006) 045 [hep-th/0605073] [INSPIRE].

[7] J.B. Hartle and S.W. Hawking, *Path Integral Derivation of Black Hole Radiance*, *Phys. Rev. D* **13** (1976) 2188 [INSPIRE].

[8] J.B. Hartle and S.W. Hawking, *Wave Function of the Universe*, *Phys. Rev. D* **28** (1983) 2960 [INSPIRE].

[9] S.W. Hawking and D.N. Page, *Thermodynamics of Black Holes in anti-de Sitter Space*, *Commun. Math. Phys.* **87** (1983) 577 [INSPIRE].

[10] J.M. Maldacena, *Eternal black holes in anti-de Sitter*, *JHEP* **04** (2003) 021 [hep-th/0106112] [INSPIRE].

[11] S.W. Hawking, *Particle Creation by Black Holes*, *Commun. Math. Phys.* **43** (1975) 199 [*Erratum ibid.* **46** (1976) 206] [INSPIRE].

[12] E. Witten, *Anti-de Sitter space, thermal phase transition, and confinement in gauge theories*, *Adv. Theor. Math. Phys.* **2** (1998) 505 [hep-th/9803131] [INSPIRE].

[13] P. Gao, D.L. Jafferis and A.C. Wall, *Traversable Wormholes via a Double Trace Deformation*, *JHEP* **12** (2017) 151 [arXiv:1608.05687] [INSPIRE].

[14] E. Witten, *On string theory and black holes*, *Phys. Rev. D* **44** (1991) 314 [INSPIRE].

[15] *V. Fateev, A. Zamolodchikov and Al. Zamolodchikov*, unpublished.

[16] V. Kazakov, I.K. Kostov and D. Kutasov, *A Matrix model for the two-dimensional black hole*, *Nucl. Phys. B* **622** (2002) 141 [hep-th/0101011] [INSPIRE].

[17] L. Eberhardt, M.R. Gaberdiel and R. Gopakumar, *Deriving the AdS_3/CFT_2 correspondence*, *JHEP* **02** (2020) 136 [arXiv:1911.00378] [INSPIRE].

[18] M.R. Gaberdiel and R. Gopakumar, *Tensionless string spectra on AdS_3*, *JHEP* **05** (2018) 085 [arXiv:1803.04423] [INSPIRE].

[19] L. Eberhardt, M.R. Gaberdiel and R. Gopakumar, *The Worldsheet Dual of the Symmetric Product CFT*, *JHEP* **04** (2019) 103 [arXiv:1812.01007] [INSPIRE].

[20] G. Giribet, C. Hull, M. Kleban, M. Porrati and E. Rabinovici, *Superstrings on AdS_3 at $k = 1$*, *JHEP* **08** (2018) 204 [arXiv:1803.04420] [INSPIRE].

[21] M. Berkooz, Z. Komargodski and D. Reichmann, *Thermal AdS_3, BTZ and competing winding modes condensation*, *JHEP* **12** (2007) 020 [arXiv:0706.0610] [INSPIRE].

JHEP10(2022)195

[22] K. Hori and A. Kapustin, *Duality of the fermionic 2-D black hole and $N = 2$ Liouville theory as mirror symmetry*, *JHEP* **08** (2001) 045 [hep-th/0104202] [INSPIRE].

[23] M. Bañados, C. Teitelboim and J. Zanelli, *The Black hole in three-dimensional space-time*, *Phys. Rev. Lett.* **69** (1992) 1849 [hep-th/9204099] [INSPIRE].

[24] M. Bañados, M. Henneaux, C. Teitelboim and J. Zanelli, *Geometry of the $(2 + 1)$ black hole*, *Phys. Rev. D* **48** (1993) 1506 [*Erratum ibid.* **88** (2013) 069902] [gr-qc/9302012] [INSPIRE].

[25] R. Dijkgraaf, H.L. Verlinde and E.P. Verlinde, *String propagation in a black hole geometry*, *Nucl. Phys. B* **371** (1992) 269 [INSPIRE].

[26] J.S. Schwinger, *Brownian motion of a quantum oscillator*, *J. Math. Phys.* **2** (1961) 407 [INSPIRE].

[27] L.V. Keldysh, *Diagram technique for nonequilibrium processes*, *Zh. Eksp. Teor. Fiz.* **47** (1964) 1515 [INSPIRE].

[28] A. Giveon, D. Kutasov and N. Seiberg, *Comments on string theory on AdS_3*, *Adv. Theor. Math. Phys.* **2** (1998) 733 [hep-th/9806194] [INSPIRE].

[29] D. Kutasov and N. Seiberg, *More comments on string theory on AdS_3*, *JHEP* **04** (1999) 008 [hep-th/9903219] [INSPIRE].

[30] J. de Boer, H. Ooguri, H. Robins and J. Tannenhauser, *String theory on AdS_3*, *JHEP* **12** (1998) 026 [hep-th/9812046] [INSPIRE].

[31] J.M. Maldacena and H. Ooguri, *Strings in AdS_3 and the $\mathrm{SL}(2, R)$ WZW model. III. Correlation functions*, *Phys. Rev. D* **65** (2002) 106006 [hep-th/0111180] [INSPIRE].

[32] J. Teschner, *Operator product expansion and factorization in the H_3^+ WZNW model*, *Nucl. Phys. B* **571** (2000) 555 [hep-th/9906215] [INSPIRE].

[33] M. Natsuume and Y. Satoh, *String theory on three-dimensional black holes*, *Int. J. Mod. Phys. A* **13** (1998) 1229 [hep-th/9611041] [INSPIRE].

[34] S. Hemming and E. Keski-Vakkuri, *The Spectrum of strings on BTZ black holes and spectral flow in the $\mathrm{SL}(2, R)$ WZW model*, *Nucl. Phys. B* **626** (2002) 363 [hep-th/0110252] [INSPIRE].

[35] S. Hemming, E. Keski-Vakkuri and P. Kraus, *Strings in the extended BTZ space-time*, *JHEP* **10** (2002) 006 [hep-th/0208003] [INSPIRE].

[36] J.M. Maldacena, *Long strings in two dimensional string theory and non-singlets in the matrix model*, *JHEP* **09** (2005) 078 [hep-th/0503112] [INSPIRE].

[37] B. Balthazar, V.A. Rodriguez and X. Yin, *Long String Scattering in $c = 1$ String Theory*, *JHEP* **01** (2019) 173 [arXiv:1810.07233] [INSPIRE].

[38] E. Witten, *The Feynman $i\epsilon$ in String Theory*, *JHEP* **04** (2015) 055 [arXiv:1307.5124] [INSPIRE].

[39] I. Bena, S. Giusto, E.J. Martinec, R. Russo, M. Shigemori, D. Turton et al., *Smooth horizonless geometries deep inside the black-hole regime*, *Phys. Rev. Lett.* **117** (2016) 201601 [arXiv:1607.03908] [INSPIRE].

[40] D.L. Jafferis and E. Schneider, *Semi-classical analysis of the string theory cigar*, *JHEP* **12** (2021) 120 [arXiv:2004.05223] [INSPIRE].

[41] A. Giveon, N. Itzhaki and D. Kutasov, *Stringy Horizons II*, *JHEP* **10** (2016) 157 [arXiv:1603.05822] [INSPIRE].

JHEP10(2022)195

[42] L. Susskind, *Some speculations about black hole entropy in string theory*, hep-th/9309145 [INSPIRE].

[43] L. Susskind and J. Uglum, *Black hole entropy in canonical quantum gravity and superstring theory*, *Phys. Rev. D* **50** (1994) 2700 [hep-th/9401070] [INSPIRE].

[44] E. Witten, *Open Strings On The Rindler Horizon*, *JHEP* **01** (2019) 126 [arXiv:1810.11912] [INSPIRE].

[45] A. Dabholkar, *Strings on a cone and black hole entropy*, *Nucl. Phys. B* **439** (1995) 650 [hep-th/9408098] [INSPIRE].

[46] N. Itzhaki, *Stringy instability inside the black hole*, *JHEP* **10** (2018) 145 [arXiv:1808.02259] [INSPIRE].

[47] A. Giveon and N. Itzhaki, *Stringy Black Hole Interiors*, *JHEP* **11** (2019) 014 [arXiv:1908.05000] [INSPIRE].

[48] A. Giveon and N. Itzhaki, *Stringy Information and Black Holes*, *JHEP* **06** (2020) 117 [arXiv:1912.06538] [INSPIRE].

[49] A. Giveon, N. Itzhaki and U. Peleg, *Instant Folded Strings and Black Fivebranes*, *JHEP* **08** (2020) 020 [arXiv:2004.06143] [INSPIRE].

[50] K. Attali and N. Itzhaki, *The Averaged Null Energy Condition and the Black Hole Interior in String Theory*, *Nucl. Phys. B* **943** (2019) 114631 [arXiv:1811.12117] [INSPIRE].

[51] N. Itzhaki and L. Liram, *A stringy glimpse into the black hole horizon*, *JHEP* **04** (2018) 018 [arXiv:1801.04939] [INSPIRE].

[52] K.P. Yogendran, *Horizon strings and interior states of a black hole*, *Phys. Lett. B* **750** (2015) 278 [arXiv:1808.05748] [INSPIRE].

[53] K.P. Yogendran, *Closed Strings in the 2D Lorentzian Black Hole*, arXiv:1808.10109 [INSPIRE].

[54] J.M. Maldacena and H. Ooguri, *Strings in AdS_3 and $\mathrm{SL}(2,R)$ WZW model. I: The Spectrum*, *J. Math. Phys.* **42** (2001) 2929 [hep-th/0001053] [INSPIRE].

[55] J.M. Maldacena, H. Ooguri and J. Son, *Strings in AdS_3 and the $\mathrm{SL}(2,R)$ WZW model. Part 2. Euclidean black hole*, *J. Math. Phys.* **42** (2001) 2961 [hep-th/0005183] [INSPIRE].

[56] K. Gawędzki, *Noncompact WZW conformal field theories*, in *NATO Advanced Study Institute: New Symmetry Principles in Quantum Field Theory*, (1991), pp. 0247–274 [hep-th/9110076] [INSPIRE].

[57] J. Teschner, *On structure constants and fusion rules in the $\mathrm{SL}(2,C)/\mathrm{SU}(2)$ WZNW model*, *Nucl. Phys. B* **546** (1999) 390 [hep-th/9712256] [INSPIRE].

[58] A. Hanany, N. Prezas and J. Troost, *The Partition function of the two-dimensional black hole conformal field theory*, *JHEP* **04** (2002) 014 [hep-th/0202129] [INSPIRE].

[59] A. Giveon and D. Kutasov, *Comments on double scaled little string theory*, *JHEP* **01** (2000) 023 [hep-th/9911039] [INSPIRE].

[60] A.B. Zamolodchikov and A.B. Zamolodchikov, *Structure constants and conformal bootstrap in Liouville field theory*, *Nucl. Phys. B* **477** (1996) 577 [hep-th/9506136] [INSPIRE].

[61] D. Harlow, J. Maltz and E. Witten, *Analytic Continuation of Liouville Theory*, *JHEP* **12** (2011) 071 [arXiv:1108.4417] [INSPIRE].

JHEP10(2022)195

[62] V.G. Knizhnik, A.M. Polyakov and A.B. Zamolodchikov, *Fractal Structure of 2D Quantum Gravity*, *Mod. Phys. Lett. A* **3** (1988) 819 [INSPIRE].

[63] A.S. Losev, A. Marshakov and A.M. Zeitlin, *On first order formalism in string theory*, *Phys. Lett. B* **633** (2006) 375 [hep-th/0510065] [INSPIRE].

[64] N.A. Nekrasov, *Lectures on curved beta-gamma systems, pure spinors, and anomalies*, hep-th/0511008 [INSPIRE].

[65] E. Frenkel and A. Losev, *Mirror symmetry in two steps: A-I-B*, *Commun. Math. Phys.* **269** (2006) 39 [hep-th/0505131] [INSPIRE].

[66] R. Argurio, A. Giveon and A. Shomer, *Superstrings on AdS_3 and symmetric products*, *JHEP* **12** (2000) 003 [hep-th/0009242] [INSPIRE].

[67] A. Giveon and D. Kutasov, *Notes on AdS_3*, *Nucl. Phys. B* **621** (2002) 303 [hep-th/0106004] [INSPIRE].

[68] G. Giribet and C.A. Núñez, *Correlators in AdS_3 string theory*, *JHEP* **06** (2001) 010 [hep-th/0105200] [INSPIRE].

[69] J. Kim and M. Porrati, *On the central charge of spacetime current algebras and correlators in string theory on AdS_3*, *JHEP* **05** (2015) 076 [arXiv:1503.07186] [INSPIRE].

[70] J.L.F. Barbón and E. Rabinovici, *Remarks on black hole instabilities and closed string tachyons*, *Found. Phys.* **33** (2003) 145 [hep-th/0211212] [INSPIRE].

[71] J.L.F. Barbón and E. Rabinovici, *Closed string tachyons and the Hagedorn transition in AdS space*, *JHEP* **03** (2002) 057 [hep-th/0112173] [INSPIRE].

[72] G.T. Horowitz and E. Silverstein, *The Inside story: Quasilocal tachyons and black holes*, *Phys. Rev. D* **73** (2006) 064016 [hep-th/0601032] [INSPIRE].

[73] J.A. Harvey, D. Kutasov, E.J. Martinec and G.W. Moore, *Localized tachyons and RG flows*, hep-th/0111154 [INSPIRE].

[74] G.T. Horowitz, *Tachyon condensation and black strings*, *JHEP* **08** (2005) 091 [hep-th/0506166] [INSPIRE].

[75] E. Silverstein, *Singularities and closed string tachyons*, in *23rd Solvay Conference in Physics: The Quantum Structure of Space and Time*, Brussels Belgium, December 1–3 2005, pp. 70–81 [hep-th/0602230] [INSPIRE].

[76] A. Adams, X. Liu, J. McGreevy, A. Saltman and E. Silverstein, *Things fall apart: Topology change from winding tachyons*, *JHEP* **10** (2005) 033 [hep-th/0502021] [INSPIRE].

[77] A. Adams, J. Polchinski and E. Silverstein, *Don't panic! Closed string tachyons in ALE space-times*, *JHEP* **10** (2001) 029 [hep-th/0108075] [INSPIRE].

[78] N. Seiberg and S.H. Shenker, *A Note on background (in)dependence*, *Phys. Rev. D* **45** (1992) 4581 [hep-th/9201017] [INSPIRE].

[79] J.L. Karczmarek, J.M. Maldacena and A. Strominger, *Black hole non-formation in the matrix model*, *JHEP* **01** (2006) 039 [hep-th/0411174] [INSPIRE].

[80] A. Giveon, D. Kutasov, E. Rabinovici and A. Sever, *Phases of quantum gravity in AdS_3 and linear dilaton backgrounds*, *Nucl. Phys. B* **719** (2005) 3 [hep-th/0503121] [INSPIRE].

[81] N. Seiberg, *Notes on quantum Liouville theory and quantum gravity*, *Prog. Theor. Phys. Suppl.* **102** (1990) 319 [INSPIRE].

JHEP10(2022)195

[82] J.J. Atick and E. Witten, *The Hagedorn Transition and the Number of Degrees of Freedom of String Theory*, *Nucl. Phys. B* **310** (1988) 291 [INSPIRE].

[83] G.T. Horowitz and J. Polchinski, *Selfgravitating fundamental strings*, *Phys. Rev. D* **57** (1998) 2557 [hep-th/9707170] [INSPIRE].

[84] P. Hořava and C.J. Mogni, *String Perturbation Theory on the Schwinger-Keldysh Time Contour*, *Phys. Rev. Lett.* **125** (2020) 261602 [arXiv:2009.03940] [INSPIRE].

[85] P. Hořava and C.J. Mogni, *Large-N Expansion and String Theory Out of Equilibrium*, arXiv:2008.11685 [INSPIRE].

[86] P. Hořava and C.J. Mogni, *Keldysh Rotation in the Large-N Expansion and String Theory Out of Equilibrium*, arXiv:2010.10671 [INSPIRE].

[87] K. Skenderis and B.C. van Rees, *Real-time gauge/gravity duality: Prescription, Renormalization and Examples*, *JHEP* **05** (2009) 085 [arXiv:0812.2909] [INSPIRE].

[88] K. Skenderis and B. C. van Rees, *Real-time gauge/gravity duality*, *Phys. Rev. Lett.* **101** (2008) 081601 [arXiv:0805.0150].

[89] J.D. Brown and M. Henneaux, *Central Charges in the Canonical Realization of Asymptotic Symmetries: An Example from Three-Dimensional Gravity*, *Commun. Math. Phys.* **104** (1986) 207 [INSPIRE].

[90] I.R. Klebanov and E. Witten, *AdS/CFT correspondence and symmetry breaking*, *Nucl. Phys. B* **556** (1999) 89 [hep-th/9905104] [INSPIRE].

[91] P. Breitenlohner and D.Z. Freedman, *Stability in Gauged Extended Supergravity*, *Annals Phys.* **144** (1982) 249 [INSPIRE].

[92] E. Keski-Vakkuri, *Bulk and boundary dynamics in BTZ black holes*, *Phys. Rev. D* **59** (1999) 104001 [hep-th/9808037] [INSPIRE].

[93] D. Birmingham, I. Sachs and S.N. Solodukhin, *Relaxation in conformal field theory, Hawking-Page transition, and quasinormal normal modes*, *Phys. Rev. D* **67** (2003) 104026 [hep-th/0212308] [INSPIRE].

[94] T. Fukuda and K. Hosomichi, *Three point functions in sine-Liouville theory*, *JHEP* **09** (2001) 003 [hep-th/0105217] [INSPIRE].

[95] H. Dorn and H.J. Otto, *Two and three point functions in Liouville theory*, *Nucl. Phys. B* **429** (1994) 375 [hep-th/9403141] [INSPIRE].

[96] J. Teschner, *Liouville theory revisited*, *Class. Quant. Grav.* **18** (2001) R153 [hep-th/0104158] [INSPIRE].

[97] P. Di Francesco and D. Kutasov, *World sheet and space-time physics in two-dimensional (Super)string theory*, *Nucl. Phys. B* **375** (1992) 119 [hep-th/9109005] [INSPIRE].

[98] D. Harlow, *Jerusalem Lectures on Black Holes and Quantum Information*, *Rev. Mod. Phys.* **88** (2016) 015002 [arXiv:1409.1231] [INSPIRE].

[99] E. Witten, *APS Medal for Exceptional Achievement in Research: Invited article on entanglement properties of quantum field theory*, *Rev. Mod. Phys.* **90** (2018) 045003 [arXiv:1803.04993] [INSPIRE].

[100] W.G. Unruh and N. Weiss, *Acceleration Radiation in Interacting Field Theories*, *Phys. Rev. D* **29** (1984) 1656 [INSPIRE].

JHEP10(2022)195

[101] K. Ohmori and Y. Tachikawa, *Physics at the entangling surface*, *J. Stat. Mech.* **1504** (2015) P04010 [arXiv:1406.4167] [INSPIRE].

[102] D. Friedan, E.J. Martinec and S.H. Shenker, *Conformal Invariance, Supersymmetry and String Theory*, *Nucl. Phys. B* **271** (1986) 93 [INSPIRE].

[103] E.P. Verlinde and H.L. Verlinde, *Chiral Bosonization, Determinants and the String Partition Function*, *Nucl. Phys. B* **288** (1987) 357 [INSPIRE].

[104] A. D'Adda, M.A. Rego Monteiro and S. Sciuto, *BRST Invariant N-Reggeon Vertex With Bosonized Ghosts*, *Nucl. Phys. B* **294** (1987) 573 [INSPIRE].

[105] D. Jafferis and N. Agia, *Angular Quantization in CFT*, arXiv:2204.11872.

[106] D. Jafferis and N. Agia, *Angular quantization in string theory*, work in progress.

[107] J. Polchinski, *String theory. Volume 1: An introduction to the bosonic string*, Cambridge Monographs on Mathematical Physics, Cambridge University Press (2007) [DOI] [INSPIRE].

[108] O. Aharony, A. Giveon and D. Kutasov, *LSZ in LST*, *Nucl. Phys. B* **691** (2004) 3 [hep-th/0404016] [INSPIRE].

[109] Y. Hikida and V. Schomerus, *The FZZ-Duality Conjecture: A Proof*, *JHEP* **03** (2009) 095 [arXiv:0805.3931] [INSPIRE].

[110] A. Maloney, A. Strominger and X. Yin, *S-brane thermodynamics*, *JHEP* **10** (2003) 048 [hep-th/0302146] [INSPIRE].

[111] J.M. Maldacena, *The Large N limit of superconformal field theories and supergravity*, *Int. J. Theor. Phys.* **38** (1999) 1113 [hep-th/9711200] [INSPIRE].

[112] S.S. Gubser, I.R. Klebanov and A.M. Polyakov, *Gauge theory correlators from noncritical string theory*, *Phys. Lett. B* **428** (1998) 105 [hep-th/9802109] [INSPIRE].

[113] E. Witten, *Anti-de Sitter space and holography*, *Adv. Theor. Math. Phys.* **2** (1998) 253 [hep-th/9802150] [INSPIRE].

[114] N. Bao, J. Pollack and G.N. Remmen, *Wormhole and Entanglement (Non-)Detection in the ER=EPR Correspondence*, *JHEP* **11** (2015) 126 [arXiv:1509.05426] [INSPIRE].

[115] D. Berenstein and A. Miller, *Can Topology and Geometry be Measured by an Operator Measurement in Quantum Gravity?*, *Phys. Rev. Lett.* **118** (2017) 261601 [arXiv:1605.06166] [INSPIRE].

[116] D. Berenstein and A. Miller, *Superposition induced topology changes in quantum gravity*, *JHEP* **11** (2017) 121 [arXiv:1702.03011] [INSPIRE].

[117] A. Almheiri, X. Dong and B. Swingle, *Linearity of Holographic Entanglement Entropy*, *JHEP* **02** (2017) 074 [arXiv:1606.04537] [INSPIRE].

JHEP10(2022)195